An investigation of the mechanism of cisplatinum-induced apoptosis in SH-SY5Y neuroblastoma cells

PRIYADHARSHINI BALARAMAN

A thesis submitted for the degree of Doctor of Philosophy

Institute of Child Health

University College London

2005

ProQuest LLC
789 East Eisenhower Parkway
P.O. Box 1346
Ann Arbor, MI 48106-1346

ACKNOWLEDGEMENTS

I wish to offer my immense gratitude to my PhD supervisor, Dr. Jonathan Ham for his enormous support and guidance during my PhD training. His continuous encouragement, persistence and attention to detail have been great lessons to me. I would like to thank Dr. Mike Hubank, my secondary supervisor, for his help and advice over the years. His support along with the help of Ms. Danielle Fletcher during the microarray experiments was of great benefit to me.

To Dr. Jonathan Ham's neuronal apoptosis group: Dr. Jonathan Gilley, Dr. Susanna Terzano, Ms. Jennefer Lindsay and Ms. Emily Towers – I am grateful to have been part of such a warm, friendly and supportive team.

I would like to thank all the staff and students of the Molecular Haematology & Cancer Biology Unit at the Institute of Child Health for their support, advice, criticism and encouragement. Special thank you to Jenny, Susi and Emily – your friendship has kept me sane over the years.

I want to take this opportunity to offer my long overdue gratitude to Mr. Cunnington, my GCSE biology teacher, whose fascinating and humorous lessons on genetics, kindled my interest in the subject and inspired me to enter the world of research. For the passion with which you imparted knowledge to young minds, I will be eternally grateful.

Without the love, support and blessings of my parents, Amma and Appa, nothing would have been achievable nor worth achieving. My dearest Swami, my best friend - thank you for your eternal guidance and support throughout my life. I dedicate this thesis to my Amamma and to the loving memories of my Apappa, Patti, Pappa and Chico.

I acknowledge and appreciate the support of the Child Health Research Appeal Trust (CHRAT) in supporting this work.

ABSTRACT

Neuroblastomas are common paediatric tumours derived from the sympathoadrenal lineage. Neuroblastoma cells may arise from neuroblasts, which failed to differentiate or which were not eliminated by apoptosis at an appropriate stage of development. The aim of this thesis was to identify the signalling pathway by which cis-diamminedichloroplatinum (II) (CDDP) a chemotherapeutic agent, triggers caspase activation and apoptosis in the SH-SY5Y neuroblastoma cell line. An understanding of this may prove to be useful for developing better therapeutic agents for treating neuroblastoma and for understanding mechanisms of drug resistance. CDDP was found to induce apoptosis in SH-SY5Y cells via the mitochondrial death pathway, with cytochrome c release and activation of caspases-9 and -3. CDDP, a DNA damaging agent, activates p53 in SH-SY5Y cells and p53 is known to induce apoptosis via the mitochondrial pathway.

Bcl-2 family members play a central role in the regulation of the mitochondrial death pathway and may have pro- or antiapoptotic activity. The pattern of expression of members of the Bcl-2 family following CDDP treatment was investigated to determine their regulatory role. PUMA (p53 upregulated modulator of apoptosis), a proapoptotic BH3-only protein and a direct transcriptional target of p53, was found to be upregulated at both the mRNA and protein levels during CDDP-induced apoptosis of SH-SY5Y cells. *PUMA* has three transcripts that encode PUMA- α, β and δ. PUMA-α and PUMA-β are proapoptotic and contain the BH3 domain. PUMA-α was identified as the transcript that increased during CDDP treatment in SH-SY5Y cells. Overexpression of PUMA-α in SH-SY5Y cells was sufficient to induce apoptosis.

To identify other genes regulated by CDDP, we performed oligonucleotide microarray analysis using Affymetrix human genome-U133A microarrays and RNA extracted from SH-SY5Y cells treated with DMSO, transplatinum (an isomer of CDDP which does not induce cell death) and CDDP. The results provide a detailed picture of the changes in gene expression that occur following CDDP treatment.

CONTENTS

LIST OF FIGURES

List of Tables

ABBREVIATIONS

ActD	Actinomycin D
AIF	Apoptosis-inducing factor
ATM	ataxia telangiectasia mutated
ATP	Adenosine triphosphate
ATR	ATM and Rad3 related
BDNF	brain-derived neurotrophic factor
BIR	Baculovirus IAP-repeat
BSA	Bovine serum albumin
CAD	Caspase-activated DNase
CARD	Caspase-activating recruitment domain
CDDP	Cis-diamminedichloroplatinum (II)
CDK	cyclin-dependent kinase
CED	*C. elegans* cell death
CHK	Checkpoint kinase
CHX	Cyclohexamide
CIP	calf intestinal alkaline phosphatase
DARK	*Drosophila* Apaf-1-related killer
DBD	DNA binding domain
DD	Death domain
DED	Death-effector domain
DEPC	Diethyl pyrocarbonate
DIABLO	Direct IAP-binding protein with low pI
DISC	Death-induced signalling complex
DLC	Dynein light chain
DMEM	Dulbecco's modified Eagle's medium
DMSO	Dimethylsulphoxide
DNA	Deoxyribonucleic acid
DTT	Dithiothreitol
EGL	Egg-laying-defective
FCS	Foetal calf serum
FKHR	Forkhead rhabdomyosarcoma
FOXO	Forkhead box, subgroup O
GULP	engulfment adaptor PTB domain containing
IAP	Inhibitor of apoptosis protein
ICE	Interleukin-1β converting enzyme
LB	Luria Bertani

MAPK	Mitogen-activated protein kinase
MDM2	Mouse double minute 2
MMP	Mitochondrial membrane potential
MOM	Mitochondrial outer membrane
MOPS	3-(N-morpholino) propanesulphonic acid
MST	mammalian sterile twenty-like
NGF	Nerve growth factor
OA	Okadaic acid
OptiMEM	Opti-MEM modification of Eagle's minimal essential medium
PAK	p21-activated kinase
PARP	Poly-ADP ribose polymerase
PBS	phosphate-buffered saline
PCR	Polymerase chain reaction
PNK	polynucleotide kinase
PTB	phosphotyrosine binding
PTEN	phosphatase and tensin homologue
RA	Retinoic acid
RNA	Ribonucleic acid
RT-PCR	Reverse-transcriptase - PCR
SDS	Sodium dodecyl sulphate
SEM	standard error of the mean
siRNA	Small interfering RNA
SMAC	Secondary mitochondrial activator of caspase
TAQ	Thermus aquaticus DNA polymerase
TBE	Tris-borate-EDTA
TBS-T	Tris-buffered saline-Tween
TDDP	Trans-diamminedichloroplatinum (II)
TM	Transmembrane
T_m	Melting temperature
TNE	Tris sodium EDTA
TNFR	Tumour necrosis factor receptor
TRK	Tyrosine kinase receptor
TUNEL	Tdt-mediated dUTP-nick end labelling
ZVAD-fmk	N-benzyloxycarbonyl-Val-Ala-Asp- (O-methyl) fluoromethyl ketone

Chapter 1: Introduction

1.1 Neuroblastoma

Neuroblastoma is one of the most common paediatric tumours and is the cause of approximately 7-10% of cancer-related deaths in children. The median age at diagnosis for neuroblastoma patients is about 18 months. About 40% are diagnosed by 1 year of age, 75% by 4 years of age and 98% by 10 years of age. There are approximately ninety new neuroblastoma cases each year in the UK (Bown, 2001). These extra-cranial, solid, malignant tumours are derived from the sympathoadrenal lineage of neural crest cells. Neuroblastomas express neuronal markers, such as neuron-specific enolase, tyrosine hydroxylase, dopamine β-hydroxylase, which suggest that neuroblastoma cells may have arisen from neuroblasts, which failed to differentiate, or which were not eliminated by programmed cell death at the appropriate stage of development (Packham *et al.*, 1996; Middlemas *et al.*, 1999). The primary sites for neuroblastoma development are predominantly the adrenal glands, followed by abdominal, thoracic, cervical and the pelvic sympathetic ganglia (Schwab, 1999).

The clinical hallmark of neuroblastoma is its variability. Approximately 75% of neuroblastoma cases with disseminated metastases (stage 4) are seen in children over the age of 1 year. These neuroblastomas are aggressive, chemo-resistant, and generally incurable. In contrast, infants with neuroblastoma tend to present with lower stage disease (stages 1, 2, and 4s), which are generally chemo-sensitive and high cure rates are obtained. A proportion of lower stage tumours show widespread dissemination in stage 4s disease (Bown, 2001).

Studies of genetic abnormalities show that there are close associations with tumour stage and aggressiveness. The three most important abnormalities associated with neuroblastoma tumours are chromosome 1p loss, 17q gain and *MYCN* amplification. Except for *MYCN* status, the relationship of the other genetic events to the clinical path of neuroblastoma has not been established (Mora *et al.*, 2001). Analysis of cell cycle defects has not yielded many clues for neuroblastoma tumourigenesis (Kawamata *et al.*, 1996; Diccianni *et al.*, 1999).

1.1.1 *MYCN* Amplification

MYCN oncogene amplification or allelic loss at sites such as chromosome 1p are linked with more aggressive neuroblastoma tumours and poor prognosis. The MYC-related oncogene, *MYCN* was found to be amplified in a group of neuroblastoma cell lines (Schwab *et al.*, 1983). *MYCN* is a proto-oncogene normally expressed in the developing nervous system and other selected tissues (Maris and Matthay, 1999). It is a member of the *MYC* gene family, which encode transcription factors that regulate cell proliferation and apoptosis (Fulda *et al.*, 1999). Addition of *MYCN* antisense RNA to MYCN-overexpressing neuroblastoma cell lines can decrease proliferation and/or induce differentiation (Maris and Matthay, 1999). *MYCN* amplification occurs in many primary neuroblastomas in untreated patients (Brodeur *et al.*, 1984). Amplification of *MYCN* is known to correlate with advanced stage disease, which has only been found in more aggressive malignant neuroblastoma variants but it is also associated with rapid tumour progression and a poor prognosis, even in infants and patients with lower stages of disease (Seeger *et al.*, 1985). It correlates with a greatly increased risk of fatal outcome and is therefore established as a powerful clinical marker of high-risk disease. Currently, *MYCN* is the only tumour genetic feature used as a basis for treatment stratification in neuroblastoma clinical trials (Bown, 2001). *MYCN* amplification is a frequent mechanism by which cells gain resistance against cytotoxic drugs (Niimi *et al.*, 1991).

There is minimal or no expression of caspase-8 in a substantial portion (25-35%) of neuroblastoma cell lines and patient samples. The caspase-8 gene (*CASP8*), which encodes a key initiator caspase in the death receptor pathway, is an anti-oncogene that can be completely inactivated by silencing through methylation or deletion exclusively in *MYCN*-amplified neuroblastoma (Teitz *et al.*, 2000).

1.1.2 Overexpression of Cyclin D1

Genetic defects and overexpression of cyclin D1 are found in many malignancies (Donnellan and Chetty, 1998). Approximately two thirds of neuroblastoma cell lines and tumours were identified as overexpressing cyclin D1 at both the RNA and protein levels (Molenaar *et al.*, 2003). D-type cyclins activate their cyclin-dependent kinase partners CDK4 and CDK6 during cell-cycle progression, which leads to the phosphorylation of the retinoblastoma protein and the regulation of

the G1 to S cell cycle progression. This pathway is often deregulated in many tumours. Molenaar *et al.* (2003) have also found a rearrangement in the 3'-UTR of the cyclin D1 gene in 1 out of 96 neuroblastoma tumours. These observations suggest a potential role for deregulated cyclin D1 gene activity in neuroblastoma tumourigenesis.

1.1.3 Trk A and neuroblastoma

TrkA, neurotrophin tyrosine kinase receptor type 1 is the receptor for nerve growth factor (NGF). TrkA is critical for the development and maturation of the central and peripheral nervous system, regulating proliferation, differentiation and programmed cell death (reviewed by Barbacid, 1994). Point mutations, deletions, or novel chimera formation due to chromosomal rearrangements causes oncogenic TrkA activation. Neuroblastoma cell lines are generally unresponsive to NGF (Azar *et al.*, 1990) and TrkA expression exhibits an inverse relationship to neuroblastoma aggressiveness, consistent with a potential marker of good prognosis (Nakagawara *et al.*, 1992; Nakagawara, 2001). The idea that the exclusive role of TrkA in neuroblastoma cells is as a tumour suppressor, which is supported by TrkA gene transduction and restoration of NGF responsiveness, has been challenged by Tacconelli *et al.*, (2004). Tacconelli *et al.* identified a hypoxia-regulated mechanism for oncogenic TrkA activation which generates a novel constitutively active TrkAIII splice variant that exhibits oncogenic properties, antagonises antioncogenic NGF/TrkAI signalling, and is expressed by primary human neuroblastomas (Tacconelli *et al.*, 2004).

1.1.4 Regression of neuroblastomas

Neuroblastomas either regress spontaneously, particularly in infants, or they mature into benign ganglioneuroma. Neuroblastoma has the highest rate of spontaneous regression observed in human cancers, so delayed activation of normal apoptotic pathways might be important in this phenomenon. Activation of programmed cell death can originate from various stimuli, such as the presence or absence of exogenous ligands or from DNA damage. The TNFR family may be involved in initiating apoptosis in neuronal cells and neuroblastomas. Intracellular molecules that are responsible for relaying the apoptotic signal include the Bcl-2

family of proteins, and Bcl-2 is highly expressed in most neuroblastomas. The Bcl-2 proteins might also be important in acquired resistance to chemotherapy (Dole *et al.*, 1994; Dole *et al.*, 1995). So neuroblastomas that are prone to undergoing apoptosis are more likely to spontaneously regress and / or respond well to chemotherapy.

1.1.5 Anti-cancer drugs and neuroblastoma

Currently used highly intensive chemotherapy regimens are better than previous methods but are ineffective in more than half of children with advanced disease. Therefore, the requirement for new additional approaches to treatment is essential. One of the major limitations to the use of drugs is when tumours that were initially responsive to the drugs acquire resistance. Possible mechanisms of acquired resistance include altered cellular drug transport, enhanced intracellular detoxification, increased DNA repair, and enhanced tolerance to platinum-DNA damage. Platinum-containing drugs, including cisplatin and carboplatin, are widely used in the treatment of solid tumours such as ovarian, testicular, head and neck, bladder and lung cancer. Understanding the cellular responses to platinum-based drugs is critical for determining mechanisms of drug resistance and for allowing the development of therapeutic approaches for increasing the effectiveness of cisplatinum or carboplatin treatment.

1.2 Cis-diamminedichloroplatinum (II)

Cis-diamminedichloroplatinum (II) (CDDP) is one of the most effective chemotherapeutic drugs used as part of combination therapy in neuroblastoma patients. However, many tumours are intrinsically resistant and even among initially sensitive tumours, acquired resistance develops commonly during treatments. The tendency of tumour cells to become resistant to CDDP with repeated exposure accounts for therapeutic failure in many cancer patients. A subpopulation of neuroblastoma is relatively resistant to chemotherapy. Approximately 10% of neuroblastoma patients show primary resistance to chemotherapy. CDDP is administered intravenously in multidrug therapy combined with other anti-tumour drugs (Gonzalez *et al.*, 2001; Kartalou and Essigmann, 2001). The problems associated with CDDP treatment are the acquisition of resistance by initially

responsive tumours and side effects such as kidney damage and provocation of nausea and vomiting.

Approximately 1% of intracellular CDDP reacts with nuclear DNA to yield a variety of adducts that include inter- and intra-strand DNA cross-links and DNA-protein cross-links (**Figure 1.1**). Intra-strand cross-links between adjacent guanines are the most common adducts (Perez, 1998). These irreparable lesions in the DNA are essential for the cytotoxic activity of the drug. The DNA adducts inhibit DNA replication and gene transcription (Sanchez-Perez *et al.*, 1998).

The *trans*-isomer, trans-diamminedichloroplatinum (II) (TDDP) is 20-fold less cytotoxic than CDDP and ineffective against tumours (Sanchez-Perez *et al.*, 1998). DNA adducts formed by TDDP are repairable and are of a different nature to those formed by CDDP. The majority of adducts formed by CDDP are intrastrand cross-links between the N7 atoms of adjacent purines. Due to its stereochemical limitations TDDP cannot form intrastrand cross-links but forms interstrand cross-links between complementary G and C residues (Gonzalez *et al.*, 2001; Kartalou and Essigman, 2001).

The DNA damage caused by CDDP is recognised by nucleotide excision repair, mismatch repair, DNA dependent-protein kinase and high mobility group proteins (Gonzalez *et al.*, 2001). Adduct formation disrupts the cytoskeleton and affects actin polymerisation. CDDP also targets the phospholipids and the phosphotidylserines in the membrane and mitochondrial DNA (Gonzalez *et al.*, 2001). Genomic DNA is considered the critical pharmacological target of CDDP-induced cytotoxicity. Like other DNA damaging agents, CDDP triggers several cellular responses, including the activation of the p53 pathway and the induction of DNA damage-inducible genes such as *gadd153, gadd45,* p21, and *c-jun* (Wetzel and Berberich, 2001).

1.2.1 p53 and CDDP

The p53 tumour suppressor protein belongs to a family of related proteins that includes two other members: p63 and p73. Both p63 and p73 share the structural and functional hallmarks of p53, however, they are both involved in normal development whereas p53 plays a role in preventing tumour development. The loss of normal p53 function occurs in almost all cancers (Hollstein *et al.*, 1991). The processes induced

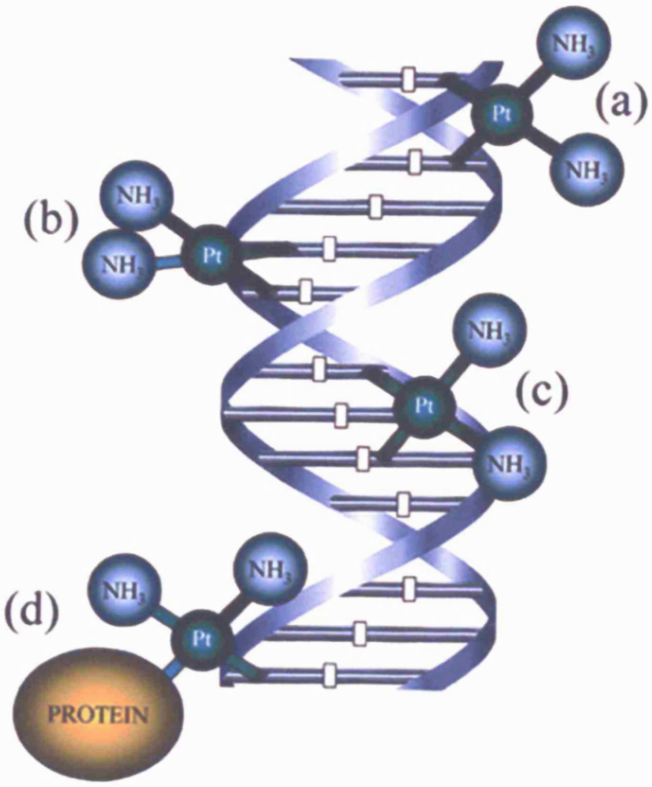

Figure 1.1 The interaction of cisplatin with DNA.

The main adducts formed are **(a)** interstrand cross-link, **(b)** 1,2-intrastrand cross-link, **(c)** 1,3-intrastrand cross-link, **(d)** protein-DNA cross-link. Taken from Gonzalez *et al.*, (2001).

by p53 in response to stress signals that can cause oncogenic changes include cell-cycle arrest, apoptosis, senescence, differentiation and DNA repair. The cellular response to p53 depends on many factors, including cell type, cell environment and whether the cell has sustained other oncogenic alterations. Mutations in p53 are found in approximately 50% of all human tumours (Keshelava *et al.*, 2001; Hickman *et al.*, 2002), but are seen in only 2% of human neuroblastoma tumours examined (Vogan *et al.*, 1993). p53 protein has been found to be abundant in human neuroblastoma cell lines (Davidoff *et al.*, 1992; Vogan *et al.*, 1993). It is possible that instead of mutations, cytoplasmic sequestration and defective translocation of p53 could be alternate mechanisms involved, but previous studies have shown that p53 function is intact in neuroblastoma cell lines (Keshelava *et al.*, 2001).

p53 is a transcriptional regulator protein whose target genes include: *p21, MDM2, Gadd45, Bax, Noxa* and *PUMA* (Keshelava *et al.*, 2001; Hickman *et al.*, 2002). Products of these genes are critical for cell cycle regulation, apoptosis and DNA repair. The p53 transcription factor directly activates the expression of genes that contain p53-binding sites within their regulatory regions. There are many genes that are regulated by p53, which can be divided into groups that might mediate a specific p53 function, such as inhibition of cell growth, DNA repair, and activation of apoptosis or regulation of angiogenesis (Vogelstein *et al.*, 2000). A number of studies have shown that a major role of p53 is in the induction of the apoptotic cascade that is associated with the release of proapoptotic proteins from the mitochondria, such as cytochrome *c* and SMAC (Schuler and Green, 2001). However, p53-inducible genes might also contribute to the induction of death-receptor signalling.

In addition to the activation of apoptotic target genes, p53 can repress gene expression and act independently of the regulation of transcription. Transcription-independent functions of p53 might include shuttling of death receptors to the cell surface (Bennett *et al.*, 1998) or activation of caspase-8 (Ding *et al.*, 2000). The identification of p53 in the mitochondria of some cells may provide a clue as to the nature of the transcription-independent activity of p53 (Marchenko *et al.*, 2000). Marchenko *et al.* showed that a fraction of p53 protein localises to the mitochondria in tumour cells undergoing p53-dependent apoptosis. Another group also reported that a similar targeting of p53 to the mitochondria occurs in normal lymphocytes induced to die in response to ionising radiation (Mihara *et al.*, 2003). p53 that is excluded from the nucleus, and therefore transcriptionally inert, is still capable of

triggering apoptosis in several different cell types. Mihara provided mechanistic insight by showing that p53 directly interacts with the antiapoptotic proteins Bcl-x_L and Bcl-2, which are known to bind to the proapoptotic family members Bak and Bax and inhibit the ability of these to induce cytochrome c release from the mitochondria. It is now proposed that the binding of p53 to Bcl-x_L and Bcl-2 liberates Bak and Bax, thereby allowing them to induce changes in the mitochondrial membrane leading to activation of the caspase cascade resulting in cell death (Mihara *et al.*, 2003). However, mice with deficiency in either of the two direct transcriptional targets of p53, *Puma* or *Noxa*, showed no requirement of these genes for normal development and physiology but a decrease in DNA-damage induced apoptosis in fibroblasts was observed, although only the loss of PUMA protected the lymphocytes from cell death (Villunger *et al.*, 2003). These results have led Villunger *et al.* to suggest that p53 promotes apoptosis mainly through transcriptional activation rather than through the other mechanisms discussed above.

One of the key regulators of p53 stability is MDM2, a protein that functions as a ubiquitin ligase for p53, mediating ubiquitination of p53 and allowing it to be recognised and degraded by the proteasome (Kubbutat *et al.*, 1997). Tumours that have wild-type p53 frequently harbour defects either in the pathways that allow for the stabilisation of p53 in response to stress, or in the effectors of the apoptotic activity of p53. MDM2 is a transcriptional target of p53 and is involved in an autoregulatory loop with p53, where p53 controls the expression of its own regulator. Different stress signals use different pathways to allow p53 to escape MDM2-mediated protein degradation, and defects in one of them might not be sufficient to prevent induction of p53 through another pathway. MDM2 is also a target for phosphorylation by the serine/threonine kinase Akt, which is activated by growth factor stimulation, and phosphorylation of MDM2 is associated with nuclear localisation of MDM2 and enhanced degradation of p53 (Mayo and Donner, 2001; Zhou *et al.*, 2001). Apart from Akt, other components of signalling pathways associated with cell proliferation, such as c-Jun can also function to block p53 activity (Schreiber *et al.*, 1999). p53 inhibition by Akt is counteracted by the ability of p53 to induce expression of PTEN, a phosphatase that can inhibit the activation of Akt (Stambolic *et al.*, 2001). PTEN is a lipid phosphatase that de-phosphorylates PIP3 and thus negatively regulates PI3K-dependent signalling. There is a p53 binding site

directly upstream of the PTEN gene. Thus p53 can negatively regulate cell survival by activating the transcription of PTEN (Stambolic *et al.*, 2001).

Activation of p53 in response to stress signals is almost always accompanied by stabilisation of the p53 protein, and several pathways leading to the inhibition of MDM2-mediated degradation in response to stress have been described (Woods and Vousden, 2001). The interaction between MDM2 and p53 can be impaired by phosphorylation of p53 within the MDM2 binding region. Phosphorylation of these residues occurs in response to stress, such as DNA damage, mediated at least in part by the kinases Chk1, Chk2, ATM and ATR, that are activated by genotoxic damage (Appella and Anderson, 2001). DNA damage-induced phosphorylation of p53 therefore allows stabilisation of p53 by reducing binding to MDM2.

p53 function is also regulated by controlling the cellular localisation of the protein. Since one of the key functions of p53 is the regulation of transcription, localisation of p53 to the nucleus plays an important role in the p53 response (Giannakakou *et al.*, 2000). Once in the nucleus, regulatory mechanisms exist to control the export of p53 back out to the cytoplasm (Montes de Oca *et al.*, 1995). The ability of p53 to be exported is greatly enhanced by the action of MDM2 (Freedman *et al.*, 1999).

Cells possessing wild type p53 protein respond to exposure to DNA-damaging agents by elevating p53 protein levels (Wetzel and Berberich, 2001). Depending on the cell type and the type of DNA damage, increased p53 protein triggers either growth arrest or apoptosis (El Deiry, 1998; Gottlieb and Oren, 1998). Involvement of p53 in CDDP-induced apoptosis has been demonstrated in several cell types (Park *et al.*, 2001). The effect of the loss of p53 function on sensitivity to CDDP is not the same in all cell types. This depends on cell type-specific interactions with other pro- or antiapoptotic pathways (Niedner *et al.*, 2001).

The p53 status of neuroblastoma tumours is unusual because these tumours are one of a small group of early onset tumours that do not have mutations in the p53 gene, yet overexpression of p53 protein is the most universal change observed in the disease (Davidoff *et al.*, 1992; Vogan *et al.*, 1993; Castresana *et al.*, 1994; Hosoi *et al.*, 1994). The overexpressed p53 accumulates in the cytoplasm of neuroblastoma cells and it was initially thought that p53 was excluded from the nucleus (Moll *et al.*, 1995). However, more recent evidence has shown that p53 is not anchored in the cytoplasm, but continually exported from the nucleus by an MDM2-dependent

pathway (Arriola *et al.*, 1999; Smart *et al.*, 1999; Stommel *et al.*, 1999; Lu *et al.*, 2000).

1.3 Forms of cell death

1.3.1 Apoptosis

Apoptosis (derived from the Greek word meaning 'falling down of leaves') is an active, genetically programmed form of physiological cell death (Wyllie, 1994), which is essential for normal embryonic development and adult tissue homeostasis (Kaipia and Hsueh, 1997). The morphological characteristics of apoptosis differ from those of necrosis (Wyllie *et al.*, 1980).

Apoptosis characteristically affects scattered single cells, which condense and separate from their neighbours when degenerating (Wyllie, 1994). Initial events in an apoptotic cell include nuclear and cytoplasmic condensation with the development of cytoplasmic vacuoles, and pyknotic nuclei, but cell organelles remain intact (Jacobson *et al.*, 1997). DNA fragmentation occurs due to the activation of a neutral Ca^{2+}/Mg^{2+}-dependent endonuclease, which cleaves DNA into 185 bp multiples (Zeleznik *et al.*, 1989), which appear as a DNA ladder when analysed by gel electrophoresis. The apoptotic cell breaks into a number of membrane-bound, ultrastructurally well-preserved fragments known as apoptotic bodies (Wyllie, 1994) which are phagocytosed by surrounding cells or macrophages, before any leakage of cell contents occurs (**Figure 1.2a**). This prevents an inflammatory response.

1.3.2 Necrosis

Cells typically die by necrosis following physical injury or trauma (Wyllie *et al.*, 1980). For example, many necrotic cells are observed in the mammalian brain following a stroke. Necrosis is characterised by progressive loss of cytoplasmic membrane integrity, rapid influx of Na^{+}, Ca^{2+}, and water, resulting in cytoplasmic swelling and cell lysis (Wyllie, 1994; Berridge *et al.*, 2000) . DNA fragmentation in necrotic cells occurs at random so, when analysed by gel electrophoresis, the DNA appears as a smear rather than a DNA ladder (as observed in apoptotic cells). Unlike the tidy engulfment of apoptotic cells, the swelling of necrotic cells causes the lysosomal and granular contents to be released into the surrounding extracellular space initiating an inflammatory response (Scaffidi *et al.*, 2002) (**Figure 1.2b**).

Figure 1.2

(a) Morphology of apoptosis

The characteristic morphological changes associated with apoptosis include:

(i) onset of apoptosis, (ii) chromatin condensation and cellular shrinkage, (iii) nuclear fragmentation and convolution of the cell membrane to form apoptotic bodies and finally, (iv) digestion by phagocytes and/or adjacent cells (Kerr *et al.*, 1994).

(b) Morphology of necrosis

The ultrastructural changes within a necrotic cell include:

(i) Swelling and increased eosinophilia, (ii) clumping of chromatin, increased swelling and appearance of flocculent densities within mitochondria and, finally, (iii) membrane disruption prior to phagocytosis (Kerr *et al.*, 1994).

a

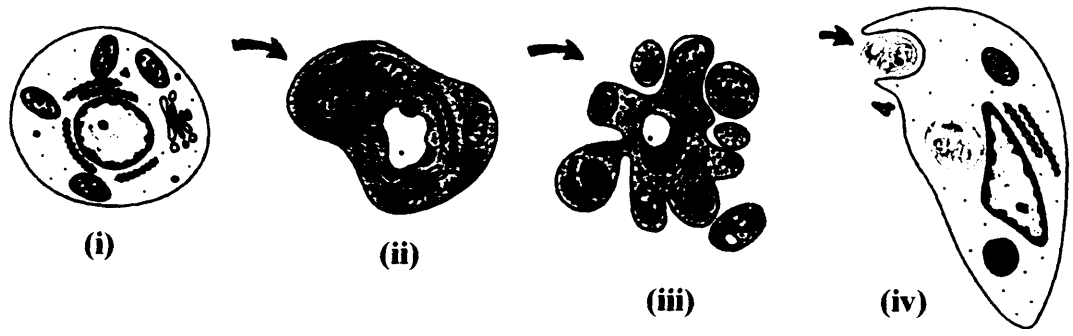

(i) (ii) (iii) (iv)

b

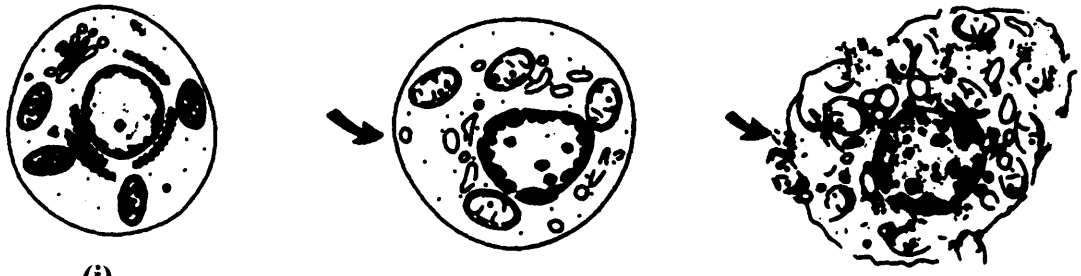

(i) (ii) (iii)

1.3.3 Role of apoptosis in development and tissue homeostasis

The neat and efficient elimination of unwanted cells in a short period of time with no accompanying inflammation makes apoptosis an ideal process in cellular replacement and tissue remodelling (Wyllie *et al.*, 1980). Apoptosis has a number of important functions during embryonic development, metamorphosis and tissue homeostasis (reviewed by Jacobson *et al.*, 1997): 1) apoptosis is used to sculpt developing tissues, e.g. the death of interdigital web cells between developing digits; 2) apoptosis is employed to eliminate structures that are no longer needed, e.g. regression of the tadpole tail when a tadpole becomes a frog; 3) apoptosis has an important role in controlling cell numbers, e.g. the number of neurons in the developing nervous system is matched to the number of target cells that they innervate, a process that is regulated by the limited availability of target-derived neurotrophic factors; 4) misplaced cells are eliminated by apoptosis because all cells are programmed to die by apoptosis in the absence of appropriate survival signals (Raff, 1992) and these signals are usually only available in the cell's normal environment; 5) harmful cells, such as lymphocytes with auto-reactive antigen receptors or cells with badly damaged DNA are eliminated by apoptosis; 6) apoptosis has a role in the response to pathogens, e.g. cytotoxic T lymphocytes kill pathogen-infected cells by inducing apoptosis.

1.3.4 Apoptosis and disease

A number of human diseases are associated with alterations in apoptosis. Unscheduled apoptosis occurs in degenerative disorders. For example, neurons are thought to die by apoptosis during neurodegenerative diseases, such as retinal degeneration, Alzheimer's disease and Parkinson's disease. However, much of the evidence for this has come from experiments with cell culture or animal models and it has been difficult to demonstrate this in patient samples (Yuan and Yankner, 2000). Similarly, autoimmune disease can result from a failure to eliminate lymphocytes that have antigen receptors that recognise self. On the other hand, inhibition of apoptosis contributes to the development of cancer.

1.4 Genetic regulation of apoptosis

1.4.1 Programmed cell death in *Caenorhabditis elegans*

Mapping of the cell lineages in *C. elegans* made this an ideal model in which to define the specific genes responsible for developmental cell fates (Sulston and Brenner, 1974; Brenner, 1974). Genetic studies of developmental cell death in the nematode worm *C. elegans* have provided much information about the core apoptotic pathway that executes cell death. The *C. elegans* hermaphrodite has 1090 somatic cells of which the same 131 cells die during development, leaving an adult nematode made up of 959 cells.

The core cell death pathway in *C. elegans,* which has been highly conserved during evolution, consists of four specific genes required for the regulation and execution of apoptosis in each of the 131 cells fated to die: *egl-1*, *ced-3*, *ced-4* and *ced-9* (reviewed by Metzstein *et al.*, 1998). Loss-of-function experiments with *egl-1*, *ced-3* or *ced-4* resulted in the survival of the 131 cells. This indicated that these genes are essential for the induction of apoptosis. However, inactivation of the *ced-9* gene caused the majority of cells to undergo programmed cell death resulting in the early demise of the nematode during development. In gain-of-function experiments with *ced-9*, the 131 cells destined to die were prevented from undergoing cell death. These experiments suggest that *ced-9* is an inhibitor of apoptosis. The CED-9 protein is homologous to mammalian Bcl-2, an antiapoptotic protein, and when Bcl-2 is expressed in *C. elegans,* it inhibits programmed cell death, indicating a conservation of function (Vaux, 1993).

Egl-1 encodes a proapoptotic protein, homologous to the BH3-only members of the Bcl-2 family, which binds the CED-9 protein at the mitochondria, displacing CED-4. This process of displacement of CED-4 from CED-9 requires the carboxy-terminal half of EGL-1 to cause structural rearrangements in CED-9 upon binding. This then results in the release of CED-4 from the CED-9/ CED-4 complex (Yan *et al.*, 2004). The *egl-1* gene promotes apoptosis by inhibiting the antiapoptotic activity of *ced-9*. The *ced-4* gene encodes an adaptor protein, which is homologous to Apaf-1 in mammals and DARK in Drosophila. When CED-4 is displaced from CED-9 at the mitochondria by EGL-1, it translocates to the perinuclear region where it undergoes oligomerisation and binds to CED-3. The *ced-3* gene encodes a cysteine protease,

homologous to the mammalian interleukin - 1β converting enzyme (ICE), a cysteine protease, which cleaves substrates after specific aspartic acid residues (a caspase).

Once, CED-3 has been activated, the execution phase of apoptosis occurs and this is followed by a process of engulfment. Seven genes have been shown to be involved in the removal of apoptotic cells (Danial and Korsmeyer, 2004). These fall into two categories: the first group of genes are involved in the recognition of apoptotic cells; the second group of genes influences cytoskeletal remodelling. Mutations in one gene from each category in double-mutant animals were required for the most dramatic engulfment defects to be seen. Genes in category one are *ced-1*, which encodes an engulfment protein, *ced-6*, which is homologous to the mammalian PTB domain-bearing adaptor GULP and *ced-7*, which encodes a protein with homology to the ABC-1 transporter and is also unique out of all the engulfment genes as it functions both in phagocytes and apoptotic cells. Category two comprises *ced-2* which is homologous to human CrkII protein, *ced-5* (DOCK180) and *ced-12* (ELMO), which all form a signalling complex in response to upstream engulfment signals and activate another member of this category, *ced-10* (Rac GTPase) to initiate rearrangement of the cytoskeleton which is necessary for the engulfment of the cell corpse (reviewed in Danial and Korsmeyer, 2004).

1.4.2 Caspases and programmed cell death

The genetic studies with *C. elegans* revealed the importance of caspases for apoptosis. Most of the visible changes that characterise apoptotic cell death depend on the activation of caspases, the central executioners of the apoptotic pathway. Caspases are a family of cysteine proteases that cleave target proteins at specific aspartate residues. They are expressed as catalytically inactive proenzymes composed of an amino-terminal pro-domain and a protease domain, which contains a large subunit and a small subunit. Active caspases are heterotetramers of two large and two small subunits. A dozen or more caspases have been identified in humans but only two-thirds of these have a role in apoptosis.

In apoptosis, caspases function as both effectors and initiators in response to proapoptotic signals. Caspases that have long pro-domains are upstream, type I, initiator caspases, such as caspase-1, -2, -4, -5, -8, -9, -10, -11 and -12. Those with short prodomains such as caspase-3, -6 and -7 are downstream, type II, effector

caspases that depend on the upstream initiator caspases for activation (Wang and Lenardo, 2000). Caspases can also be classified according to the sequence motifs in their pro-domains. Caspases with the death-effector domain (DED), which include caspase-8 and caspase-10, are activated by interacting with adaptor proteins that bind to the intracellular domains of death receptors, such as the Fas (Apo-1/ CD95) and tumour necrosis factor (TNF) receptors. Caspases with caspase-activating recruitment domains (CARDs), which includes caspases-1, -2, -4, -5, -9, -11 and -12, are most probably activated through an intracellular activating complex such as the cytochrome c /Apaf-1/ caspase-9 (apoptosome) complex. Caspases with short domains may be activated by most, if not all, caspase pathways (Hengartner, 2000).

The *ced-3* gene was found to have sequence homology with the mammalian interleukin -1β converting enzyme (ICE), which is involved in processing of proinflammatory cytokines and was the first member of the mammalian caspase family to be identified (caspase-1). However, studies of substrate specificity indicated that CED-3 was more like caspase-3 than caspase-1/ICE. Caspase-3 activation leads to the processing of its substrates, cleavage of which causes most of the morphological changes associated with apoptosis: DNA degradation, chromatin condensation and membrane blebbing.

In mammals, elimination or mutation of caspases can slow or prevent apoptosis. Studies with caspase knockout mice have been informative. For example, inactivation of the *caspase-3* or *caspase-9* genes leads to an increase in the number of neurons in the brain due to a decrease in apoptosis during neural development (Kuida *et al.*, 1996; Kuida *et al.*, 1998). Studies with *caspase-8* knockout mice indicate that caspase-8 is critical for early embryonic development, especially for the generation of heart muscle and haematopoietic progenitor cells (Wang and Lenardo, 2000).

1.4.3 Mechanisms of caspase activation

Caspases are activated by proteolytic cleavage by one of three mechanisms. Effector caspases are activated by being cleaved by upstream caspases, which is useful for the amplification and integration of proapoptotic signals. The other two mechanisms are used to activate the initiator caspases. One mechanism is known as the induced proximity mechanism, in which multiple procaspase molecules are brought into close proximity creating a high concentration of the zymogens allowing

the various proenzyme molecules to mutually cleave and activate each other. This is the mechanism by which caspase-8 is activated by death receptors, such as Fas (section 1.5.1).

The other mechanism of caspase activation is exemplified by caspase-9 and involves its association with a regulatory subunit, Apaf-1, and cytochrome c released from the mitochondria to form an "apoptosome complex". Apaf-1 transmits apoptotic signals from mitochondrial damage to activate caspases. Apaf-1 forms the apoptosome by binding to cytochrome c via its WD40 domains to be able to engage caspase-9 in the presence of ATP. This is mediated by the caspase recruitment domains (CARDs), which are present in both Apaf-1 and caspase-9. The CARD of Apaf-1 is bound by two of the WD40 domains, but is freed when cytochrome c binds to the WD40 within Apaf-1. Binding of ATP to Apaf-1, causes a conformational change forming a wheel-shaped heptamer - the apoptosome. Activated caspase-9 then cleaves and activates caspase-3 (Hengartner, 2000).

1.4.4 Caspase substrates

A large number of caspase substrates have been described. Cleavage of some of these can be related to the changes that typically occur in apoptotic cells. For example, CAD (caspase-activated DNase) cleaves nuclear DNA during apoptosis and is found in normal cells as an inactive complex with an inhibitory subunit ICAD. Caspase-3 mediated cleavage of ICAD results in the release of CAD, which can then cleave nuclear DNA.

Cleavage of another substrate, PAK2, a member of the p21-activated kinase family, leads to the blebbing characteristic of apoptotic cells (Rudel and Bokoch, 1997). Other substrates such as nuclear lamins are cleaved for nuclear shrinking and budding; fodrin and gelsolin are cytoskeletal proteins that are cleaved resulting in the loss of cell shape.

Poly (ADP-ribose) polymerase-1 (PARP-1) is a 116 kDa zinc-finger nuclear protein which is activated by DNA breaks. It has three distinct functional domains of which the DNA binding domain (DBD) located at the N-terminus contains a bipartite nuclear localisation sequence (NLS) and utilises two zinc-finger motifs that recognise either single or double stranded breaks. In response to DNA damage, PARP-1 activity is rapidly increased and it takes part in DNA-base-excision repair.

Caspases cleave PARP-1 at a DEVD site within the DBD, thus splitting the NLS and this cleavage of PARP-1 inactivates the poly (ADP-ribosylation) process. Poly (ADP-ribosylation) is a post-translational modification of proteins that, in eukaryotic cells, plays a crucial role in DNA repair and replication, transcription and cell death, and represents a cellular emergency reaction. Caspase-3 cleaves PARP-1 during apoptosis (Tewari *et al.*, 1995).

Chromatin condensation may be regulated by post-translational histone modification. Mst1 (mammalian sterile twenty-like) kinase is a 34 kDa caspase-cleaved apoptosis-induced H2B kinase. In mammalian cells, the only core histone modification that has been uniquely associated with apoptosis is histone H2B phosphorylation (Ajiro, 2000). H2B phosphorylation may be important for apoptotic chromatin condensation. Cheung *et al.*, (2003) identified an apoptosis induced 34 kDa H2B S14 kinase as the caspase-3 cleaved form of Mst1. Furthermore, H2B S14 phosphorylation is not dependent on CAD suggesting that this modification is associated with the apoptotic chromatin condensation pathway.

1.5 Caspase activation pathways

1.5.1 The extrinsic death-receptor pathway

Death effector domain-containing caspase-8 is the key initiator caspase activated by death-receptors, such as TNFR1, Fas (APO-1/ CD95) and DR4/5. These receptors depend on intracellular signalling proteins that contain the protein modules death domain (DD) and death effector domain (DED). The binding of ligands such as FasL and tumour necrosis factor (TNF) to Fas and TNFR1 respectively induces the formation of the death-induced signalling complex (DISC). The DISC contains adaptors such as FADD, which have both the DD and DED motifs, and so can bind to the DD of Fas and recruit caspase-8 via the DED motif. The activation of caspase-8 in the DISC complex proceeds via the induced proximity model mentioned previously where the high localised concentration of procaspase-8 as a result of receptor trimerisation and recruitment of FADD or other adaptors which in turn recruit multiple caspase-8 molecules which then activate each other *in trans* (**Figure 1.3**).

Type I cells, e.g. thymocytes, and type II cells, e.g. hepatocytes, differ in which of two different Fas signalling pathways are used. In both type I and II cells,

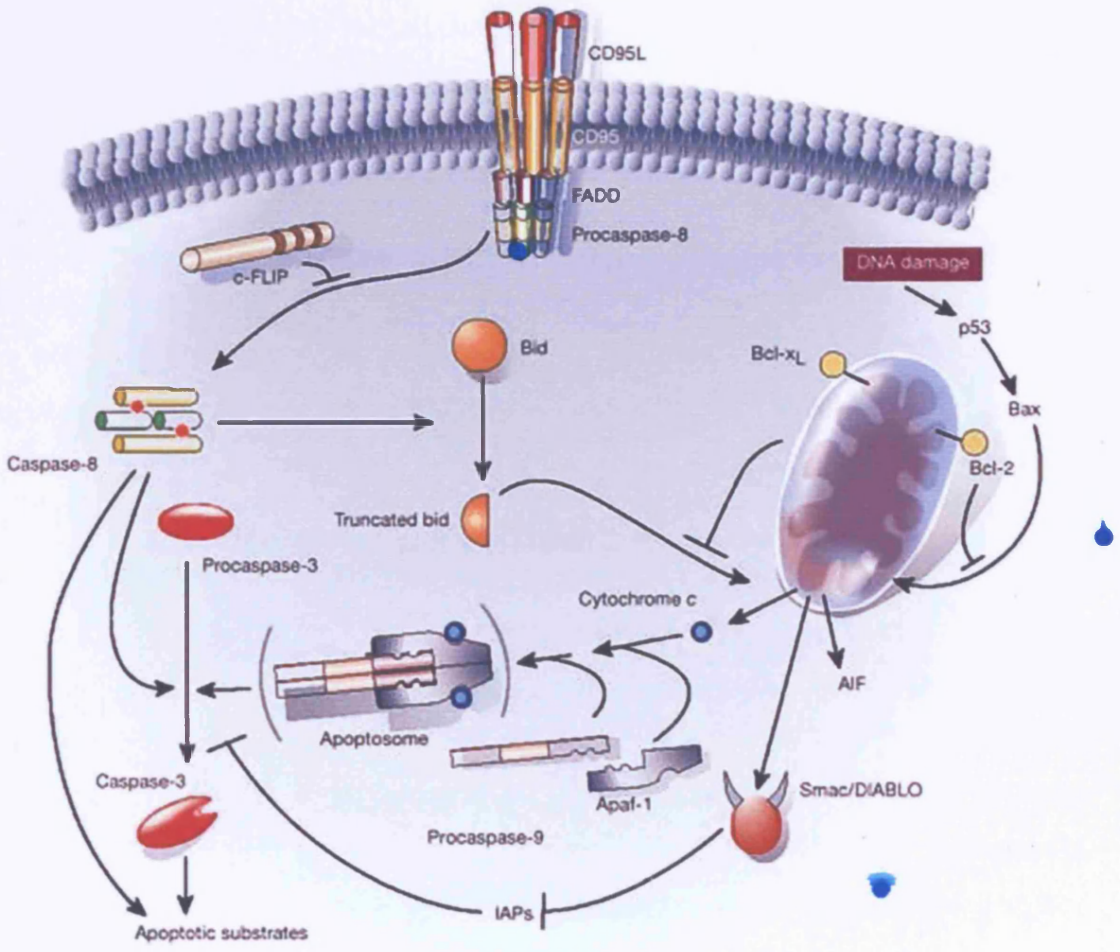

Figure 1.3 The two major apoptotic pathways in mammalian cells

The extrinsic death-receptor pathway is shown on the left-hand side of the figure and the intrinsic mitochondrial pathway is shown on the right. Both pathways converge at the mitochondria often due to the activation of a proapoptotic Bcl-2 family member. Figure taken from Hengartner, (2000).

the mitochondria are activated during Fas-induced apoptosis. In type I cells, DISC formation activates a large amount of caspase-8 leading to swift cleavage of caspase-3 prior to the loss of mitochondrial membrane potential (MMP) during apoptosis. However, in type II cells, DISC formation is considerably reduced and caspase-8 and caspase-3 activation occur subsequent to the loss of MMP. High levels of Bcl-2 overexpression block caspase-8 and caspase-3 activation, and thus apoptosis, in type II but not type I cells. This is due to the requirement for a mitochondrial amplification loop wherein Bid cleavage by caspase-8 results in truncated Bid translocating to the mitochondria, inducing mitochondrial outer membrane permeabilisation leading to cytochrome c release and the execution of apoptosis. So Fas-mediated apoptosis in type I cells is independent of mitochondrial permeabilisation whereas type II cells are dependent on the mitochondrial pathway to initiate the executioner caspase cascade.

1.5.2 The intrinsic mitochondrial pathway

The mitochondrion serves as a fundamental integrator of many apoptotic pathways (**Figure 1.3**). Many proapoptotic molecules are located in the mitochondrial intermembrane space before being released into the cytoplasm following an apoptotic signal (Hengartner, 2000). Cytochrome c is one of the most important of these as it is one of the components, together with Apaf-1, required for activation of caspase-9 in the cytosol by formation of the apoptosome complex (section 1.4.3).

Apoptosis-inducing factor (AIF), also resides in the mitochondrial intermembrane space, translocates from the mitochondria to the nucleus and causes chromatin condensation and DNA-fragmentation. AIF functions with endo G, another mitochondrial protein which translocates to the nucleus causing DNA fragmentation. Overexpression studies of AIF and endo G indicated that together they have stronger cytotoxic activity than on their own (Wang *et al.*, 2002). They also both induce apoptotic changes in the presence of caspase inhibitors suggesting that they can function independently of caspases (Susin *et al.*, 1999; Cande *et al.*, 2002).

PARP-1 activity triggers the translocation of AIF from the mitochondria to the nucleus to promote cell death through a caspase-independent pathway. The use of caspase inhibitors did not prevent PARP-1 mediated cell death, however, AIF was

found to translocate immediately after PARP-1 activation (Yu *et al.*, 2002). So, AIF released from the mitochondria can function independently of caspases. In some cells when caspase-inhibitors are used and there is a lack of Apaf-1, which is required for caspase-dependent- cell death, cells die via an AIF-dependent mechanism (Cregan *et al.*, 2002).

Smac / DIABLO and Omi/HtrA2 are also released from the mitochondria during apoptosis and are inhibitors of IAP proteins (section 1.6.2).

1.6 Regulators of caspase activity

1.6.1 Regulation by the Bcl-2 family

Members of the Bcl-2 family regulate the release of cytochrome c and other proapoptotic proteins from the mitochondria. The Bcl-2 family of proteins have a crucial role in intracellular apoptotic signal transduction. The family includes both antiapoptotic and proapoptotic proteins that contain one or more Bcl-2 homology (BH) domains. Mammalian Bcl-2, Bcl-x_L, Bcl-w, Mcl-1 and A1 all promote cell survival (**Figure 1.4**). Bax, Bak and Bok are related to Bcl-2 at BH1-3 but instead promote cell death. BH3-only proteins, such as Bad, Bik, Hrk/Dp5, Bid, Bim, Noxa and PUMA, are members of the Bcl-2 family but have only one of the Bcl-2 homology regions, BH3. These BH3-only proteins are essential initiators of apoptosis. Bcl-2 family proteins play a critical role in mammalian development (Huang and Strasser, 2000). The proapoptotic activity of BH3-only proteins is regulated by transcriptional and posttranscriptional mechanisms to prevent inappropriate cell death during development. Overexpression of Bcl-2 can promote cancer and affect sensitivity of tumour cells to chemotherapeutic drugs. Mutations in the BH3-only proteins or their regulators may therefore also be pathogenic (Huang and Strasser, 2000).

The *bcl-2* (B cell lymphoma gene-2) oncogene was the first member of the Bcl-2 family to be identified. Early studies showed that unlike other oncogenes, Bcl-2 expression did not promote cell proliferation but inhibited cell death (Vaux *et al.*, 1988) thus establishing a link between apoptosis and tumourigenesis. Bcl-2 blocked all morphological characteristics of apoptosis and was found to localise to the mitochondria (Hockenbery *et al.*, 1990).

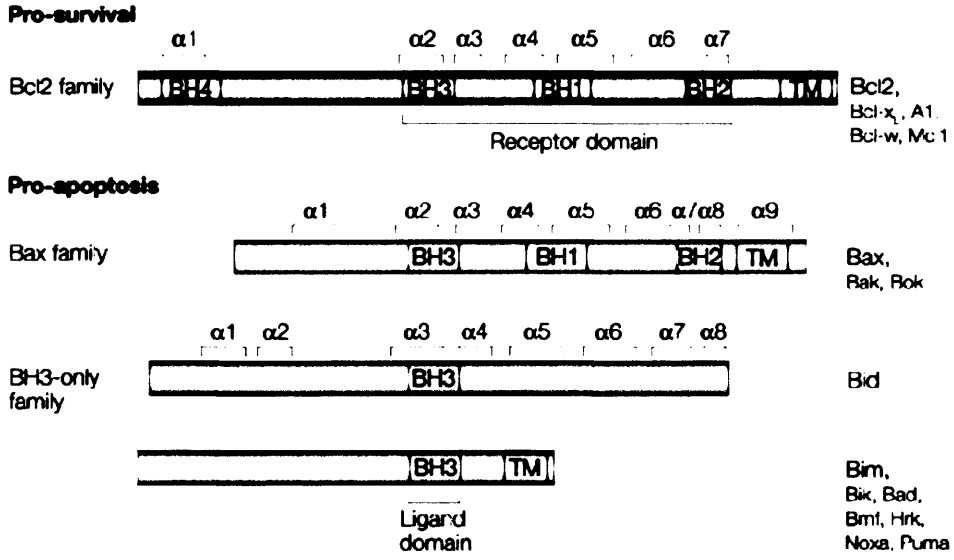

Figure 1.4 Three subfamilies of the Bcl-2 family proteins: antiapoptotic, proapoptotic and BH3-only families

In mammals, Bcl-2 has at least 20 relatives, all of which share at least one conserved Bcl-2 homology (BH) domain. The four domains (BH1-4) that are most highly conserved among the family members are shown. α1 - α9 represent α-helical regions of the proteins. TM represents the transmembrane domain that enables the proteins to insert into intracellular membranes, such as the mitochondrial outer membrane. The BH3 domain of BH3-only proteins binds to a hydrophobic region on the surface of the Bcl-2 subfamily formed from the BH1, BH2 and BH3 domains. This is analogous to a ligand-receptor interaction. Figure taken from Cory and Adams, (2002).

In *C. elegans*, the Bcl-2 homologue, CED-9 protects cells from dying by directly binding to and sequestering CED-4 (Metzstein *et al.*, 1998). This interaction is not observed in mammals. However, Bcl-2 can rescue some cells in *C. elegans* from dying when expressed in ced-9 deficient mice (Vaux *et al.*, 1992; Hengartner and Horvitz, 1994). This shows the conservation of function.

Plasmacytomas from *bcl-2* transgenic mice contained rearrangements of the c-*myc* protoncogene (McDonnell and Korsmeyer, 1991; Strasser *et al.*, 1993). *c-myc* on its own promotes abnormal cell proliferation and tumourigenesis (Adams *et al.*, 1985). Double transgenic mice (*bcl-2/c-myc*) developed undifferentiated hematopoetic leukemia (Strasser *et al.*, 1990). Loss-of-functions studies in mice showed apoptosis of lymphocytes, developmental renal cell death and loss of melanocytes indicating that Bcl-2 is required for maintaining normal cellular homeostasis (Veis *et al.*, 1993).

The *bcl-2* gene was originally identified as a transcriptional unit linked to an immunoglobulin locus by chromosomal translocation in follicular lymphoma (Vaux *et al.*, 1988) associating the activities of Bcl-2 and its homologues with cancer.

1.6.1.1 The antiapoptotic proteins

There are four other antiapoptotic homologues of Bcl-2: Bcl-x_L, Bcl-w, A1 and Mcl-1. At least one of these Bcl-2 homologues is required to protect cells from undergoing cell death. Their hydrophobic carboxy-terminal domain enables them to target the mitochondrial outer membrane (MOM), the endoplasmic reticulum (ER) and the nuclear envelope. Their BH1, 2 and 3 domains form hydrophobic pockets at their surfaces, which play an important role in their inhibitory binding to the proapoptotic proteins, in particular, the binding of the BH3 domain of BH3-only proteins **(Figure 1.5)**. Bcl-2 is always integrally inserted into the membranes in healthy cells whereas, Bcl-x_L and Bcl-w are found in a soluble, loosely attached form. Following a cytotoxic stimulus, Bcl-x_L and Bcl-w become tightly associated with the membranes (Janiak *et al.*, 1994; Hsu *et al.*, 1997; O'Reilly *et al.*, 2001; Kaufmann *et al.*, 2003).

Experiments with transgenic mice have shown that over-expression of the antiapoptotic proteins can promote tumourigenesis. Transgenic overexpression of

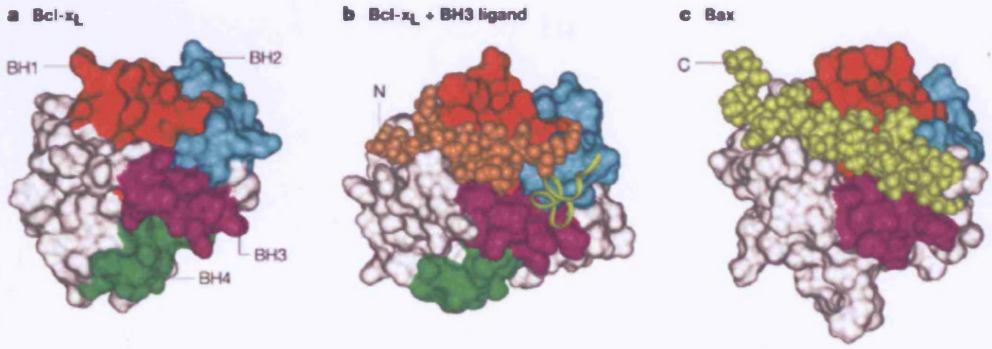

Figure 1.5 Three-dimensional structures of Bcl-x_L and Bax showing their similarity

Bcl-x_L consists of a globular bundle of five amphipathic α-helices that surround two central hydrophobic α-helices **(a)**, and a hydrophobic groove formed by residues from BH1, BH2 and BH3, can bind the BH3 α-helix (brown) of an interacting BH3-only relative **(b)**. **(c)** Bax showing its c-terminal tail (yellow) tucked into the groove. Figure taken from Cory and Adams,. (2002).

Bcl-x_L was shown to induce lymphomagenesis or development of pancreatic β-cell lymphoma. Bcl-2 is required for the survival of kidney and melanocyte stem cells and mature lymphocytes (Veis *et al.*, 1993), Bcl-x_L for neuronal and erythroid cells (Motoyama *et al.*, 1995), Bcl-w for sperm progenitors in adult mice (Print *et al.*, 1998; Ross *et al.*, 1998), A1 for neutrophils (Hamasaki *et al.*, 1998) and Mcl-1 for zygote implantation (Rinkenberger *et al.*, 2000). Mcl-1 is essential early in development and later in the maintenance of resting B and T-lymphocytes. Degradation of Mcl-1, which is needed prior to mitochondrial translocation of Bcl-x_L and Bax, initiated cytochrome c release following genotoxic damage of Hela cells (Nijhawan *et al.*, 2003).

1.6.1.2 The proapoptotic multidomain proteins

The mitochondrion was thought to play an important role in apoptosis when Bcl-2 was found to localise there during inhibition of apoptosis (Hockenberry *et al.*, 1990). The proapoptotic proteins promote the release of cytochrome c from the mitochondrion whereas the antiapoptotic proteins function to prevent this by blocking MOM permeabilisation. Initially, the proapoptotic proteins: Bax, Bak and Bok were reported to target the MOM where they function to promote apoptosis. However, they are also found to localise to the ER.

Bax was the first proapoptotic homologue to be discovered and was identified by its interaction with Bcl-2 (Oltvai *et al.*, 1993). In healthy cells, Bax is found as a soluble protein in the cytosol but it translocates to and inserts into the MOM during apoptosis (Hsu *et al.*, 1997; Wolter *et al.*, 1997). Inactive Bax is located in the cytosol or is loosely attached to membranes and its pocket is covered by its c-terminal helix (Suzuki *et al.*, 2000). When a death stimulus occurs, Bax inserts into the MOM. Bak, in its inactive state resides at the mitochondria but in response to a death stimulus, undergoes an allosteric conformational activation resulting in its oligomerisation and the permeabilisation of the MOM with release of the proteins in the intermembrane space of the mitochondria, such as cytochrome c.

Bax or Bak single knockout mice showed very few phenotypic abnormalities. In the case of *bax*$^{-/-}$ mice sympathetic and cerebellar granule neurons were protected against survival factor withdrawal-induced death (Deckwerth *et al.*, 1996). However, in the case of double knockout mice cells deficient for both Bax and Bak were

resistant to all tested intrinsic death pathway stimuli (Lindsten *et al.*, 2000; Wei *et al.*, 2001). The direct activation of Bax/Bak-like proteins by BH3-only proteins generates mitochondrial membrane disruptions and apoptogenic factors, such as cytochrome c are released (Gross *et al.*, 1999).

1.6.1.3 The BH3- only proteins

The BH3-only members function as upstream sentinels that selectively respond to developmental signals or intracellular damage (Huang and Strasser, 2000). Their functions are death stimulus-specific and cell type-restricted. Different mechanisms such as sequestering, phosphorylation, proteolytic cleavage and transcriptional activation function to control individual BH3-only proteins. BH3-only proteins are sequestered in the cytoplasm, but are suggested to function in association with the multidomain Bcl-2 family members, which are located mainly in the MOM, ER and nuclear envelope.

Gene knockout studies in mice have shown that the BH3-only proteins and Bax/Bak-like proteins are both essential for programmed cell death and stress-induced apoptosis. Bcl-2 deficiency can bring about degenerative diseases (Veis *et al.*, 1993), but all such degenerative defects can be rescued by simultaneous loss of its BH3-only antagonist Bim (Bouillet *et al.*, 2001). However, overexpression of Bcl-2 or loss of Bim can promote tumourigenesis (Vaux *et al.*, 1988; Strasser *et al.*, 1990). Bim is essential for cytokine withdrawal-induced apoptosis (Bouillet *et al.*, 1999) and essential for neuronal death (Putcha *et al.*, 2001; Whitfield *et al.*, 2001). Bmf is activated by loss of cell attachment (anoikis) (Puthalakath *et al.*, 2001) a process that is thought to safeguard against metastatic tumours. Bim and Bmf are sequestered by forming complexes with two different dynein light chains (DLC1 or DLC2 respectively) that are associated with the microtubular dynein motor complex (Bim) and actin-based myosin V motor complex (Bmf) (Puthalakath *et al.*, 1999; Puthalakath *et al.*, 2001).

In response to growth or survival factors, Bad undergoes phosphorylation by kinases such as Akt and protein kinase A which causes Bad to be bound by 14-3-3 scaffold proteins (Zha *et al.*, 1996) which then promote its sequestration in the cytosol. Mice were generated with point mutations in the *bad* gene that abolish Bad phosphorylation at specific sites. These mice displayed no clear anatomical or

developmental defects but were hypersensitive to various apoptotic stresses (Datta *et al.*, 2002). This emphasises the importance of Bad phosphorylation *in vivo*.

Bid, is essential for amplifying death receptor signalling in the extrinsic apoptotic pathway. The activation of caspase-8 is required for the proteolytic cleavage of inactive Bid in the cytosol to form truncated Bid (tBid) which can translocate and participate in the intrinsic apoptosis pathway. tBid acts as a membrane-targeted ligand which translocates to the mitochondria where its BH3 domain is required to interact and activate the oligomerisation of Bak or Bax to release cytochrome c (Desagher *et al.*, 1999; Wei *et al.*, 2001).

Like EGL-1 in *C. elegans,* Noxa, PUMA and Hrk/Dp5 are also controlled mainly at the transcriptional level. Noxa and PUMA are transcriptional targets of p53, which is activated in response to DNA damage. PUMA was initially identified as a gene activated by p53 in cells undergoing p53-induced apoptosis (Nakano and Vousden, 2001; Yu *et al.*, 2001) and as a protein interacting with Bcl-2 (Han *et al.*, 2001).

1.6.2 Regulation by the IAP proteins

The release of proapoptotic factors from the mitochondria is often considered to be the point of no return in a cell's commitment to the apoptotic programme. However, evidence indicates that occasionally cells can still be rescued at this stage. For instance, pharmacological inhibitors of caspases can often rescue cells from apoptosis, as can IAP proteins, an evolutionarily conserved protein family found in mammals, drosophila and some viruses, that encode powerful caspase inhibitors.

The characteristic structural motif of inhibitor of apoptosis proteins (IAPs) is the baculovirus IAP-repeat (BIR) of which IAPs contain between one and three of these 70 amino acid domains. IAPs can also have additional motifs such as the RING and CARD domains. Their role is to protect cells from false or accidental caspase activation. Strong anti-apoptotic activity has only been established for a subset of IAPs: XIAP (Liston *et al.*, 1997; Vitte-Mony *et al.*, 1997), cIAP1, cIAP2 (Deveraux *et al.*, 1998) and ML-IAP (Vucic *et al.*, 2000) in mammals. However, IAPs resembling mammalian survivin (Ambrosini *et al.*, 1997) are required for chromosome segregation, the NAIP gene (Roy *et al.*, 1995) appears to participate in

the innate immune response and the exact role of BRUCE is not yet established in mammals.

XIAP, an extremely potent suppressor of apoptosis, binds directly to the small (carboxyl-terminal) subunit of caspase-9 via its BIR3 domain. Inhibition of caspase-9 by the BIR3 domain of XIAP requires the cleavage of caspase-9. This would explain why caspase-9 is cleaved during caspase-9 independent apoptosis, when it is not required for its activation (Srinivasula *et al.*, 2001). XIAP binds to caspase-3 and -7 via its BIR2 domain thus preventing the normal substrates of these caspases from binding to them.

As a further safeguard mechanism, the IAPs have to be removed by additional mitochondrial proteins: Smac/DIABLO and Omi/HtrA2 which bind to and antagonise IAPs. These IAP antagonists are released from mitochondria before the executioner caspases can become fully active to produce the typical apoptotic morphology.

SMAC (secondary mitochondrial activator of caspase) /DIABLO (direct IAP-binding protein with low pI) is a mammalian IAP inhibitor which binds to IAP family members neutralising the antiapoptotic activity of IAPs. A cell will commit to apoptosis by releasing its mitochondrial contents. At this time, SMAC (in human, DIABLO in mice), a mitochondrial protein is released into the cytosol where it sequesters IAP proteins ensuring that they do not inhibit the apoptotic programme (Du *et al.*, 2000; Verhagen *et al.*, 2000).

The addition of DIABLO to extracts in which XIAP is inhibiting a caspase, causes the release of caspase activity (Du *et al.*, 2000). Overexpression of DIABLO in cells surviving by virtue of transfected XIAP causes them to undergo apoptosis (Verhagen *et al.*, 2000). Major interaction of dimeric DIABLO with IAPs occurs via its processed N-terminal four residues that bind to a groove in BIR2 and BIR3 of XIAP.

Like DIABLO, HtrA2 is targeted to the mitochondrial inter-membrane space where the targeting peptide is removed to generate a GRIM, HID, REAPER, DIABLO-like N-terminus (Hegde *et al.*, 2002).

IAPs are considered to be 'the brakes' of the caspase cascade during the execution phase of apoptosis. In *Drosophila*, cells are not preloaded with sufficient levels of IAP-inhibited processed caspases to achieve cell killing. This has led to a 'gas and brake ' model, whereby simultaneous input from Dark, together with removal of IAP inhibition, drives caspase activation to levels that exceed a threshold necessary for apoptosis (Rodriguez *et al.*, 2002).

1.7 Survival signalling pathways and apoptosis

All normal cells require survival signals to survive and die by apoptosis in their absence (Raff, 1992). The activation of cell survival signals that block apoptosis is associated with tumourigenesis and resistance to chemotherapeutic drugs. A number of signalling pathways that protect cells from apoptosis appear to block mitochondrial cytochrome c release, which is regulated in an antagonistic manner by pro- and antiapoptotic members of the Bcl-2 protein family (reviewed by Gross *et al.*, 1999). Also, trophic factors such as NGF, insulin-like growth factor I, or BDNF activate a variety of signalling pathways, including the phosphotidylinositol-3-OH kinase (PI3K)-Akt and Ras-mitogen-activated protein kinase (MAPK) pathways (Hunter, 2000).

1.7.1 The PI3K-Akt pathway

The PI3K-Akt pathway regulates the Forkhead box, class O (FOXO) subfamily of Forkhead transcription factors, FKHR (FOXO1), FKHRL1 (FOXO3a) and AFX (FOXO4). In 1999, three groups (Biggs *et al.*, 1999; Brunet *et al.*, 1999; Kops *et al.*, 1999), provided evidence that in mammalian cells, Akt directly phosphorylates the FOXOs causing the relocalisation of these transcription factors from the nucleus to the cytoplasm. In the absence of survival factors, Akt activity is reduced, FOXO factors became dephosphorylated and relocalise to the nucleus and activate gene transcription. So the relocalisation of the FOXOs from the nucleus to cytoplasm, when AKT is activated in the presence of survival factors leads to the FOXOs being taken away from their target genes, which are consequently not induced (Biggs *et al.*, 1999; Brunet *et al.*, 1999; Kops *et al.*, 1999). The gene encoding FasL is one target of FOXO factors, as its promoter contains several FOXO binding sites. FOXO-induced apoptosis is diminished when FasL signalling is blocked (Brunet *et al.*, 1999). Another target is the gene encoding Bim, a proapoptotic BH3-only protein induced in neurons following NGF withdrawal (Whitfield *et al.*, 2001). The Bim protein contains two FOXO binding sites and FOXO-induced apoptosis in neurons is blocked when Bim expression is inhibited by antisense oligonucleotides (Gilley *et al.*, 2003).

As well as its effects on transcription, the PI3K-Akt pathway also directly regulates the apoptotic machinery. Akt has been proposed to act both prior to the

release of cytochrome c, by regulating the activity of Bcl-2 family members and thereby mitochondrial function, and then after the release of cytochrome c, by regulating components of the apoptosome. Previously it was shown that Akt can phosphorylate procaspase-9 suggesting a mechanism for regulation of caspases by protein phosphorylation (Cardone *et al.*, 1998). However, the Akt phosphorylation sites in procaspase-9 are not conserved across species.

The absence of survival factors leads to Bad forming a complex with the antiapoptotic Bcl-2 family member, Bcl-x_L, thus inhibiting Bcl-x_L from promoting cell survival. In the presence of survival factors, when Akt is activated, it phosphorylates Bad, thereby inhibiting the proapoptotic functions of Bad (Datta *et al.*, 1997; del Peso *et al.*, 1997).

Bad phosphorylation occurs at a specific amino acid residue, serine 136, which creates a binding motif for the chaperone molecule 14-3-3. The binding of Bad to 14-3-3 allows survival factors to bring about a second phosphorylation event at serine 155, which is necessary to promote the complete release of Bad from Bcl-x_L. The phosphorylation of serine 155, which is located within the BH3 domain of Bad, interferes with the interaction of Bad with Bcl-x_L, which then promotes cell survival by inhibiting the release of cytochrome c (Datta *et al.*, 2000).

1.7.2 The Ras-Raf-MEK-ERK pathway

The MAP kinase family includes at least three major kinase cascades that control cellular responses to a wide variety of signals, including growth factors: the JNK, p38 and ERK MAPK pathways. ERK1/2 are serine-threonine protein kinases. The activation of the Ras-Raf-MEK-ERK mitogen-activated protein kinase (MAPK) pathway is associated with protection of cells from apoptosis and the inhibition of caspase-3 activation (Erhardt *et al.*, 1999; Le Gall *et al.*, 2000; von Gise *et al.*, 2001), despite release of cytochrome c from mitochondria (Erhardt *et al.*, 1999; Tashker *et al.*, 2002).

Recently, a group investigating the potential of signalling pathways to regulate caspase activation at the post-translational level, showed that the ERK MAPK pathway inhibits caspase-9 activity by direct phosphorylation (Allan *et al.*, 2003). They showed using okadaic acid (OA), an inhibitor of protein phosphatases PP-1 and PP-2, that protein phosphatase activity was required for cytochrome c-induced activation of caspase-9 and subsequent activation of caspase-3. The phosphorylation

site on caspase-9 was found to be Thr 125, which is followed by a proline residue, a characteristic of sites phosphorylated by proline-directed kinases such as ERK. Thr 125 is the main phosphorylation site for ERK2 but an additional minor phosphorylation site was also identified as Thr 107, which is followed by a proline residue as well. So the ERK2-mediated phosphorylation of Thr 125 on caspase-9 is sufficient to inhibit the processing of caspase-9 associated with its enzymatic activation and is an important mechanism by which ERK2 inhibits caspase-3 activation. It may also be an important mechanism through which growth factor and survival signals that activate the ERK MAPK pathway can inhibit apoptosis.

This regulation of caspase-9 by ERK may play a role in the developmental control of cell death and suppression of apoptosis in tumourigenesis. Cancer cells, which often have a constitutively activated ERK MAPK pathway, will need to be examined to establish the extent of caspase-9-Thr 125 phosphorylation and whether this affects the cytotoxic response to chemotherapeutic drugs.

As well as phosphorylating procaspase-9, the ERK1/2 pathway functions independently of the PI3-K pathway to inhibit the expression of the BH3-only protein Bim_{EL} in order to prevent apoptosis due to serum withdrawal (Weston *et al.*, 2003). The activation of the ERK1/2 pathway is required for Bim_{EL} to undergo phosphorylation making it a target for ubiquitination and degradation by the proteasome pathway (Ley *et al.*, 2003). Following serum withdrawal, the rapid expression of Bim_{EL} occurs by the inactivation of the ERK 1/2 pathway which dephosphorylates and stabilises pre-existing and newly synthesised Bim_{EL}, together with an increase in *bim* mRNA due to JNK activation (Whitfield *et al.*, 2001) or loss of PI3K (Dijkers *et al.*, 2000) or ERK1/2 activity (Weston *et al.*, 2003), depending on the cell type.

1.8 Aims of this thesis

Currently used highly intensive chemotherapy regimens are better than previous methods but are ineffective in more than half of children with advanced neuroblastoma. There are different types of neuroblastoma: a third of these have MYCN amplification and this correlates with advanced disease. Approximately 10% of neuroblastoma patients show primary resistance to chemotherapy. Therefore, the development of new approaches to treatment is essential. The aim of this thesis is to

identify the signalling pathway by which CDDP, a chemotherapeutic agent that is used for treating neuroblastoma tumours triggers caspase activity and apoptosis in a representative human, SH-SY5Y neuroblastoma cell line.

The SH-SY5Y neuroblastoma cell line, is the third successive sub-clone of the parental neuroblastoma cell line, SK-N-SH, isolated from a bone marrow biopsy of a neuroblastoma patient. This cell line has no *MYCN* amplification. SH-SY5Y cells proliferate in serum containing medium. All *trans*-retinoic acid (RA) induces *trkB* expression in cultured human SH-SY5Y neuroblastoma cells (Kaplan *et al.*, 1993; Matsumoto *et al.*, 1995). The receptors are functional and mediate BDNF-induced morphologic differentiation. Under serum-free growth conditions, the RA-BDNF-treated cells appear to differentiate into neuron-like cells (Encinas *et al.*, 2000).

It has previously been shown that CDDP treatment induces apoptosis in SH-SY5Y cells (Cece *et al.*, 1995). Further understanding of the cellular responses to CDDP is critical for determining mechanisms of drug resistance and for allowing the development of therapeutic approaches for increasing the effectiveness of CDDP treatment or for developing new approaches.

Chapter 2: Materials and Methods

2.1 Materials

2.1.1 Chemicals and equipment

List of suppliers

Affymetrix	Human genome U133A microarrays
Amersham Biosciences	ECL western blotting detection reagents, ECL Plus western blotting detection reagents, Hybond-C extra nitrocellulose membrane, MOPS
ATCC	SH-SY5Y human neuroblastoma cells
BDH Laboratory services	Glycine (molecular biology grade), sodium chloride, sodium hydroxide pellets, Tris, methanol, isopropanol, chloroform, coverglass (13 mm diameter),
Beckton Dickinson	Bacto tryptone, Bacto agar
Bio-Rad	Prestained Kaleidoscope marker, Mini Protean II electrophoresis system, minitransblot electrophoretic transfer cell, Bio-Rad protein assay, TEMED
Calbiochem	Bisbenzamide H33342 fluorochrome, trihydrochloride (Hoechst dye)
Citifluor Ltd	Citifluor glycerol / PBS solution AF1
Difco	Yeast extract
Gibco	Sterile phosphate buffered saline (PBS) (for cell culture), Dulbecco's modified Eagle's medium (DMEM), Penicillin/streptomycin (100X), L-glutamine (100X), MEM (100X) non-essential amino acids, OptiMEM
Globepharm	Foetal calf serum
Hayman Ltd	Absolute ethanol
Insight Biotech	Z-Val-Ala-Asp (Ome) -FMK (ZVAD-fmk), X-gal

Invitrogen	Lipofectamine 2000, TRIzol®, DH5α™ competent cells, 1 kb DNA Ladder, agarose
Marvel	Non-fat dried milk
Molecular Probes	Live/Dead® Viability/Cytotoxicity assay kit
National Diagnostics	Protogel acrylamide solution, 10 X TBE
New England Biolabs	T4 DNA ligase, T4 DNA ligase buffer, T4 polynucleotide kinase (PNK), 10 X kinase buffer
Oxoid	PBS tablets
Promega	Restriction enzymes, pGEM®-T Easy vector system
Qiagen	QIAprep spin miniprep kit, HiSpeed plasmid maxiprep kit, QIAquick gel extraction kit
Roche	In Situ Cell Death Detection Kit, Fluorescein, GC-rich PCR System
Sarstedt	Rohre 13 ml 95 X 16.8mm polypropylene centrifuge tubes
Sigma	Cis-platinum(II)-diammine dichloride, Trans-platinum(II)-diammine dichloride, dithiothreitol, dimethyl sulphoxide, formaldehyde, formamide, goat serum, protease inhibitor cocktail, Tween-20, trypsin-EDTA, PBS (-Ca^{2+}/Mg^{2+}) (for cell staining), Ponceau S, ampicillin, kanamycin, sodium dodecyl sulphate, actinomycin D, Triton X-100, gelatin, bovine serum albumin, Red Taq, cyclohexamide
Techne	Touchgene gradient PCR machine
Whatman Scientific	3 mm paper
Zeiss	Axiovert S100 inverted fluorescence microscope, Axioplan 2 fluorescence microscope

2.1.2 Antibodies

ANTIBODY	SUPPLIER	Cat / Clone No.	Type
BAD (H-168)	Santa Cruz	SC-7869	Rabbit polyclonal
BAK NT	Upstate Biotech.	06-536	Rabbit polyclonal
BAX NT	Upstate Biotech.	06-499	Rabbit polyclonal
BCL-2	Santa Cruz	SC-4096	Rabbit polyclonal
BCL-W	Chemicon Int.	MAB17002	Rat monoclonal
BCL-X (S-18)	Santa Cruz	SC-634	Rabbit polyclonal
BID (N-19)	Santa Cruz	SC-6539	Goat polyclonal
BIK/NBK (FL-160)	Santa Cruz	SC-10770	Rabbit polyclonal
BIM	Chemicon	AB17003	Rabbit polyclonal
BMF	Alexis Biochemicals	210-831-R100	Mouse monoclonal
CASPASE-3	Upstate Biotech.	06-735	Rabbit polyclonal
CASPASE-8Ab-3	Oncogene	AM46	Mouse monoclonal
CASPASE-9	Upstate Biotech.	#05-572, CLONE 96-2-22	Mouse monoclonal
CYTOCHROME C	Pharmingen	556432 CLONE 6H2.B4	Mouse monoclonal
ERK	Cell Signaling Tech.	#9102	Rabbit polyclonal
FLAG M2	Sigma	A9469	Mouse monoclonal
HRK	G.Nunez (University of Michigan)		Rabbit polyclonal
MCL-1 (S-19)	Santa Cruz	SC-819	Rabbit polyclonal
NOXA	Eri Oda (University of Tokyo)		Rabbit polyclonal
P21 (C-19)	Santa Cruz	SC-397	Rabbit polyclonal
P53 (FL-393)-G	Santa Cruz	SC-6243	Goat polyclonal
P53 (Ab-1)	Oncogene Research Products	Clone Pab421	Mouse monoclonal
PUMA	Abcam	AB9643	Rabbit polyclonal
ALPHA-TUBULIN	SEROTEC	MCAP77	Rat monoclonal

Table 2.1 Antibodies used for immunoblotting and immunocytochemistry

SECONDARY ANTIBODY	SUPPLIER	Cat / Clone No.
GOAT IgG HRP	Santa Cruz	SC-2020
MOUSE Ig HRP	Amersham	NA931V
RABBIT Ig HRP	Amersham	NA934V
GOAT ANTI-RAT IgG HRP	Santa Cruz	SC-2032

Table 2.2 Secondary antibodies used for immunoblotting and immunocytochemistry

2.1.3 Bacterial strains

DH5α competent cells – F^- ϕ80*lac*ZΔM15 Δ(*lac*ZYA-*arg*F)U169 *rec*A1 *end*A1 *hsd*R17(r_k^-, m_k^+) *pho*A *sup*E44 *thi*-1 *gyr*A96 *rel*A1 λ^-

2.1.4 Plasmids

pEGFP-N1 - Clonetech

pcDNA1 – Invitrogen

pCMVneoBam, pCMVneoBam-FLAG-PUMA-α, pCMVneoBam-FLAG-ΔLRR-PUMA-α provided by K.Vousden, CRUK (Nakano and Vousden, 2001).

2.1.5 Stock Solutions

All solutions were prepared in MilliQ deionised water unless specified otherwise.

LB medium	1% w/v bacto-tryptone, 0.5% w/v yeast extract, 17 mM NaCl
LB-agar	LB medium containing 1.5% w/v bacto agar
Ampicillin	100 mg/ml in water

Kanamycin	100 mg/ml in water
Chloramphenicol	34 mg/ml in ethanol
Immunoblot transfer buffer	25 mM Tris base, 192 mM Glycine, 20% v/v methanol
SDS electrophoresis buffer (5X)	0.125 M Tris base, 0.96 M Glycine, pH 8.3, 0.5% SDS
TBS-T	20 mM Tris-Cl, pH 8.0, 500 mM NaCl, 0.1% v/v Tween-20
6 X SDS sample buffer	1M Tris-Cl, pH 6.8, 10% w/v SDS 30% v/v Glycerol, 0.6 M DTT, 1.2 mg/ml bromophenol blue, make up to 10 ml with water, aliquots at -70°C.
SDS lysis buffer	10 mM Tris-Cl, pH 7.6, 150 mM NaCl, 0.5 mM EDTA, 1 mM EGTA, 1% w/v SDS, 2% v/v protease inhibitor cocktail (added just before use)
4 X Tris-Cl/SDS pH 6.8	0.5 M Tris base, 0.4% w/v SDS

4 X Tris-Cl/SDS pH 8.8	1.5 M Tris base, 0.4% w/v SDS
4% paraformaldehyde	0.1 mM $CaCl_2$, 0.1 mM $MgCl_2$, 4% paraformaldehyde, pH 7.4
SH-SY5Y cell medium	10% FCS, 1% penicillin/streptomycin (100X), 1% glutamine (100X), 1% MEM (100X) non-essential amino acids, in Dulbecco's modified Eagle's medium
Immunoblot Stripping solution	100 mM 2-β-mercaptoethanol, 2% w/v SDS, 62.5 mM Tris-Cl, pH 6.7
TE buffer	10 mM Tris-Cl, pH 8.0 1 mM EDTA
TNE buffer	0.1 M NaCl 10 mM Tris-Cl, pH 8.0 1 mM EDTA
Buffer P1 (resuspension buffer)	50 mM Tris-Cl, pH 8.0 10 mM EDTA, 100 μg/ml RNase A
Buffer P2 (lysis buffer)	200 mM NaOH 1% w/v SDS
Buffer P3	3 M potassium acetate,

(neutralisation buffer)	pH 5.5
Buffer N3 (miniprep)	contains guanidine hydrochloride Acetic acid
Buffer PB (miniprep and QIAquick)	contains guanidine hydrochloride Isopropanol
QBT (equilibration buffer)	750 mM NaCl 50 mM MOPS, pH 7.0 15% isopropanol (v/v) 0.15% Triton® X-100 (v/v)
QC (wash buffer)	1 M NaCl 50 mM MOPS, pH 7.0 15% isopropanol (v/v)
QF (elution buffer)	1.25 M NaCl 50 mM Tris-Cl, pH 8.5 15% isopropanol (v/v)
Buffer EB	10 mM Tris-Cl, pH 8.5
Buffer PN (QIAquick)	sodium perchlorate Isopropanol
Buffer QG (QIAquick)	guanidine thiocyanate

2.2 Methods

2.2.1 Cell culture

SH-SY5Y human neuroblastoma cells were obtained from the ATCC and were cultured in DMEM (-glu-pyruvate) containing L-glucose at 4.5 g/L supplemented with 10% FCS (PAA; later changed to Globepharm), 2 mM glutamine, penicillin / streptomycin and non-essential amino acids. The cells were maintained in T25 or T75 flasks at 37°C in 5% CO_2 and passaged when 80-100% confluent, usually once a week. Cells recovered from liquid nitrogen were passaged at least twice before being used for experiments. Medium in the flasks was changed every four days. Cells were used for up to 9 passages.

2.2.2 Treatment of SH-SY5Y cells with chemical compounds

2.2.2.1 CDDP and TDDP

The platinum compounds were weighed out carefully in a fume hood (because of their toxicity) and dissolved in DMSO. The dissolved compounds were mixed into the medium of SH-SY5Y cells grown on 3.5 cm or 9 cm tissue culture dishes or on 1.3 cm diameter glass coverslips placed in 3.5 cm dishes and left to incubate at 37°C in 5% CO_2 for the required amount of time.

2.2.2.2 Other compounds

Actinomycin D (Act D) was dissolved in DMSO before being use to pre-treat the cells. Cyclohexamide (CHX) was diluted to the working concentration in 50% ethanol. Z-Val-Ala-Asp (OMe)-FMK (ZVAD-fmk) was dissolved in anhydrous DMSO to make up the stock and working concentrations. In the case of Act D, CHX and ZVAD-fmk, the SH-SY5Y cells were pre-treated for an hour at 37°C in 5% CO_2 with the compound, prior to treatment with CDDP or TDDP.

2.2.3 Live - Dead cell viability / cytotoxicity assay

The Live-Dead cell viability / cytotoxicity assay kit from Molecular Probes was used according to the manufacturer's instructions. The two stains used in this assay are calcein AM, and ethidium homodimer-1. Calcein AM is converted by viable cells to calcein, which fluoresces green. Ethidium homodimer-1 is excluded by viable cells but taken up by apoptotic cells, which have lost membrane integrity

allowing the dye to bind to chromosomal DNA resulting in the apoptotic cells having red nuclei.

SH-SY5Y cells were plated at a density of 1 X 10^5 cells in 2 ml of medium per 3.5 cm tissue culture dish and grown at 37°C in 5% CO_2 until 80-100% confluent. The medium was changed every four days and the final change of medium was added just before the cells were treated with the compounds under investigation.

A 10 X stock solution of calcein AM and ethidium homodimer in 0.8 ml of pre-warmed DMEM was prepared and 0.22 ml of this 10 X working solution was added to the cells in 2 ml of medium. Following incubation for 30 minutes at 37°C in 5% CO_2, the cells were counted on a Zeiss Axiovert S100 inverted fluorescence microscope on 40X magnification. The total number of live and dead cells was determined in 10 fields around the circumference of each dish.

% of viable cells = [N° of live cells / (N° of live cells + N° of dead cells)] X 100

2.2.4 TUNEL analysis

In order to detect which cells are committed to death, the TdT-mediated dUTP-nick end labelling (TUNEL) technique was used (Gavrieli *et al.*, 1992). The process of apoptotic cell death results in DNA fragmentation and 3'OH-ends are generated, to which TdT catalyses template-independent addition of labelled deoxyuridine triphosphate (dUTPs). Labelling can be observed by fluorescence microscopy. Since necrotic and autolytic cells, along with apoptotic cells, generate a sufficiently high number of stainable DNA ends (Grasl-Kraupp *et al.*, 1995), technique cannot differentiate between apoptosis and necrosis in cells (Grasl-Kraupp *et al.*, 1995; Thomas *et al.*, 1995). The use of Hoechst dye (bisbenzimide H33342 fluorochrome trihydrochloride) to stain nuclear DNA enables the morphology of the nuclei to be clearly observed.

2.2.4.1 Coverslip sterilisation

Glass coverslips were incubated for two hours in 2N NaOH in a fume hood following vigorous tapping to release trapped air bubbles between the coverslips. The coverslips were washed extensively in tissue culture quality water prior to being stored in sterile 70% ethanol. Each coverslip was allowed to dry inside a class II tissue culture hood prior to use.

2.2.4.2 Cell preparation

Cells were plated onto 1.3 cm coverslips placed in 3.5 cm tissue culture dishes. 4 X 10^4 cells in 100 µl of medium were plated onto each coverslip. The cells were allowed to attach to the coverslips by incubating for 2 hours at 37°C in 5% CO_2 before each dish was filled with 2 ml of medium. Medium was changed every four days. The final change of medium was added when the cells were 80-100% confluent and were ready to be treated with the compounds under investigation.

2.2.5 *In Situ* 3' -end DNA labelling

The quantity of each solution used in this assay was 100 µl and the coverslips were washed in PBS three times unless otherwise stated. Using a pair of forceps, culture medium was drained from the coverslips before they underwent three washes in PBS. Once the PBS had been drained away, the cells on each coverslip were fixed in 100 µl of 4% paraformaldehyde. Following incubation for 30 minutes at room temperature and washing in PBS, the cells were permeabilised in 0.5% Triton X-100 in PBS for 5 minutes at room temperature.

After washing in PBS, 50 µl of the TUNEL reaction mixture was added to each coverslip and these were incubated at 37°C for 1 hour in a dark humidified chamber. The TUNEL reaction mixture was prepared with reagents supplied in the *In Situ* cell death detection kit supplied by Roche. The TUNEL reaction mixture was prepared immediately before use by adding 50 µl of enzyme solution (10 X TdT in storage buffer) to 450 µl of label solution (nucleotide mixture in reaction buffer). The components of the TUNEL reaction mixture were mixed carefully and stored on ice until used.

After the TUNEL reaction, the coverslips were washed in PBS before the cells were treated with Hoechst dye (10 µg/ml in water) for 5 minutes at room temperature in the dark. Following two washes in water, the coverslips were allowed to dry prior to mounting onto glass slides using Citifluor AF1 mounting solution. The edges of the coverslips were sealed with nail varnish. The glass slides were left for 30 minutes in the dark to dry before being examined on a Zeiss Axioplan 2 fluorescence microscope. Images were captured using a Photometrix Quantix digital camera and SmartCapture VP software. The files were exported as JPEG files for analysis in Adobe Photoshop 5.5.

The Hoechst dye stains the nuclei blue. The nuclei with DNA fragmentation are stained green due to the incorporation of fluorescein-labelled dUTP. The slides were stored in the dark at 4°C.

2.2.6 Cytochrome c relocalisation assay

Cells undergoing apoptosis via the mitochondrial pathway release cytochrome c, which is required for caspase activation and thus DNA fragmentation and chromatin condensation. The release of cytochrome c from the mitochondria into the cytosol, can be visualised by performing immunocytochemistry with an anti-cytochrome c antibody (Neame *et al.*, 1998).

2.2.6.1 Cell preparation and treatment

Cells were grown on coverslips as described in section 2.2.4.2. The quantity of each solution used in this assay was 100 µl per coverslip. The coverslips were washed in PBS three times unless otherwise stated. Using a pair of forceps, culture medium was drained from the coverslips before they underwent three washes in PBS. Once the PBS had been drained away, the cells on each coverslip were fixed in 100 µl of 4% paraformaldehyde. Following incubation for 20 minutes at room temperature, the coverslips were washed in two changes of 10 mM glycine in PBS, after which the cells were incubated in 100 µl of blocking / permeabilisation solution (50% goat serum, 0.5% Triton X-100, 0.2% gelatin, 0.5% BSA, 0.5 X PBS) for 30 minutes at room temperature. The blocking / permeabilisation solution was then drained off, and anti-cytochrome c monoclonal antibody diluted 1:100 in blocking/ permeabilisation solution was added to each coverslip and incubated for 2 hours at room temperature. The coverslips were washed in PBS, and fluorescein-conjugated anti-mouse IgG secondary antibody, diluted 1:100 in blocking/permeabilisation solution, was added. Following incubation with the secondary antibody for one hour at room temperature in the dark, the coverslips were washed three times in PBS before the cells were treated with Hoechst dye (10 µg/ml) for 5 minutes at room temperature in the dark. Following two washes in water, the coverslips were allowed to dry prior to mounting onto glass slides in Citifluor mounting solution. The glass slides were left for 30 minutes in the dark to dry before being examined on a Zeiss Axioplan 2 fluorescence microscope. Images were captured using a Photometrix Quantix digital camera and

SmartCapture VP software. The files were exported as JPEG files for analysis in Adobe Photoshop 5.5.

The Hoechst dye stains the nuclei blue. The cytochrome c specific immunostaining will be green due to the binding of the anti-cytochrome c primary antibody and fluorescein-conjugated secondary antibody. The slides were stored in the dark at 4°C.

2.2.7 Protein analysis

2.2.7.1 Cell preparation

Cells (6.5 X 10^5) were plated in 10 ml of medium per 9 cm tissue culture dish and grown at 37°C in 5% CO_2 until 80-100% confluent. The medium was changed every four days and the final change of medium was added just before the cells were treated with the compounds under investigation prior to protein extraction.

2.2.7.2 Protein extraction

The dishes containing the SH-SY5Y cells for protein extraction were placed on ice. The growth medium from the dishes (containing detached, apoptotic cells) was removed and transferred to centrifuge tubes, which were also kept on ice. The attached cells were harvested by scraping them off the dish in a small volume of ice cold PBS. The adherent and floating cells were pooled in one tube and pelleted by centrifugation at 738 x g for 5 minutes at 4°C. The pellet was resuspended in 1 ml of ice cold PBS and transferred to a microfuge tube to be spun for 5 minutes at 4°C at 16,100 x g. The cell pellet was resuspended in 50-200 µl of SDS lysis buffer containing 2% v/v of a protease inhibitor cocktail (Sigma). The cell lysate was heated at 90°C for 20 minutes and then pipetted up and down to assist the disruption of the cells. Following centrifugation of the lysate for 20 minutes at 4°C at 16,100 x g, the supernatant was aliquoted into fresh tubes and snap-frozen in dry ice before being stored at -80°C.

2.2.7.3 Protein assay

Various concentrations of the standard, γ-globulin, and 2 µl of each protein sample were diluted in 800 µl of water. Bio-Rad protein assay dye (200 µl) was then added and the samples were mixed well and incubated at room temperature for 10

minutes. The absorbance at 595 nm was then measured using a spectrophotometer and protein concentration was calculated by drawing a graph using Cricket Graph software.

2.2.7.4 SDS-polyacrylamide gel electrophoresis of proteins

Protein extracts were mixed with SDS sample buffer and heated at 100°C for 10 minutes before being separated on 10%, 12% or 15% SDS-polyacrylamide gels using a Bio-Rad mini Protean II electrophoresis system. Protein extract (15 μg) was loaded into each lane of the gel. After SDS-PAGE, the proteins were transferred onto Hybond-ECL nitrocellulose using a Bio-Rad minitransblot electrophoretic transfer cell. Success of the transfer was determined by staining the nitrocellulose with ponceau S for 5 minutes. Ponceau S was washed off with water and the stained nitrocellulose was photographed using a camera on a UV-doc gel imaging system.

2.2.7.5 Immunoblotting

The nitrocellulose membrane was blocked in 5% non-fat dried milk in 1 X TBS-T for one hour at room temperature and probed overnight with the primary antibody (**Table 2.1**). Antibody dilutions were according to the manufacturer's instructions. Following three washes for 15 minutes each in 1 X TBS-T, the nitrocellulose was incubated for 2 hours at room temperature with a horseradish peroxidase-conjugated secondary antibody (**Table 2.2**). After washing three times for 15 minutes each in 1 X TBS-T the proteins were detected by using enhanced chemiluminescence (ECL) reagents.

2.2.8 DNA Manipulations

2.2.8.1 Bacterial transformation

E.coli DH5α competent cells (50 μl) were thawed on ice and then mixed with 0.5 ng of plasmid DNA. The mixture was incubated on ice for 30 minutes and then heat shocked at 37°C for 20 seconds to stimulate DNA uptake. Following a further 2 minutes on ice, 400 μl of LB medium was added to the cells and incubated at 37°C for one hour to allow the transformed cells to recover. Using aseptic technique, 50-300 μl of the transformation mix was plated out onto LB agar plates containing 100

μg/ml of ampicillin or 50 μg/ml of kanamycin (as appropriate) to select for antibiotic resistant transformants. The plates were then incubated overnight at 37°C.

2.2.8.2 Small-scale plasmid preparation (miniprep)

Small-scale purification of plasmid DNA was performed using the QIAprep spin miniprep protocol (Qiagen). This protocol is designed for purification of up to 20 μg of high-copy plasmid DNA from 1–5 ml overnight cultures of *E.coli* in LB medium. Overnight cultures were prepared by inoculating single colonies into 3 ml of LB medium containing 100 μg/ml of ampicillin and then shaking overnight at 37°C. All the following steps were performed at room temperature.

Glycerol stocks were made by mixing 0.5 ml of the overnight culture with 0.5 ml of 50% glycerol and storing at -70°C. The remainder of the overnight culture was harvested in a 1.5 ml tube by centrifugation at 16,100 x g for 10 minutes in a microcentrifuge. The supernatant was discarded and the pellet was resuspended vigorously in 250 μl of the cell resuspension solution, buffer P1 until no cell clumps were observed and then 250 μl of cell lysis solution, buffer P2 was added. The solutions were mixed by gently inverting the tubes until the solution appeared clear indicating complete cell lysis. After 5 minutes, 350 μl of ice-cold neutralisation solution, buffer N3 was added to neutralise the reaction. The solutions were mixed thoroughly by gentle inversion. Following centrifugation for 10 minutes at 16,100 x g, the supernatant was transferred into the QIAprep spin column held within a 2 ml collection tube. The spin column was centrifuged at 16,100 x g for 30 – 60 seconds and the flow-through discarded. The spin column was washed by the addition of 0.75 ml of buffer PE and centrifuged for 30 – 60 seconds. The flow-through was discarded and the column was centrifuged for a further 1 minute to remove any residual wash buffer. The spin column was transferred to a new tube and 50 μl of buffer EB was added to the column and left for 1 minute, after which the plasmid DNA was eluted by centrifugation at 16,100 x g for 1 minute.

Approximately 4 μl of the DNA was digested with restriction enzymes to determine the structure of the plasmid. The rest of the plasmid DNA preparation was stored at -20°C.

2.2.8.3 Large-scale plasmid preparation (maxiprep)

Large-scale preparation of plasmid DNA was carried out using the HiSpeed plasmid maxi kit (Qiagen) and 400 ml of overnight culture inoculated with 500 µl of a 5 ml overnight starter culture of bacteria in LB medium containing the appropriate selective antibiotic.

Using aseptic technique, a single colony was used to inoculate 5 ml of LB containing the appropriate selective antibiotic and shaken vigorously for approximately 8 hours at 37°C. An aliquot of this culture was used to inoculate 400 ml of LB in a 2 litre flask containing the appropriate selective antibiotic. The cultures were grown overnight at 37°C in an orbital shaker at approximately 225 rpm.

In the case of some plasmids, such as pcDNA1, the yield was improved by chloramphenicol amplification. Cultures (400 ml) were grown to an OD_{600}=1.5 and chloramphenicol was added to 170 µg/ml. The culture was then incubated for 12 - 16 hours at 37°C.

The overnight culture was harvested by centrifugation at 6000 x g for 15 minutes at 4°C. The resulting pellet was resuspended in 10 ml of cell resuspension solution, buffer P1 (Tris-EDTA containing RNase A at 4°C). To help resuspension, the pellet was manually disrupted by pipetting up and down until clumps were no longer visible. The solution was then transferred to a 50 ml tube to which 10 ml of cell lysis solution, buffer P2 was added and the solutions were mixed by gently inverting the tube. After 5 minutes, 10 ml of ice-cold neutralisation solution, buffer N3 was added to the lysate and mixed immediately. The lysate was transferred into the QIAfilter cartridge (which completely removes SDS precipitates and clears bacterial lysates) and left to incubate for 10 minutes at room temperature to allow the precipitate to float so that filtration would be easy. The cell lysate was filtered into a HiSpeed Maxi Tip, which had been equilibrated with 10 ml of buffer QBT.

Once the cell lysate had entered the resin by gravity flow, the tip was washed with 60 ml of buffer QC. The DNA was eluted with 15 ml of buffer QF and precipitated by incubating for 5 minutes at room temperature with 10.5 ml (0.7 volumes) of isopropanol.

The eluate-isopropanol mixture was passed through a QIAprecipitator maxi module that traps the precipitated DNA while the isopropanol–buffer mixture flows through. This allows the DNA to be washed by passing 2 ml of 70% ethanol through

the module. The DNA was then eluted from the QIAprecipitator into a tube with 0.5 – 1 ml of TE buffer or water. An aliquot of the DNA (5 µl) was used in a 1:100 dilution to determine DNA concentration by measuring absorbance at 260 and 280 nm using a spectrophotometer. Pure DNA has an A_{260} / A_{280} ratio of 1.7-1.9.

2.2.8.4 Restriction endonuclease digestion

The restriction enzyme (10U/µl) was added to a 1.5 ml tube containing 1 µg of the plasmid DNA diluted with distilled water and one-tenth of the total reaction volume of restriction enzyme buffer. After gentle mixing, the reaction was incubated at 37°C for 2 hours and then stopped by placing in ice for 5 minutes.

2.2.8.5 Agarose gel electrophoresis of DNA

This procedure was used to analyse the size and conformation of nucleic acids in samples, to quantify DNA and to separate and extract DNA fragments. Restriction enzyme-digested DNA was analysed by running against the uncut plasmid DNA and a 1 kb DNA ladder, as a size standard, on a 1.5% agarose gel (made with 1 X TBE and 0.5 µg/ml ethidium bromide) with loading dye at 80V. DNA was observed using a UV transilluminator and then photographed. The sizes of the bands observed were calculated by comparing them to the known DNA fragment lengths of the standard.

For gel extraction, the appropriate DNA fragments were excised from the gel and DNA extracted using the QIAQuick gel extraction kit (Qiagen). The manufacturer's protocol was followed and the DNA was eluted in 30 µl of buffer EB (elution buffer). DNA was stored at -20°C.

2.2.8.6 Cloning of PCR products

For the cloning of PCR products, the pGEM®-T Easy vector system was used since these linearised vectors have single 3'-T overhangs at the insertion site. This significantly improves the efficiency of ligation of a PCR product into the plasmid by preventing recircularisation of the vector and providing compatible overhangs for PCR products. The vector also contains T7 and SP6 RNA polymerase promoters flanking the multiple cloning region within the α-peptide coding region of the enzyme β-galactosidase. Thus the presence of inserts can be detected using the blue-white colony screening.

Ligation reactions were set up on ice using 50 ng of the pGEM®-T Easy vector in a 10 µl reaction with 1µl of T4 DNA ligase, 1 µl of 10 X T4 DNA ligase buffer and the PCR product made up the remainder of the volume. The reaction was incubated at 4°C overnight.

DH5α cells were allowed to thaw on ice and then 50 µl of these competent cells was added to 2 µl of the ligation reaction and mixed gently. The mix was incubated on ice for 20 minutes, heat shocked for 45 - 50 seconds at 42°C and allowed to cool for 2 minutes on ice. Next, 950 µl of LB was added to the transformed cells, which were incubated for 90 minutes at 37°C in a water bath. Each transformation culture was plated (100 µl) onto duplicate LB/ampicillin/IPTG/X-Gal plates and incubated overnight at 37°C. White colonies were selected for minipreps.

2.2.8.7 DNA sequencing

Each DNA sequencing reaction was prepared in a 200 µl PCR tube. Approximately 400 ng of double stranded DNA was added to 6 µl of BigDye Terminator and 2.4-3.2 ρmoles of T7 primer and the total volume of the reaction was made up to 15 µl with PCR-grade water. Control reactions were also prepared using 2 µl of pGEM-DNA supplied with the BigDye Terminator kit, 4 µl of M13 primer (also supplied) and 6 µl of the BigDye Terminator and made up to 15 µl with PCR-grade water. Cycle sequencing of double stranded DNA was carried out using a Techne Touchgene thermal cycler according to the manufacturer's instructions.

The 15 µl reaction mixture was transferred to a 1.5 ml tube and 50 µl of absolute ethanol and 3 µl of 3M sodium acetate, pH 4.6, were added and mixed well. The DNA was left at -20°C for 30 - 45 minutes to precipitate. Following centrifugation at 16,100 x g for 45 minutes at 4 °C, the supernatant was discarded and the pellet was washed twice with 70% ethanol, first with 200 µl of 70% ethanol and then with 50 µl of ethanol. Each wash was centrifuged at 16,100 x g at room temperature for 20 minutes, and the supernatant was discarded. After the last wash step, the pellet was dried in a DNA concentrator for 1 - 2 minutes until dry. If necessary, the dried pellet was stored at -20°C until sequenced. The sequencing was carried out on an ABI 377 DNA Sequencer and the resulting DNA sequences were analysed using MacVector software.

2.2.8.8 Transient transfection

Cells for transfection followed by immunofluorescence were grown on coverslips at a cell density of 8 X 10^5 per coverslip in 200 µl of SH-SY5Y medium. Coverslips were sterilised and dried as described in section 2.2.4.1, then each coverslip was placed in a well of a 24-well plate. After the 200 µl of cell suspension had been pipetted onto each coverslip, the 24-well plate was placed in a 37°C CO_2 incubator for 2 hours to allow cells to attach to the coverslip, after which 300 µl of SH-SY5Y medium was added to each coverslip making the total volume of plating medium 500 µl. If the next day, the cells were approximately 90-95% confluent, they were ready to be transfected. The total concentration of DNA used for transfecting each coverslip was 0.8 µg in 50 µl.

For PUMA-α overexpression experiments, the cells were co-transfected with a GFP expression vector to assess transfection efficiency. The other expression vectors were pCMVneoBam, pCMVneoBam-FLAG-PUMA-α, pCMVneoBam-FLAG-ΔLRR-PUMA-α (provided by K.Vousden, CRUK; Nakano and Vousden, 2001). Cells were transfected at a 1:3 ratio of GFP: PUMA expression vector. Therefore 0.2 µg of GFP expression vector and 0.6 µg of DNA were mixed with 50 µl of OptiMEM. For each coverslip, 2 µl of Lipofectamine 2000 was mixed in 50 µl of OptiMEM and left to incubate for 5 minutes at room temperature. The diluted DNA was then added and left at room temperature for 30 minutes to allow the DNA-Lipofectamine 2000 complexes to form. During this incubation period, the SH-SY5Y medium covering the cells to be transfected was removed and the cells were washed with basic DMEM. Following aspiration of the DMEM, 400 µl of SH-SY5Y medium without antibiotics was added. DNA-Lipofectamine mixture (100 µl) was then added to the cells. The plate was rocked gently and then incubated at 37°C for 5 hours after which the transfection medium was aspirated and complete SH-SY5Y medium was added. In experiments to block caspase activity, ZVAD-fmk was added to the SH-SY5Y medium at a concentration of 100 µM after the transfection medium had been aspirated.

At 16 hours after transfection, the cells were viewed on a Zeiss Axiovert S100 inverted fluorescence microscope using 40X magnification. The number of green

GFP-expressing transfected cells was counted in ten fields of view along the coverslip. Cells were then prepared for immunofluorescence (section 2.2.8.10).

2.2.8.9 siRNA

A pSUPER construct that expresses siRNA against human PUMA was designed using the human PUMA-α mRNA sequence (AF354654). Potential 19-nucleotide siRNAs were identified using Oligoengine software, out of which three sequences were selected: 437, 452 and 518. Sequence 518 relates to the sequence reported in Gu *et al.*, 2003. Three pairs of 60-nucleotide oligos were designed using the selected sequences and incorporating BglII and HindIII restriction enzyme sites according to the Oligoengine design protocol (**Figure 2.1**). Oligos were made by Sigma Genosys and were dissolved in TE to a concentration of 1 μg/μl.

Phosphorylation of 0.5 μg of each oligo pair (forward and reverse) was performed using 10 X kinase buffer, 10 mM ATP and T4 polynucleotide kinase (PNK) made up to a total volume of 20 μl with water and incubated for one hour at 37°C. The reaction contained a concentration of 50 ng of double stranded (ds) DNA per μl. The kinased ds DNA (100 ng) was annealed by mixing with 98 μl of TNE buffer to make a total volume of 100 μl and incubated in a 65°C water bath for 30 minutes. The mixture was then allowed to cool slowly to room temperature in a container of water.

pSUPER was linearised by digestion with BglII and HindIII restriction enzymes simultaneously. The linearised vector was then dephosphorylated using calf intestinal alkaline phosphatase (CIP), 10 X CIP buffer and incubated for 30 minutes at 37°C. Next, EGTA was added a final concentration of 20 mM and the reaction was incubated for 10 minutes at 65°C. The linearised vector was run on a 0.8% agarose gel to separate it from any undigested plasmid and the fragment between the BglII and HindIII sites. The CIP-treated pSUPER band was excised and purified using the QIAquick gel extraction kit and eluted in 30 μl of buffer EB.

The CIP-treated pSUPER vector and the phosphorylated oligos were ligated as described in section 2.2.8.6 but the ligation reaction was carried out at 16°C overnight. DH5α cells were transformed with the ligation reaction and plated onto LB agar plates containing 100 μg/ml of ampicillin and left to incubate overnight. Colonies were selected for inoculation of 5 ml overnight cultures for minipreps. The

plasmid DNA was checked for the presence of the oligos by digesting with EcoRI and HindIII. As a control, pSUPER was digested with the same restriction enzymes. The digested DNA was run on a 2% agarose gel and plasmids containing the oligos were identified and some of these were sequenced. Four siPUMA constructs with the correct sequences were selected: 437.1, 452.1, 452.2 and 518.6. Glycerol stocks of the correct siPUMA sequences were used to make overnight cultures for large scale plasmid preparation.

SH-SY5Y cells were co-transfected with FLAG-PUMA-α and siPUMA constructs for 16 hours with 50 μM ZVAD-fmk (to reduce PUMA-induced cell death). Cells for co-transfection followed by protein extraction were plated in 6 cm dishes at a cell density of 8 X 10^6 in 4 ml of medium to be approximately 90-95% confluent the next day for transfection. A total concentration of up to 8 μg of DNA is ideal for transfections. For the siRNA and PUMA-α co-transfections, 6 μg of total DNA was used in 500 μl of OptiMEM and 20 μl of Lipofectamine 2000 was used in 500 μl of OptiMEM. The pBluescript vector was used to make up the volume of total DNA transfected to 6 μg. The transfection protocol in section 2.2.8.8 was followed. Protein extraction and immunoblotting was performed at 16 hours after transfection.

Figure 2.1 siPUMA sequences (a) 437, **(b)** 452 and **(c)** 518

2.2.8.10 Immunofluorescence

Cells grown on coverslips were fixed with 4% paraformaldehyde for 30 minutes at room temperature. The paraformaldehyde was removed by washing the coverslips three times with PBS. The cells were then permeabilised using 0.5% Triton X-100 in PBS for 5 minutes at room temperature. Cells were washed three times in PBS before blocking with 50% goat serum in 1% BSA in PBS for 30 minutes at room temperature. Cells were washed three times in PBS prior to a one hour incubation at room temperature with the M2 monoclonal antibody diluted 1:200 in 1% BSA in PBS. The primary antibody was washed off with PBS and a Rhodamine-conjugated anti-mouse antibody diluted 1:100 in 1% BSA in PBS was added and left to incubate for one hour at room temperature in the dark. Following three washes with PBS, the cells were stained with 10 μg/ml of Hoechst dye in water for 5 –10 minutes at room temperature in the dark. The cells were washed twice in water before mounting on to glass slides using Citifluor mounting solution. The coverslips were fixed to the slides with clear nail varnish. The glass slides were left for 30 minutes in the dark to dry before being examined on a Zeiss Axioplan 2 fluorescence microscope. Images were captured using a Photometrix Quantix digital camera and SmartCapture VP software. The files were exported as JPEG files for analysis in Adobe Photoshop 5.5.

2.2.9 RT-PCR

Sterile technique was used when working with RNA to minimise RNase contamination. Any isolated RNA was kept on ice. RNase-free water was used throughout the following procedures.

2.2.9.1 RNA Extraction

SH-SY5Y cells were grown and prepared for RNA extraction as described in section 2.2.4.7. The medium from the dishes was transferred into 50 ml tubes kept on ice and then centrifuged for 5 minutes at 738 x g to retain a pellet of the detached cells. Approximately 7 ml of TRIzol reagent, a monophasic solution of phenol and guanidine isothiocyanate was added to the attached cells in the dishes. A cell scraper was used to detach cells and these were transferred to the 50 ml tube containing the

pellet. The tube was vortexed to completely resuspend the pellet. At this stage the extraction procedure could be paused by storing the cell suspension in TRIzol at – 70°C. The samples were transferred to autoclaved 13 ml Sarstedt polypropylene centrifuge tubes to which 1.4 ml (20% of the volume of TRIzol used) of chloroform was added and mixed by vortexing. The solution was incubated at room temperature for 2-3 minutes and then centrifuged for 15 minutes at 4°C at 4,700 x g to separate the solution into aqueous and organic phases. The RNA containing aqueous upper phase was transferred into fresh centrifuge tubes and mixed with 10 μg of glycogen as carrier. Isopropanol (50% of the volume of TRIzol used) was added to the solution, mixed and left at room temperature for 10 minutes before centrifugation for 10 minutes at 4°C at 5365 x g to precipitate the RNA. The RNA pellet was washed with 75% ethanol and dried in a dessicator to remove all traces of ethanol. The pellet was resuspended in 50 μl of water and incubated at 42°C for 10 minutes to facilitate solution of the RNA.

The 50 μl RNA was treated with DNase I by adding 10X DNase I buffer (7 μl), 10 μl of DNase I, water to 70 μl and incubating for 15 minutes at 37°C. An equal volume of phenol was added to the reaction and the tube was vortexed and centrifuged for 3 minutes at 16,100 x g. The upper phase was extracted and the phenol step was repeated with the remaining phenol phase. After the second extraction, an equal volume of TE (pH 8) was added and the tube vortexed. Following centrifugation for 4 minutes at 16,100 x g, the upper phase was transferred to a new 1.5 ml tube and the lower phase underwent repetition of the TE step until all of the RNA was recovered. To the total volume of recovered RNA, an equal volume of chloroform was added. The solution was vortexed and centrifuged at 16,100 x g for 4 minutes. The RNA was precipitated by adding 10 μg of glycogen as carrier, 1/10 of the total RNA volume of 3M sodium acetate pH 5.2 and 2.5 volumes of 100% ethanol. The tube was vortexed and left to incubate for one hour at -20°C. Following a 15 minute centrifugation at 16,100 x g at 4°C, the recovered pellet was washed in 100 μl of 70% ethanol by vortexing, and centrifuged at 16,100 x g for 5 minutes at 4°C. The pellet was vacuum-dried and resuspended in 50 μl of water. The purified RNA was stored at -20°C or -70°C in water.

2.2.9.2 Quantitative and qualitative analysis of RNA

RNA concentration was determined by measuring the absorbance at 260 nm (A_{260}) in a spectrophotometer using a quartz cuvette. A solution of RNA whose A_{260} = 1 contains 40 µg of RNA per ml.

RNA integrity was assessed by denaturing gel electrophoresis and ethidium bromide staining. Gel electrophoresis equipment was soaked in 3% hydrogen peroxide in MilliQ water for 10 minutes. A formaldehyde agarose gel was prepared by boiling 0.48 g of agarose, 28 ml of DEPC-treated water and 8 ml of 5 X MOPS and then cooling the solution until the container could be touched. Under a fume hood, 4 ml of formaldehyde was mixed into the cooled agarose and the 1.2% agarose gel mixture was poured into the gel tank and allowed to set.

The sample mix was prepared for loading using 0.8 µl of 5 X MOPS, 1.4 µl of formaldehyde, 4 µl of formamide, 1 µl of 0.5 µg/µl ethidium bromide and 100 ng - 1 µg of RNA in a 1.5 ml tube. The sample mix was heated for 5 minutes at 65°C and placed on ice immediately afterwards. The contents were collected by briefly spinning the tube. The sample mix was mixed with 1 µl of loading dye and the samples loaded onto the gel. The gel was run at 70 V in 1 X MOPS running buffer and viewed using a transilluminator.

In undegraded RNA preparations, the 28S ribosomal RNA band should appear twice as intense as the 18S ribosomal RNA band. If the RNA is degraded, this would appear as a smear of smaller sized RNAs or the 28S and 18S ribosomal RNA bands will show equal intensities.

2.2.9.3 cDNA Synthesis

Superscript™ II RNase H$^-$ reverse transcriptase (Invitrogen) was used for first strand cDNA synthesis for RT-PCR. In a 1.5 ml tube, a mixture of 500 µg/ml of oligo $(dT)_{12\text{-}18}$, 350 ng of total RNA and 1 µl of 10 mM dNTP mix made up to 12 µl with water was heated at 65°C for 5 minutes. The reaction mix was chilled quickly on ice and the contents collected at the bottom of the 1.5 ml tube by brief centrifugation. Next, 4 µl of 5 X First-Strand buffer and 2 µl of 0.1 M DTT were added, mixed and incubated at 42°C for 2 minutes. To this reaction, 1 µl of Superscript™ II RT was gently mixed in and the mixture was incubated for 50 minutes at 42°C. The reaction was inactivated by heating at 70°C for 15 minutes.

2.2.9.4 Primer Design

The PUMA primers used for RT-PCR were 5'-TGTAGAGGAGACAGGAATCCACGG-3' from exon 1 and 5'-AGGCACCTAATTGGGCTCCATCTC-3' from exon 4 as described in Nakano and Vousden, 2001. The GAPDH primer sequences (from Gabriella Pagnan) were 5'-ACCACAGTCCATGCCATCAC-3' for the forward primer and 5'-TCCACCACCCTGTTGCTGTA-3' for the reverse primer. Primers were made by Sigma Genosys.

2.2.9.5 PCR product analysis

PUMA amplification was difficult due to a high GC content in the transcript so the GC-rich PCR system (Roche) was used to overcome this problem. The GC-rich PCR system contains a blend of thermostable *Taq* DNA polymerase and *Tgo* DNA polymerase a thermostable enzyme with a proofreading (3'-5' -exonuclease) activity. The GC-rich PCR reaction buffer in combination with the separately included GC-rich resolution solution allows efficient amplification of GC-rich targets. Titration of the GC-rich resolution solution indicated that its optimal concentration for amplification of PUMA transcripts was 0.5M. Standard conditions for the other PCR components were used according to the GC-rich PCR system protocol.

During optimisation of the PCR, multiple unspecific products were generated often to the exclusion or low amplification of the desired PUMA products. The PCR reaction was optimised using an approach similar to 'touchdown' PCR (Don *et al.*, 1991) to favour the amplification of the desired products and not artifacts or primer dimers. The programme designed involved multiple cycles where the annealing segments in sequential cycles ran at incrementally lower temperatures. The annealing temperature is generally set approximately 5°C below the T_m. The estimated T_m for the primers corresponding to PUMA exon 1 and PUMA exon 4 were 69.3°C and 70.8°C respectively. The T_m was taken to be the average of the two, i.e. 70°C. So the annealing-segment temperature, which was initially set equal to the T_m, gradually declined and fell below 60°C. This strategy was used in the hope that the first primer-template hybridisation to occur involves only those reactants with the greatest specificity to PUMA thus amplifying the specific PUMA targets. Even though the annealing temperature eventually drops to the T_m of non-specific hybridisations, the

specific targets would have already begun amplification and thus will be in a position to compete out any non-specific PCR products during remaining cycles.

The PCR programme used for the amplification of PUMA transcripts commenced using a preheated lid at 110°C and initial denaturing occurred at 96°C for 5 minutes. Then a series of five cycle sequences were programmed starting with denaturing at 96°C for 30 seconds, annealing at 70°C for 30 seconds and extension at 72°C for 4 minutes. Every following set of five cycle sequences had the same denaturing and extension conditions but the annealing temperature was dropped by 2°C until the temperature reached 60°C when 25-30 cycles (depending on template) were performed. Final extension was carried out at 72°C for 5 minutes and the reaction was cooled to 10°C.

Following optimisation of conditions, the PCR for GAPDH amplification was performed using Red Taq (Sigma) at an annealing temperature of 58°C for 15 – 20 cycles.

PCR reactions (10 µl) were run on a 1.5% agarose gel alongside the 1 kb DNA ladder until each of the amplified products was clearly separated. To identify each PCR product the DNA bands were excised from the gel and the DNA was extracted using the QIAquick gel extraction kit according to manufacturer's instructions. The PCR products were ligated as described in section 2.2.8.6 followed by minipreps to isolate the DNA for restriction enzyme digestion to determine the presence of PUMA transcripts. The restriction enzymes used were EcoR1 (to release the PCR product inserts), Nco1 (which specifically cuts PUMA-α), SacII (specific for PUMA-α and -β) and RsaI (specific for PUMA-δ). PCR products with correct restriction enzyme digest results were selected for sequencing. The sequences were put through the NCBI Blast search to confirm the presence and identity of the PUMA transcripts.

2.2.10 Microarray analysis

Cells were grown and prepared as described in section 2.2.7.1. When 90% confluent, the dishes were treated with DMSO, CDDP and TDDP for 12 hours before RNA was extracted as described in section 2.2.9.1. RNA prepared for microarray analysis was not treated with DNase I and glycogen was not used as a carrier. Biotin-labelled cRNA was prepared from the total RNA using T7-$(dT)_{24}$ primer using Superscript Choice system (Gibco), BioArray™ HighYield™ RNA transcript

labelling kit (ENZO) and purified using Qiagen RNeasy columns. The purified labelled cRNA was fragmented and hybridised to the Human Genome U133A Array (Affymetrix, UK), which contains 22,215 human gene cDNA probes. Three independent experiments were performed to assess array reproducibility. The procedure of processing total RNA for Affymetrix GeneChip® Hybridisation was performed by Danielle Fletcher as described in the Affymetrix GeneChip® Expression Analysis Manual (Affymetrix, UK).

The arrays were analysed using GeneSpring 5 software.

Chapter 3: Characterisation of CDDP treated SH-SY5Y neuroblastoma cells

3.1 Introduction

It has been previously shown that CDDP treatment induces apoptosis in SH-SY5Y cells (Cece *et al.*, 1995). We wished to confirm this and further define the apoptotic process by analysing the biochemical changes that occur during CDDP-induced apoptosis. Although all cells contain the cell death machinery, in some situations activation of the cell death programme requires macromolecular synthesis, e.g. when sympathetic neurons are deprived of nerve growth factor, genes are induced that encode proteins that stimulate mitochondrial cytochrome c release and caspase activation (Putcha *et al.*, 2001; Whitfield *et al.*, 2001). Most of the visible changes that characterise apoptotic cell death depend on the activation of caspases, the central executioners of the apoptotic pathway. Caspase activation was studied by immunoblotting. Two major death pathways, the extrinsic and intrinsic pathways, can mediate the response to cytotoxic agents, and both rely on the ultimate activation of caspases. Approximately 70% of neuroblastoma cell lines do not express caspase-8 and are defective in the extrinsic pathway. The gene for caspase-8 is silenced or deleted and complete inactivation occurs in neuroblastoma cells with *MYCN* amplification (Teitz *et al.*, 2000). SH-SY5Y cells have no *MYCN* amplification.

To analyse the requirement for caspase activity in CDDP–induced apoptosis in SH-SY5Y cells I used the pan-caspase-inhibitor, ZVAD-fmk. The mitochondrion serves as a fundamental integrator of many apoptotic pathways. Many pro-apoptotic molecules are located in the mitochondrial intermembrane space before being released into the cytoplasm following an apoptotic signal (Hengartner, 2000). Cytochrome c is one of the most important of these because it is one of the components (with the apoptotic protease-activating factor 1, Apaf-1) required for activation of caspase-9 in the cytosol. Activated caspase-9 in turn cleaves and activates caspase-3 (Hengartner, 2000). I studied cytochrome c release by immunofluorescence using an anti-cytochrome c antibody (Neame *et al.*, 1998).

Like other DNA damaging agents, CDDP triggers several cellular responses, including the activation of the p53 pathway and the induction of DNA

damage-inducible genes, such as *gadd153, gadd45, p21*, and *c-jun* (Wetzel and Berberich, 2001).

The p53 tumour suppressor is a transcriptional regulatory protein whose target genes include: *p21, MDM2, Gadd45, Bax, Noxa* and *PUMA* (Keshelava *et al.*, 2001; Hickman *et al.*, 2002). Products of these genes are critical for cell cycle regulation, apoptosis and DNA repair. Mutations of p53 are found in approximately 50% of all human tumours (Keshelava *et al.*, 2001; Hickman *et al.*, 2002) but are seen in only 2% of human neuroblastoma tumours examined (Vogan *et al.*, 1993). p53 protein has been found to be abundant in human neuroblastoma cell lines (Davidoff *et al.*, 1992; Vogan *et al.*, 1993). It is possible that instead of mutations, cytoplasmic sequestration and defective translocation of p53 could be alternate mechanisms involved but previous studies have shown that p53 function is intact in neuroblastoma cell lines (Keshelava *et al.*, 2001). Cells possessing wild type p53 protein respond to exposure to DNA-damaging agents by elevating p53 protein levels (Wetzel and Berberich, 2001). Depending on the cell type and the type of DNA damage, increased p53 protein triggers either growth arrest or apoptosis (El Deiry, 1998; Gottlieb and Oren, 1998). Involvement of p53 in CDDP-induced apoptosis has been demonstrated in several cell types (Park *et al.*, 2001). To measure p53 protein levels in CDDP and TDDP treated SH-SY5Y cells, I performed immunoblotting experiments with a p53-specific antibody.

3.2 Results

3.2.1 Effects of cisplatinum and transplatinum on SH-SY5Y cells

SH-SY5Y cells adhere to tissue culture dishes and grow in clusters with multiple short, neuritic processes (**Figure 3.1a**). To determine the effect of cisplatinum and transplatinum on cell morphology, SH-SY5Y cells were plated in 3.5 cm dishes and treated with CDDP or TDDP (each at 30 μg/ml) for 24 hours. The morphology of the cells did not alter when they were treated with DMSO, the solvent used to dissolve the platinum compounds, (**Figure 3.1a**), or with TDDP (**Figure 3.1c**). However, cells treated with CDDP were found to round up and detach from the base of the dish and had a morphology characteristic of cells undergoing apoptosis (**Figure 3.1b**).

3.2.2 Dose-response and time-course of CDDP-induced death

To compare the effect of CDDP and its isomer TDDP on SH-SY5Y cells at different concentrations, a dose-response assay was performed. SH-SY5Y cells were grown until 80-100% confluent in 3.5 cm tissue culture dishes and treated with CDDP at 1, 3, 6, 10 and 30 μg/ml or TDDP at 3, 10 and 30 μg/ml for 24 hours. Cell viability was then determined using the Live-Dead cell viability/cytoxicity assay (**Figure 3.2a**). After 24 hours of platinum treatment, CDDP at 10 μg/ml had killed approximately 45% of the SH-SY5Y cells and at 30 μg/ml 67% of the cells had been killed. At higher concentrations of CDDP, the majority of cells detach from the dish and float around making it difficult to determine viability using the Live-Dead assay. On the other hand, the percentage of viable cells remained constant with increasing concentrations of TDDP. This indicates that TDDP, the isomer of CDDP is not cytotoxic. To determine the kinetics of CDDP-induced death, time course experiments were performed. Cells were treated with DMSO or CDDP at 10 μg/ml for various lengths of time up to 48 hours. The Live-Dead cell viability assay was performed on the cells at 0, 8, 16, 24 and 48 hours after treatment with DMSO or CDDP. The results are shown in **Figure 3.2b**. In this time-course experiment, 50% of the cells had died after 16 hours of CDDP treatment whereas the cells treated with DMSO remained viable throughout the 48 hour time-course.

Figure 3.1 Morphology of platinum-treated SH-SY5Y cells

SH-SY5Y cells were grown on 3.5 cm dishes until 80-100% confluent. The cells were then treated with (**a**) DMSO, (**b**) CDDP (30 μg/ml) and (**c**) TDDP (30 μg/ml) for 24 hours. The cells were examined on a Nikon TMS-F microscope using 20X magnification and photographed using a Nikon camera and FP4 black and white film. The images shown are representative of the cell morphologies observed in several independent experiments.

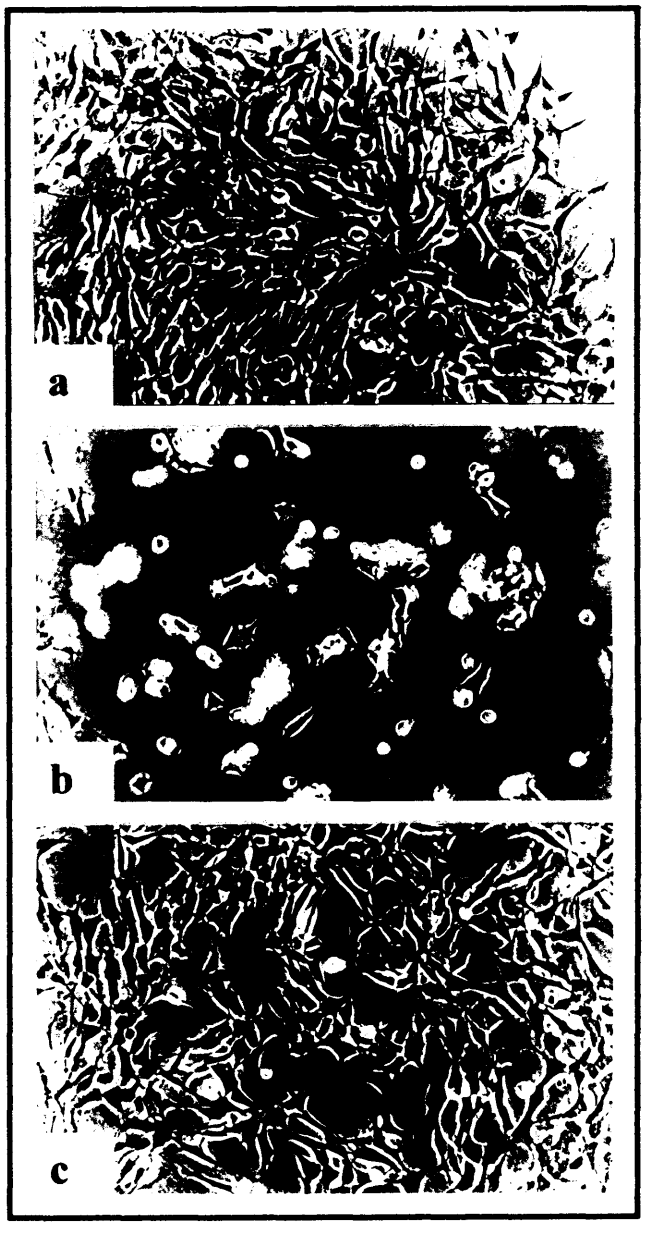
a
b
c

Figure 3.2 Dose-response and time-course of CDDP - induced death

SH-SY5Y cells were grown until 80-100% confluent in 3.5 cm tissue culture dishes and (**a**) treated with CDDP at 1, 3, 6, 10 and 30 μg/ml or TDDP at 3, 10 and 30 μg/ml for 24 hours and (**b**) cells were treated with DMSO or CDDP at 10 μg/ml for 0, 16, 24 and 48 hours. Cell viability was then determined using the Live-Dead assay. Each graph represents the average of at least three independent experiments ± SEM.

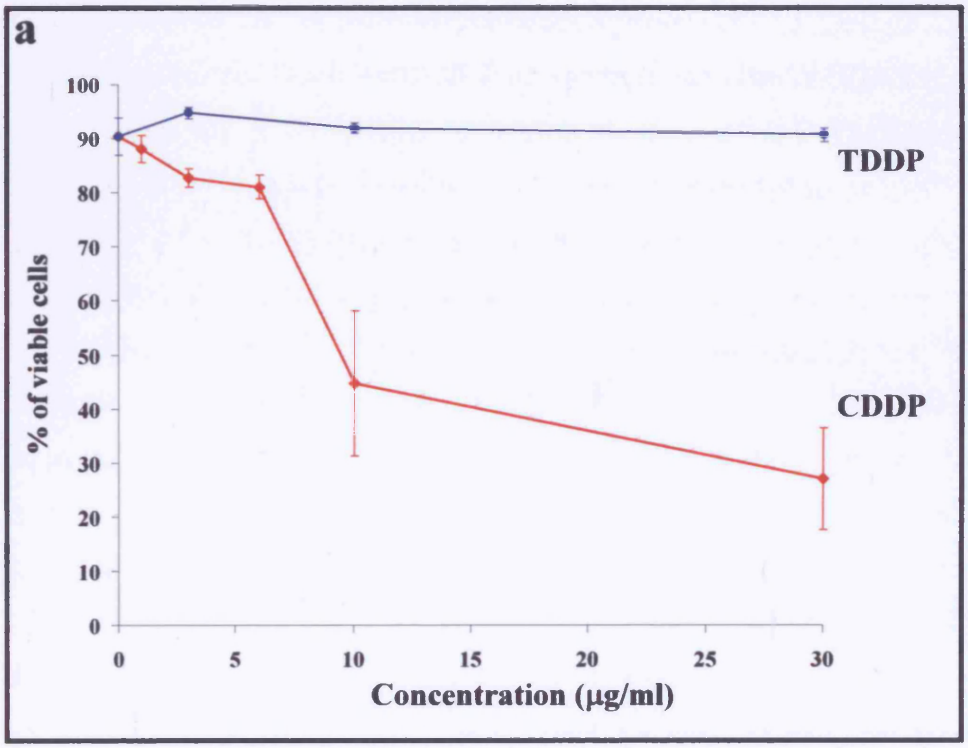
a
100
90
80
70
60
50
40
30
20
10
0
% of viable cells
TDDP
CDDP
0
5
10
15
20
25
30
Concentration (µg/ml)

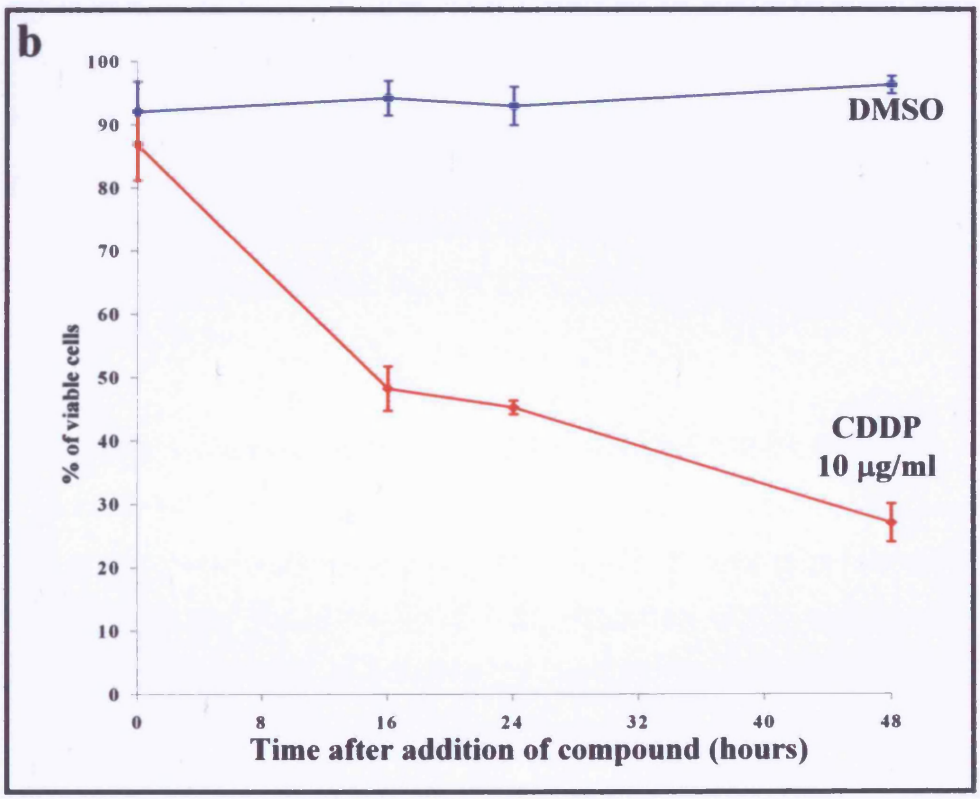
b
100
90
80
70
60
50
40
30
20
10
0
% of viable cells
DMSO
CDDP
10 µg/ml
0
8
16
24
32
40
48
Time after addition of compound (hours)

3.2.3 Requirement for macromolecular synthesis

Programmed cell death often (but not always) requires transcription and protein synthesis, e.g. the death of developing sympathetic neurons following NGF withdrawal (Martin *et al.*, 1988). To determine whether the CDDP–induced death of SH-SY5Y cells requires macromolecular synthesis, $1X10^5$ cells were pre-treated for one hour with various concentrations of actinomycin D and cyclohexamide, inhibitors of transcription and protein synthesis respectively, before being treated with CDDP (10 μg/ml) and the compounds for 24 hours. Actinomycin D inhibits transcription by binding to DNA and blocking RNA polymerase movement. Cyclohexamide blocks the translocation reaction of protein synthesis on ribosomes in the cytosol but not on ribosomes in the mitochondria. A Live-Dead cell viability assay was used to quantitate the effects of these inhibitors on CDDP-induced death. The percentage of viable cells was plotted against the concentration of each inhibitor and each graph represents the average of at least three independent experiments ± SEM. **Figure 3.3a** shows that actinomycin D killed some of the cells when added on its own but up to 50% of the cells that would normally be killed by CDDP could be rescued by actinomycin D at 1 μg/ml. **Figure 3.3b** shows that approximately 50% of the cells killed by CDDP could be saved by cyclohexamide at 1-5 μg/ml. Cyclohexamide by itself was not cytotoxic. These results suggest that CDDP-induced death requires new gene expression, in part.

3.2.4 p53 protein levels increase in CDDP–treated SH-SY5Y cells

As mentioned previously, CDDP has been shown to induce an increase in the level of the tumour suppressor, p53 (section 1.2.1). To determine whether this is also the case in our line of SH-SY5Y cells, the pattern of p53 expression was investigated by performing immunoblotting experiments with protein extracts from SH-SY5Y cells treated over 24 hours with CDDP. Protein extracts were prepared, separated by SDS-PAGE and then transferred to nitrocellulose. Following blocking and overnight incubation with an appropriate primary antibody, the proteins were detected using ECL reagents. A representative immunoblot is shown in **Figure 3.4a**. The blot (**Figure 3.4a**) was stripped and incubated with an anti-ERK antibody as a loading control. The level of p53

Figure 3.3 Effect of actinomycin D and cyclohexamide on CDDP-induced death

Approximately 1 X 10^5 SH-SY5Y cells were pre-treated for one hour with (**a**) 0, 0.5, 1 and 2 μg/ml of actinomycin D or (**b**) 0, 1, 2 and 5 μg/ml of cyclohexamide, before being treated with CDDP (10 μg/ml) and the inhibitors for 24 hours. A Live-dead cell viability assay was used to quantitate the effects of these inhibitors on CDDP-induced death. The percentage of viable cells was plotted against the concentration of each inhibitor and each graph represents the average of at least three independent experiments ± SEM.

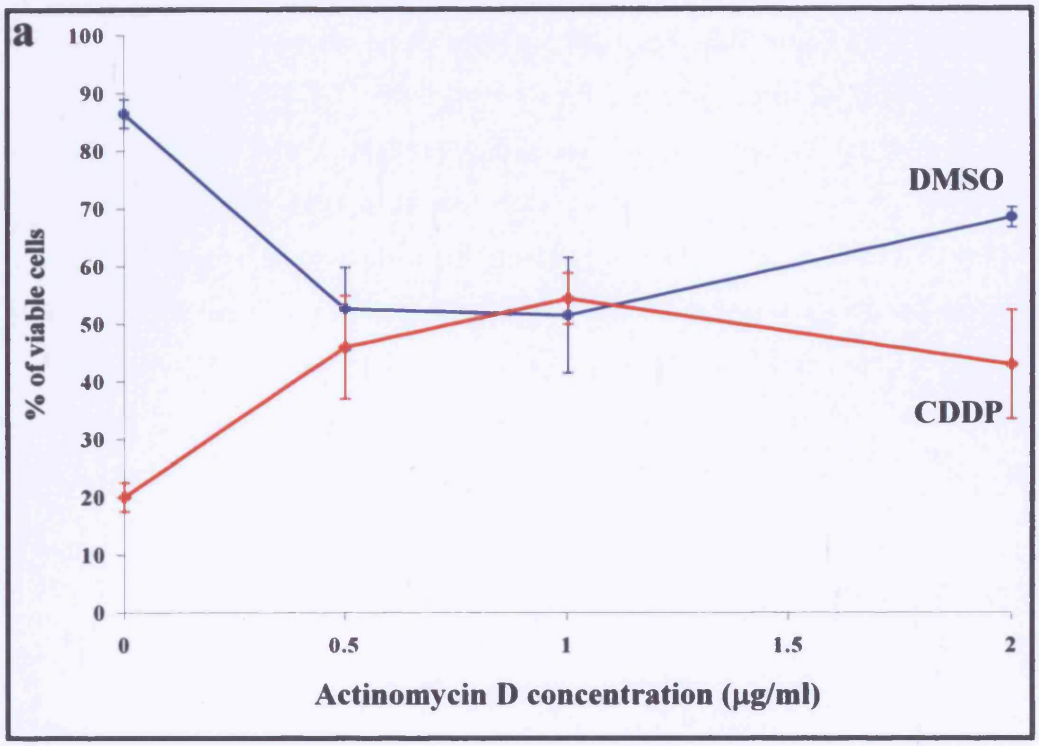
a
100
90
80
70
60
50
40
30
20
10
0
% of viable cells
DMSO
CDDP
0
0.5
1
1.5
2
Actinomycin D concentration (μg/ml)

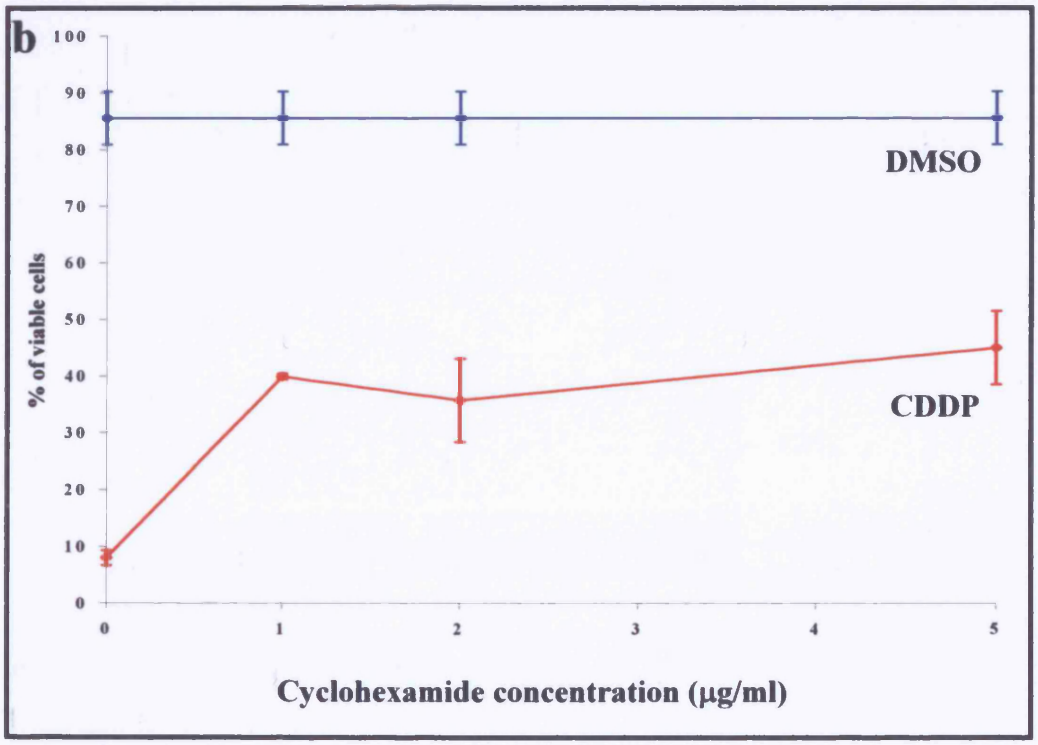
b
100
90
80
70
60
50
40
30
20
10
0
% of viable cells
DMSO
CDDP
0
1
2
3
4
5
Cyclohexamide concentration (μg/ml)

Figure 3.4 p53 protein levels increase during CDDP and TDDP treatment
SH-SY5Y cells (6.5 X 10^5) were grown in 10 cm dishes until 80-100% confluent. Cells were treated with CDDP (10μg/ml) and TDDP (10μg/ml) for 0, 4, 8, 12, 16 and 24 hours. The pattern of p53 expression was investigated by performing immunoblotting experiments with protein extracts from SH-SY5Y cells. A representative immunoblot is shown in (**a**). This blot was stripped and incubated with an anti-ERK antibody as a loading control. (**b**) ERK loading control is compared to the commonly used Tubulin loading control on the same blot that was stripped and reprobed. The two controls show distinct similarity in loading.

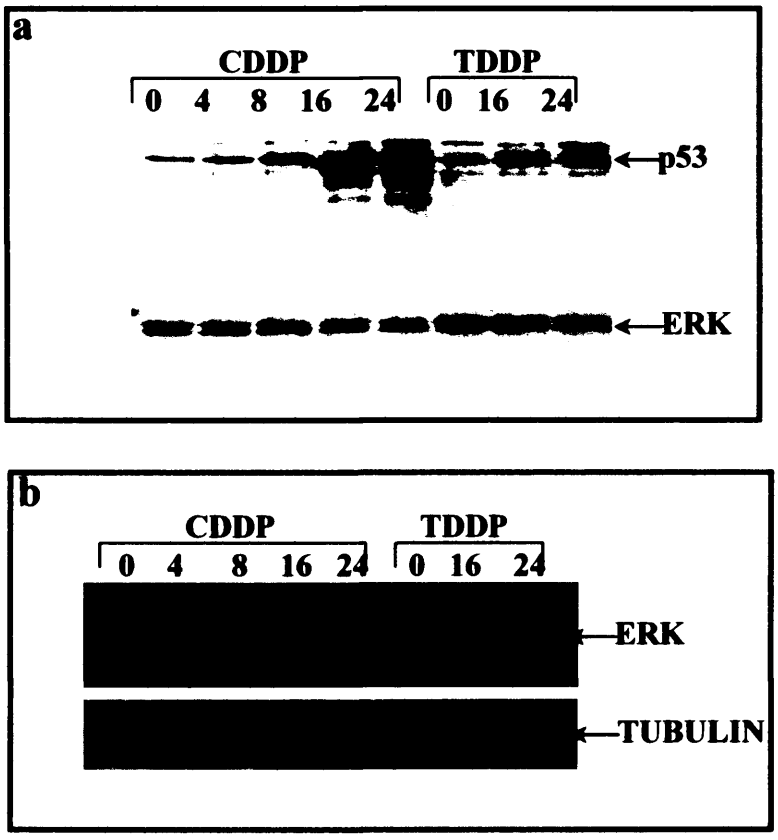

remained constant between 0 - 8 hours of CDDP treatment but between 8 - 24 hours, the level increased significantly. This is supported by the lower level of the loading control, ERK at 16 and 24 hours compared to 0 - 8 hours. ERK was a suitable loading control because ERK protein levels did not alter during CDDP or TDDP treatment and they mirrored tubulin levels. **Figure 3.4b** shows the comparison of protein levels of tubulin and ERK on the same blot. TDDP treatment also caused an increase in p53 level but this was much smaller than that seen after CDDP treatment. These results are in agreement with previous findings that p53 is expressed in SH-SY5Y cells and induced by CDDP (Tieu *et al.,* 1999; Rodriguez-Lopez *et al.,* 2001; Wetzel and Berberich, 2001).

3.2.5 CDDP induces biochemical changes characteristic of apoptosis in SH-SY5Y cells

As described in section 3.2.1, SH-SY5Y cells die when treated with cisplatin. It has previously been shown that cisplatin induces apoptosis in various cell types and the morphology of the dying SH-SY5Y cells was consistent with this. Most of the visible changes that characterise apoptotic cell death are dependent on caspases, the central executioners of the apoptotic pathway. Caspase-3-mediated cleavage of ICAD (inhibitor of CAD) activates caspase-activated DNase (CAD), which is the nuclease that cuts genomic DNA between nucleosomes, to generate DNA fragments with lengths corresponding to 185 base pairs. Eliminating caspase activity, either through targeted mutation of the caspase genes (in mice) or the use of small molecule inhibitors, such as ZVAD-fmk, will slow down or even prevent apoptosis.

3.2.5.1 CDDP induces nuclear DNA fragmentation

The TUNEL assay and Hoechst staining were used to study the nuclear changes in cells treated with CDDP at 30 μg/ml for 24 hours. Control cells were treated with DMSO. The cells were then examined by fluorescence microscopy. The results are shown in **Figure 3.5**. In the version of the TUNEL assay used here, nuclei in which DNA fragmentation has occurred are stained green due to the incorporation of fluorescein-labelled dUTP. The TUNEL assay cannot differentiate between apoptotic and necrotic death as both types of cell death can exhibit a high number of stainable DNA ends. However, bisbenzamide (Hoechst)

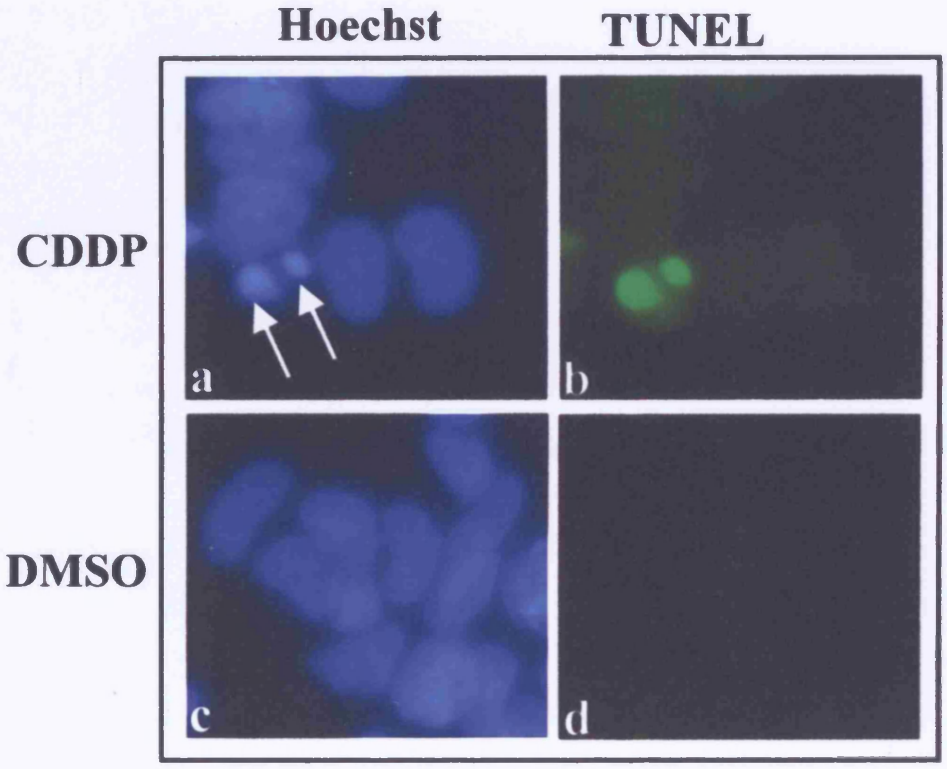

Figure 3.5 CDDP induces nuclear condensation and DNA fragmentation. SH-SY5Y cells (4 X 10^4) were grown on coverslips until 80-100% confluent. The cells were treated with 30 μg/ml of CDDP (**a** and **b**) or DMSO as a control (**c** and **d**) for 24 hours and then fixed for immunocytochemistry. The TUNEL assay and Hoechst staining were used to study the nuclear changes in the cells. The stained cells were examined by fluorescence microscopy on a Zeiss Axioplan 2 fluorescence microscope. Representative images of nuclei stained with Hoechst dye (**a** and **c**) and TUNEL staining (**b** and **d**) are shown. CDDP induced changes typical of apoptosis such as the appearance of pyknotic nuclei (arrows in **a**) and DNA fragmentation (**b**).

dye, which stains the nuclei blue, can be used to study the morphology of the nuclei and identify morphological changes typical of apoptosis. CDDP induced changes typical of apoptosis such as the appearance of pyknotic nuclei (see arrows in **Figure 3.5a**) and DNA fragmentation (**Figure 3.5b**). The control cells treated only with DMSO had nuclei with a normal morphology (**Figure 3.5c**) and did not exhibit DNA fragmentation (**Figure 3.5d**).

3.2.5.2 Procaspase-3 cleavage

The execution phase of apoptosis requires the activity of effector caspases such as caspase-3. To determine whether caspase activity was required for CDDP-induced death, SH-SY5Y cells were pre-treated for one hour with different concentrations of the broad-range caspase inhibitor ZVAD-fmk before one set of cells was treated with CDDP (10 μg/ml) and ZVAD-fmk for 24 hours. A Live-Dead cell viability assay was preformed as previously described (section 3.2.2) and the percentage of viable cells was plotted against the concentration of ZVAD-fmk. The results shown in **Figure 3.6a** represent the average of at least three sets of independent experiments ± SEM.

The results indicate that ZVAD-fmk on its own is not toxic to the cells and that at 50 μM, it can rescue almost half of the cells that would have been killed by CDDP. At 100 μM, most of the cells are protected. This indicates that caspase activity is required for the CDDP-induced death of SH-SY5Y cells. We confirmed that ZVAD-fmk had indeed inhibited caspase activity by examining procaspase-3 cleavage (a caspase-dependent event) in immunoblotting experiments. SH-SY5Y cells were treated with 100 μM ZVAD-fmk for one hour after which CDDP was added to one set of ZVAD-fmk pre-treated cells for 24 hours. Protein extracts were prepared, separated by SDS-PAGE and then transferred to nitrocellulose. Following blocking and overnight incubation with an anti-caspase-3 antibody, the proteins were detected using ECL reagents. A representative immunoblot is shown in **Figure 3.6b**. After treatment with CDDP for 24 hours, the cleavage of procaspase-3 into active caspase-3 is near to completion (**Figure 3.6b**). However, in extracts from the SH-SY5Y cells treated with ZVAD-fmk before and during CDDP exposure, there was little cleavage of procaspase-3 into active caspase and cells treated only with DMSO

Figure 3.6 CDDP-induced apoptosis requires caspase activity and cleavage of procaspase-3 occurs after CDDP treatment

(a) Duplicate sets of SH-SY5Y cells were grown in 3.5 cm dishes until 80-100 % confluent. The cells were pre-treated for one hour with the broad-range caspase inhibitor ZVAD-fmk (at 0, 50 and 100 μM) before one set of cells were treated with CDDP (10 μg/ml) plus ZVAD-fmk, and the other with DMSO for 24 hours. A Live-Dead cell viability assay was performed and the percentage of viable cells was plotted against the concentration of ZVAD-fmk. The results shown represent the average of at least three sets of independent experiments ± SEM.

(b) SH-SY5Y cells (6.5×10^5) were grown in 10 cm dishes until 80-100% confluent. One set of cells was treated with 100 μM ZVAD-fmk for one hour after which CDDP (10μg/ml) was added to the ZVAD-fmk pre-treated cells for 24 hours. The expression and cleavage of procaspase-3 was investigated by performing immunoblotting experiments with protein extracts from these cells. A representative immunoblot is shown.

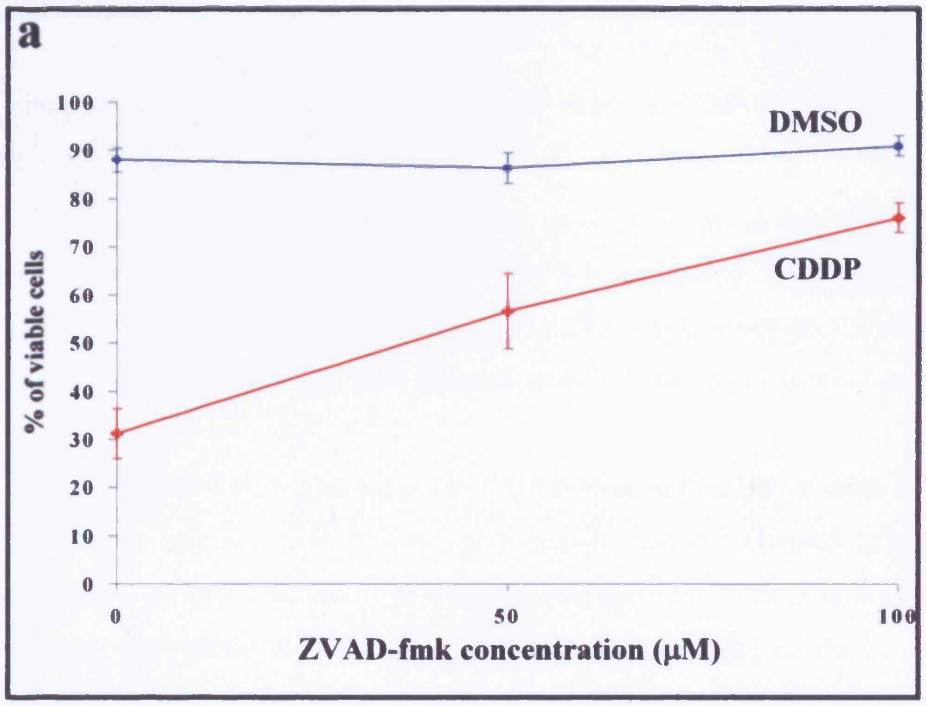
a
100
90
80
70
60
50
40
30
20
10
0
% of viable cells
DMSO
CDDP
0
50
100
ZVAD-fmk concentration (μM)

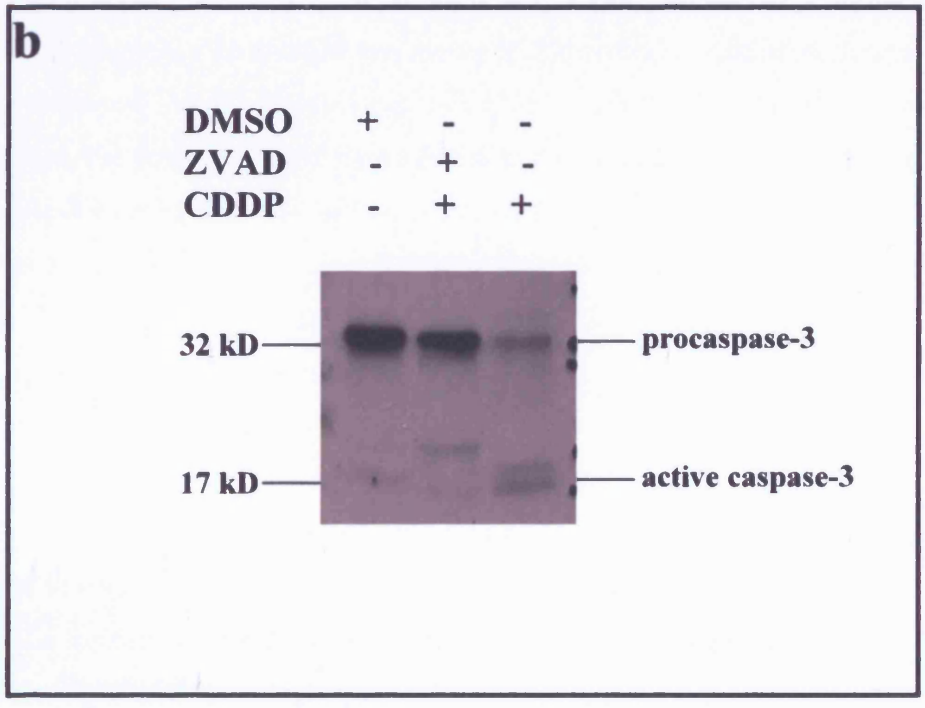
b
DMSO + - -
ZVAD - + -
CDDP - + +
32 kD
17 kD
procaspase-3
active caspase-3

have no active caspase. Thus, caspase activity is required for CDDP-induced death of SH-SY5Y cells and, consistent with this, cleavage of procaspase-3, an executioner caspase, occurs after CDDP treatment.

3.2.6 Identifying the death pathway by which CDDP induces caspase-3 activation

Cleavage and activation of caspase-3 can be induced via two upstream initiator pathways: the extrinsic death receptor signalling pathway involving procaspase-8 cleavage or the intrinsic mitochondrial death pathway involving the release of cytochrome c from the mitochondria and the cleavage of procaspase-9.

3.2.6.1 Procaspase-9 cleavage occurs in CDDP-treated SH-SY5Y cells

To investigate whether procaspase-8 and/or -9 were cleaved after CDDP treatment, protein extracts were prepared, separated by SDS-PAGE and then transferred to nitrocellulose. Following blocking and overnight incubation with an anti-caspase-8 antibody or an anti-caspase-9 antibody, the proteins were detected using ECL reagents. The results are shown in **Figure 3.7**. Neither procaspase-8 nor active caspase-8 were detected in SH-SY5Y cells. In this immunoblotting experiment, the positive control was a Jurkat cell extract that contained cleaved forms of caspase-8 because the cells had been treated for 6 hours with anti-Fas (CH11) IgM antibody to induce apoptosis. In contrast to caspase-8, procaspase-9 was expressed in SH-SY5Y cells. At 16 hours after CDDP treatment, the cleaved form of caspase-9 can be observed at 34 kDa, thus indicating the involvement of the mitochondrial pathway in CDDP-induced apoptosis in SH-SY5Y cells.

3.2.6.2 Cytochrome c is released from mitochondria during the CDDP-induced death of SH-SY5Y cells.

To further investigate the role of the mitochondrial pathway in CDDP-induced apoptosis of SH-SY5Y cells, the distribution of cytochrome c was investigated by immunocytochemistry. SH-SY5Y cells grown on coverslips were treated with CDDP for 12 hours. Representative images of the cells stained with a monoclonal antibody against cytochrome c are shown in **Figure 3.8**. Cells were also stained with Hoechst

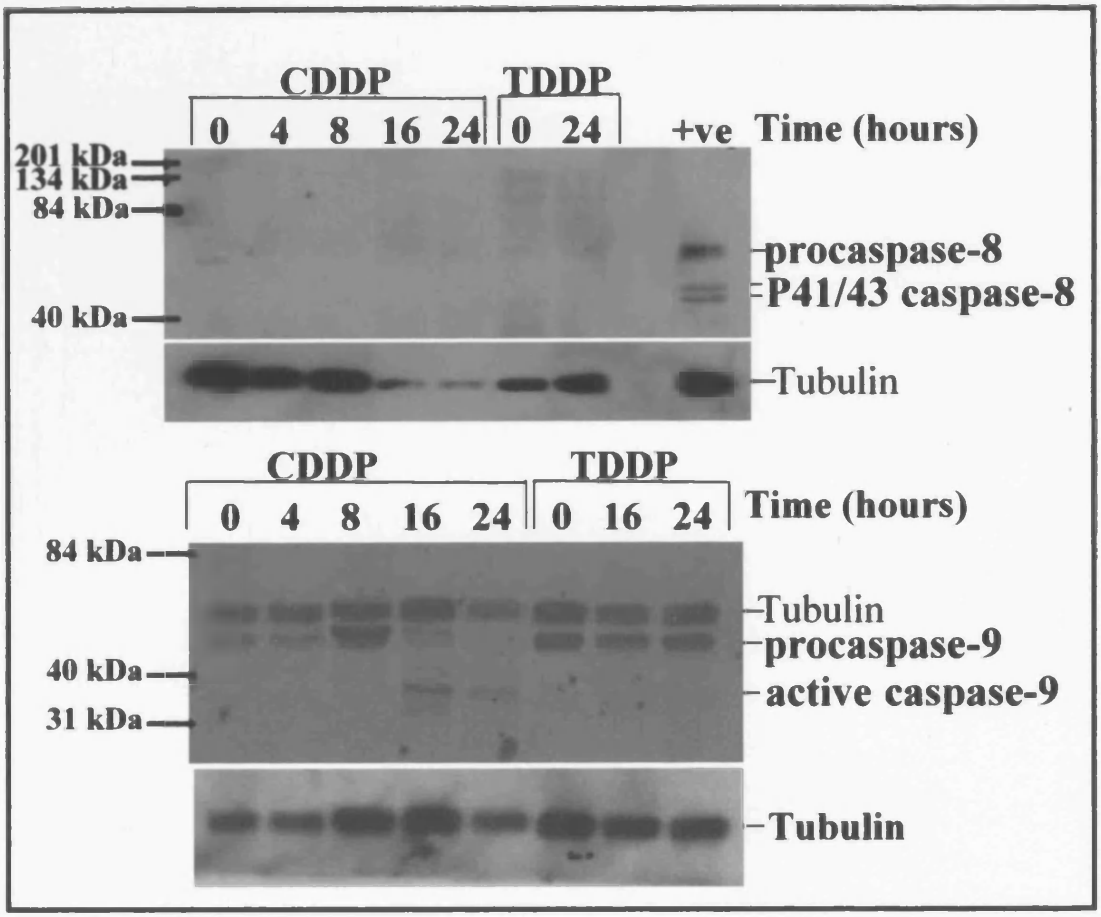

Figure 3.7 Procaspase-9 cleavage occurs in CDDP-treated SH-SY5Y cells

SH-SY5Y cells (6.5 X 10^5) were grown in 10 cm dishes until 80-100% confluent. The cells were treated with CDDP (10μg/ml) for 0, 4, 8, 16 and 24 and TDDP (10μg/ml) for 0, 16 and 24 hours. The expression of caspase-8 and caspase-9 was investigated by performing immunoblotting experiments with protein extracts from these cells. Representative immunoblots are shown. In the case of caspase-8, an extract from Jurkat cells treated with anti-fas antibody (**+ve**) was used as a control. Following stripping procedures to remove the tubulin antibody from the caspase-9 membrane, the tubulin can still be observed even though the two antibodies have different secondary antibodies.

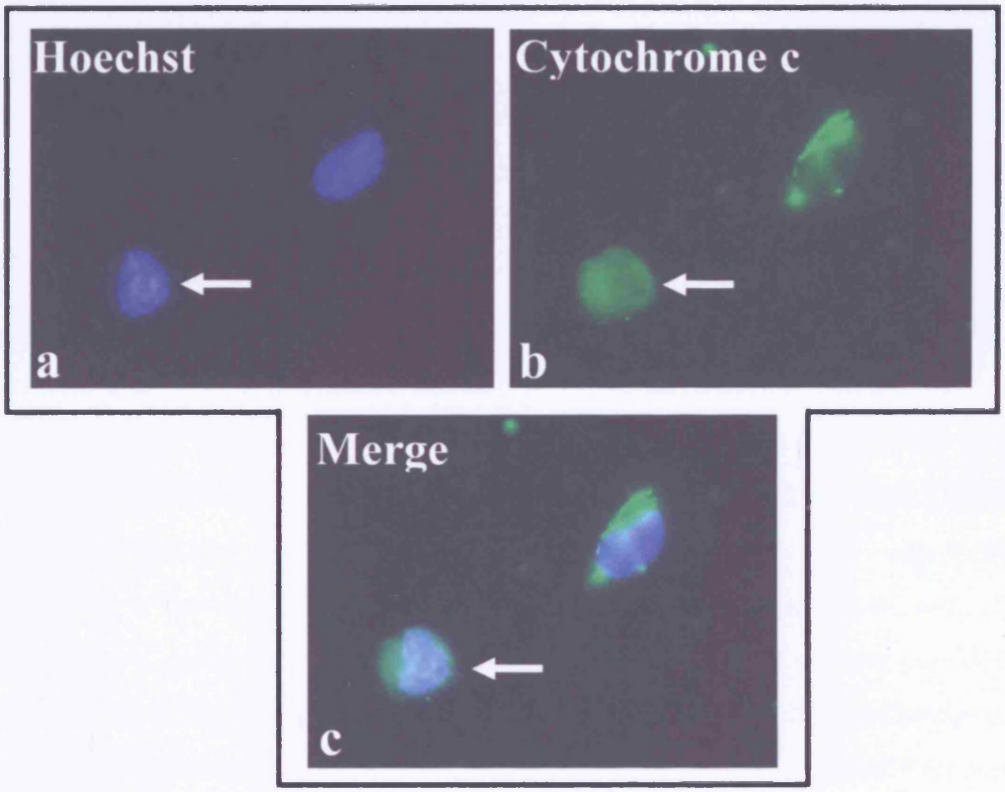

Figure 3.8 Cytochrome c is released from mitochondria during the CDDP-induced death of SH-SY5Y cells.

SH-SY5Y cells (4 X 10^4) were grown on coverslips until 80-100% confluent. The cells were treated with 30 μg/ml of CDDP (**a** and **b**) for 12 hours then fixed for immunocytochemistry. (**a**) Nuclear morphology detected by Hoechst staining. A pyknotic nucleus (arrowed) and a normal nucleus are shown. Cells were also incubated with cytochrome c antibody to detect cytochrome c distribution (**b**). The normal cell shows normal (punctate) cytochrome c staining excluded from the nucleus (see **c**) whereas the apoptotic cell (arrowed) has diffuse cytochrome c staining throughout the cytoplasm (**b**) and nuclear space (**c**). Representative images captured on a Zeiss Axioplan 2 fluorescence microscope are shown.

dye to reveal the nuclear morphology. In normal cells, cytochrome c staining was predominantly cytoplasmic whereas in apoptotic cells, cytochrome c staining was diffused throughout the cytoplasm and nuclear space.

The caspase inhibitor, ZVAD-fmk inhibits caspase-3 cleavage in SH-SY5Y cells treated with CDDP (section 3.2.7). The effect of ZVAD-fmk on cytochrome c release was investigated by treating the SH-SY5Y cells grown on coverslips with 100 μM ZVAD-fmk for one hour prior to and during CDDP treatment. The percentage of SH-SY5Y cells exhibiting normal or pyknotic nuclei, and normal or diffuse cytochrome c was determined for cells treated with DMSO alone, CDDP alone, or ZVAD-fmk alone, or ZVAD-fmk and CDDP (**Figure 3.9**). The results indicate that cytochrome c release in CDDP-treated SH-SY5Y cells is independent of caspase activity. CDDP treatment for 12 hours induces 20% of the cells to have pyknotic nuclei with a diffuse cytochrome c distribution. Treatment with both CDDP and ZVAD-fmk resulted in 10% of the cells having pyknotic nuclei with a diffuse cytochrome c distribution but 40% of the cells showed normal nuclei with diffuse cytochrome c. This indicates that caspase activity leading to nuclear condensation and fragmentation was inhibited by ZVAD-fmk but the release of cytochrome c from the mitochondria was not prevented. Thus cytochrome c release in CDDP treated SH-SY5Y cells is caspase independent.

Figure 3.9 Cytochrome c release in CDDP-treated SH-SY5Y cells is independent of caspase activity.

SH-SY5Y cells (4 X 10^4) were grown on coverslips until 80-100% confluent. Some of the cells were treated with 100 μM ZVAD-fmk for one hour prior to and during 30 μg/ml of CDDP for 12 hours. Other cells were treated with only DMSO or 30 μg/ml of CDDP for 12 hours. The cells were then fixed for immunocytochemistry with Hoechst dye and anti-cytochrome c. The graphs show the percentage of SH-SY5Y cells treated with (**a**) DMSO, (**b**) CDDP, (**c**) ZVAD-fmk and CDDP, and (**d**) ZVAD-fmk that exhibit either normal nuclear morphology and normal cytochrome c distribution (*white bars*), normal nuclear morphology and diffuse cytochrome c distribution (*grey bar*) or pyknotic nuclei and diffuse cytochrome c (*black bars*). The results shown represent the average of three independent experiments ± SEM.

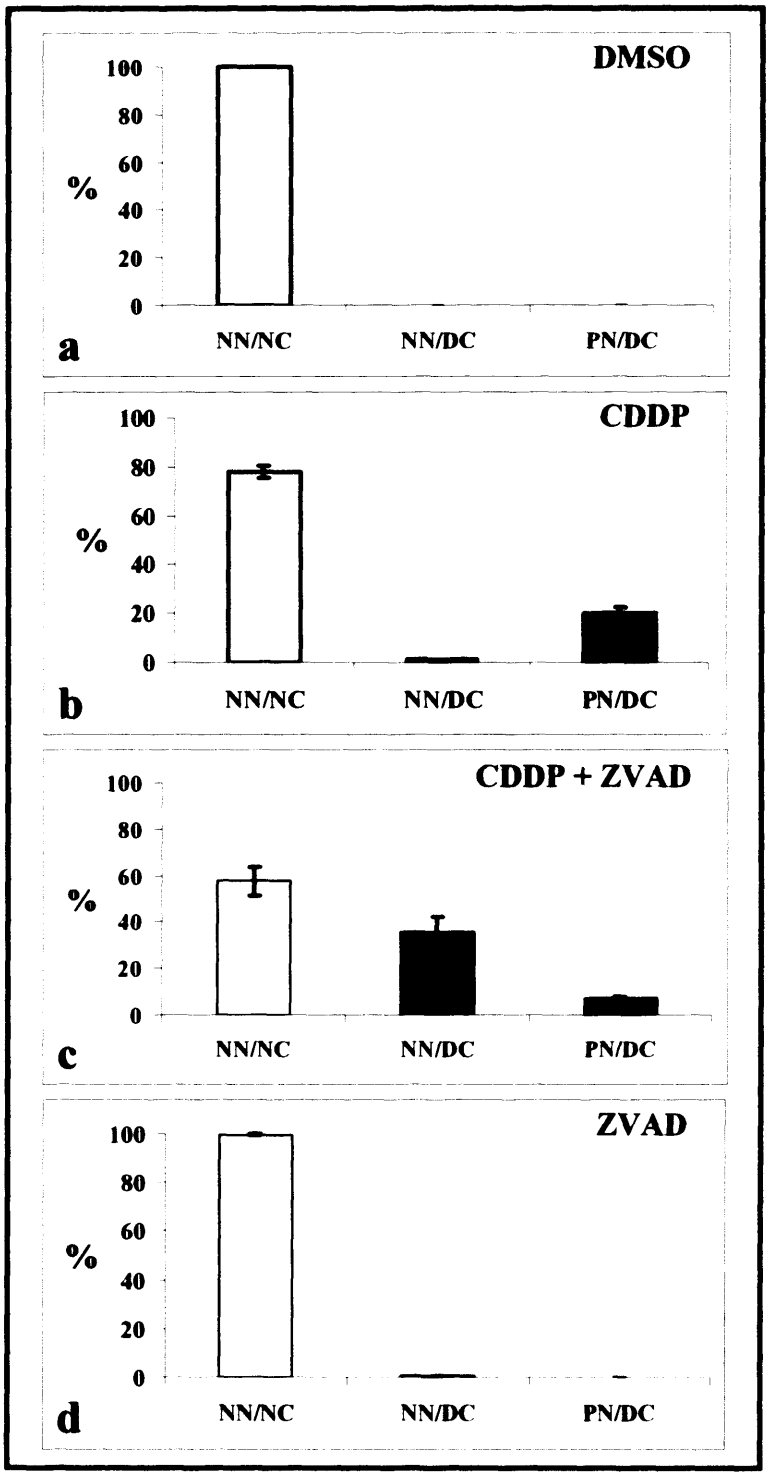
DMSO
100
80
60
%
40
20
0
a
NN/NC
NN/DC
PN/DC
CDDP
100
80
60
%
40
20
0
b
NN/NC
NN/DC
PN/DC
CDDP + ZVAD
100
80
60
%
40
20
0
c
NN/NC
NN/DC
PN/DC
ZVAD
100
80
60
%
40
20
0
d
NN/NC
NN/DC
PN/DC

3.3 Discussion

In this chapter, I have described experiments in which I characterised some of the basic features of the cell death process initiated in CDDP-treated SH-SY5Y neuroblastoma cells (see hypothetical model **Figure 3.10**). I found that the cell death process triggered by CDDP was dose-dependent. CDDP at 10 μg/ml killed approximately 45% of SH-SY5Y cells in 16 hours whereas TDDP and DMSO were not cytotoxic. Higher concentrations or longer exposures to CDDP resulted in high levels of death and the majority of the cells would detach from the dishes or coverslips and therefore could not be quantified. Cells undergoing death were loosely attached to surfaces so in the case of cell staining processes involving multiple washing steps, many cells were lost. I therefore used 10 μg/ml as the standard CDDP concentration throughout the experiments but altered the number of hours of CDDP exposure according to the experiment involved. For example, with assays where the entire medium was collected, we were able to treat cells for up to 24 hours as detached cells were collected and used as part of the assay. In cell staining experiments, 16 hours was the maximum length of time the cells were exposed to CDDP.

I investigated the question of whether there is a requirement for new protein synthesis for the CDDP-induced death of SH-SY5Y cells by treating the cells with cyclohexamide and actinomycin D in a dose-dependent manner with 10 μg/ml of CDDP. These experiments indicated that CDDP-induced death in SH-SY5Y cells requires new gene expression in part.

The inability of both TDDP and DMSO to induce cell death in SH-SY5Y cells made them ideal controls for future experiments. TDDP causes DNA damage that is repairable so its non-toxic characteristic in SH-SY5Y cells may be due to the efficient action of DNA damage recognition and repair proteins. DNA damage by CDDP activates the checkpoint kinase, ATR (Damia *et al.*, 2001; Zhao and Piwnica-Worms, 2001) which phosphorylates the p53 protein at serine-15 to initiate activation of the p53 protein (Appella and Anderson, 2001). During genotoxic stress, a rapid stabilization of the p53 protein and its activation leads to cell cycle arrest and/or apoptosis; the arrest allows cells to repair damaged DNA, whereas apoptosis removes damaged cells from the replicative pool to maintain genome integrity (el-deiry, 2002).

I found that both CDDP and TDDP treatment induces an increase in p53 protein levels due to DNA damage. However, the level of p53 does not increase very much with TDDP compared to CDDP. The small increase in p53 protein in TDDP-treated cells may be sufficient to promote DNA repair protein activity rendering the repairable DNA damage caused by TDDP not to be cytotoxic. It is also possible that p53 levels probably need to be above a certain threshold to be cytotoxic. Since p53 is activated when SH-SY5Y cells are treated with CDDP, p53 target genes are likely to have a role in promoting cytochrome c release and apoptosis in SH-SY5Y cells. p53 RNA levels were not measured so I cannot exclude that there might be some change in the rate of p53 transcription or a change in RNA stability.

Consistent with the results of previous studies (Cece *et al.,* 1995), I found that CDDP induces apoptosis in SH-SY5Y cells as evidenced by TUNEL and Hoechst staining. I supported this further, by showing that caspase activity is required for CDDP-induced death of SH-SY5Y cells and that the executioner caspase, caspase-3 is cleaved after CDDP treatment. This would be predicted to lead to an increase in caspase-3 activity, which could be measured by performing a DEVD-ase assay. Alternatively, cleavage of poly (ADP-ribose) polymerase (PARP) could have been detected by western blotting.

I found that procaspase-9 was cleaved in SH-SY5Y cells treated with CDDP whereas no expression of active caspase-8 was observed. This indicates that the mitochondrial death pathway is activated in CDDP-treated SH-SY5Y cells whereas the death receptor pathway is not. To further investigate the involvement of the mitochondrial pathway, we characterised the translocation of cytochrome c from the mitochondria to the cytoplasm in CDDP-treated cells. Investigating the effect of ZVAD-fmk treatment on cytochrome c release and apoptosis showed that caspase activity was downstream of cytochrome c release and that many cells with diffuse cytochrome c were prevented from undergoing apoptosis. Cytochrome c release could have been measured by using biochemical fractionation to separate the cell extract into a mitochondrial (heavy membrane) fraction and cytosolic fraction to confirm the results of the immunostaining assay. Members of the Bcl-2 family regulate the release of cytochrome c and other proapoptotic proteins from the mitochondria. I therefore investigate the expression pattern and role of these proteins in CDDP-treated SH-SY5Y cells in the experiments described in the next chapter (**Figure 3.10**).

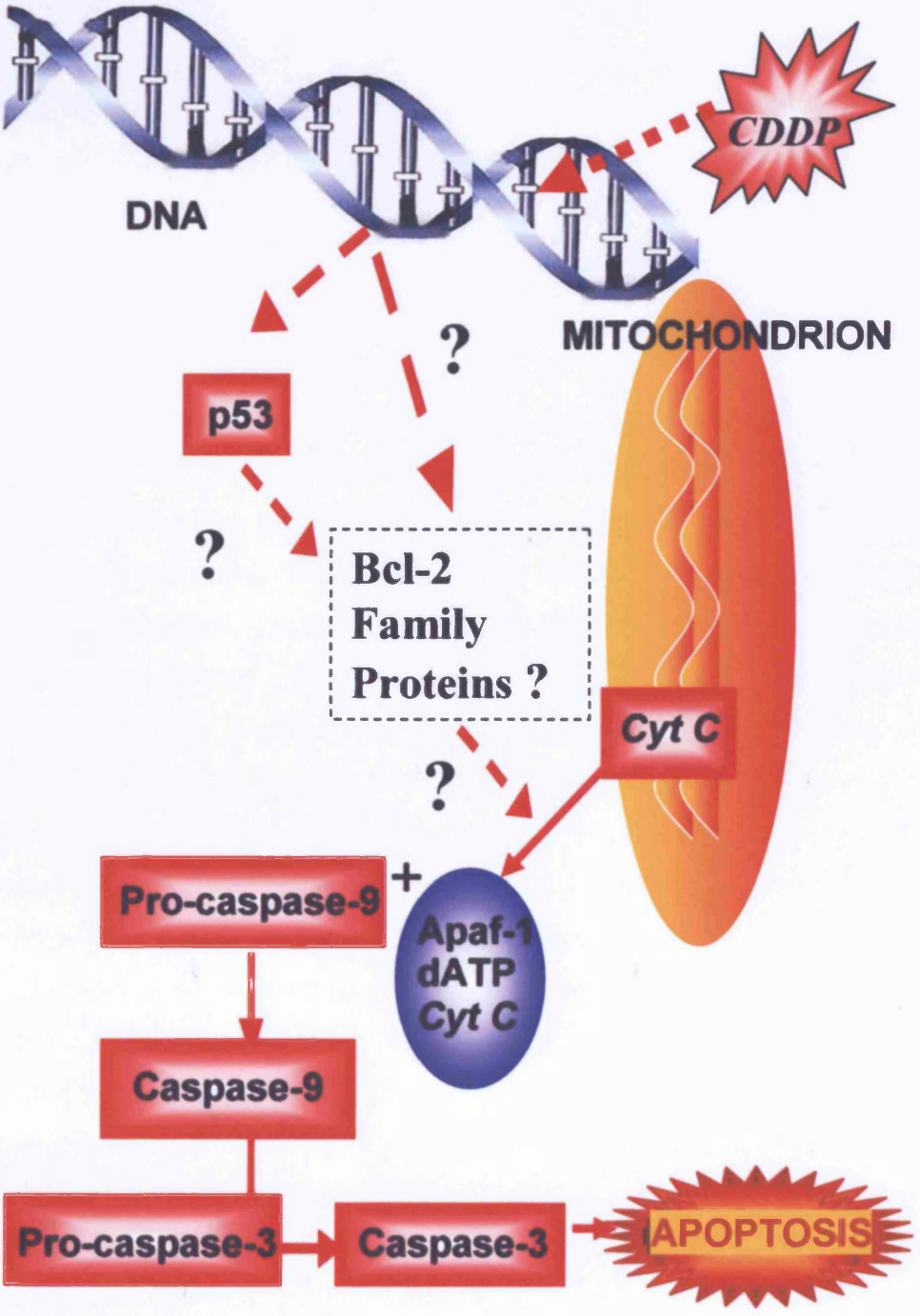

Figure 3.10 Hypothetical model of CDDP-induced death

Summary model of results so far. Dotted lines indicate unknown mechanisms and future work.

Chapter 4: Role of Bcl-2 family proteins in CDDP-induced apoptosis of SH-SY5Y neuroblastoma cells

4.1 Introduction

In the previous chapter, I described results that suggest that CDDP induces apoptosis in SH-SY5Y cells by activating caspases via the intrinsic mitochondrial pathway with the release of cytochrome c. Members of the Bcl-2 family regulate the release of cytochrome c and other proapoptotic proteins from the mitochondria. The Bcl-2 family of proteins has a crucial role in intracellular apoptotic signal transduction. The family includes both antiapoptotic and proapoptotic proteins that contain one or more Bcl-2 homology (BH) domains. There are three subfamilies. The first includes Bcl-2, Bcl-x_L, Bcl-w, Mcl-1 and A1, which all contain BH1-4 domains and promote cell survival. The second group includes Bax, Bak and Bok and these are related to Bcl-2 at BH1-3, but instead promote cell death. The third group, the BH3-only proteins, such as Bad, Bik, Hrk/DP5, Bid, Bim, Noxa and PUMA, only have one of the Bcl-2 homology regions, the BH3 domain. These BH3-only proteins are essential initiators of apoptosis. They play a critical role in mammalian development (Huang and Strasser, 2000). The proapoptotic activity of BH3-only proteins is regulated by transcriptional and post-translational mechanisms to prevent inappropriate cell death during development. Overexpression of Bcl-2 can promote cancer and can affect the sensitivity of tumour cells to chemotherapeutic drugs. Mutations in the BH3-only proteins or their regulators may therefore also be pathogenic (Huang and Strasser, 2000).

In the work described in this chapter, I investigated which Bcl-2 family members are expressed in SH-SY5Y cells and whether their level changes or post-translational modifications occur following CDDP treatment by performing immunoblotting and RT-PCR experiments.

4.2 Results

4.2.1 The role of Bcl-2 family members in CDDP-induced apoptosis of SH-SY5Y cells

To investigate whether CDDP causes any change in the pattern of expression or in the size of Bcl-2 family members present in SH-SY5Y cells, immunoblotting experiments were performed with protein extracts from SH-SY5Y cells treated for up to 24 hours with CDDP and TDDP. Protein extracts were prepared at various times during treatment, separated by SDS-PAGE and then transferred to nitrocellulose. Following blocking and overnight incubation with an appropriate primary antibody, the proteins were detected using ECL reagents. Representative immunoblots are shown in **Figure 4.1** for the antiapoptotic proteins and in **Figure 4.2** for the multidomain proapoptotic and BH3-only proteins. In figure 4.1, Bcl-w appears to increase after 24 hours of CDDP treatment, this however was not observed when the experiment was repeated atleast three times. This blot was chosen due to its low background and clear visibility of the Bcl-w band.

No consistent change was observed in the level of any of the antiapoptotic members of the Bcl-2 family except Mcl-1, which decreased in level after 8 hours of CDDP treatment, whereas its level in TDDP-treated cells remained constant (**Figure 4.1a**). Any Bcl-2 family member that plays an essential role in the regulation of CDDP-induced apoptosis in SH-SY5Y cells is likely to function upstream of caspase activity since cytochrome c release is caspase-independent. Since the level of Mcl-1 altered during CDDP treatment, its expression was studied in SH-SY5Y cells treated with ZVAD-fmk alone or with ZVAD-fmk and CDDP. The results of this experiment are shown in **Figure 4.1b**. The level of Mcl-1 decreased after CDDP treatment, but in cells treated with the caspase inhibitor ZVAD-fmk for one hour before and during CDDP treatment, Mcl-1 levels were similar to the controls. This indicates that the change in the level of Mcl-1 protein is a result of caspase activity and this rules out the decrease in Mcl-1 as a key event regulating cytochrome c release, since the latter occurs in a caspase-independent manner in SH-SY5Y cells treated with CDDP.

Immunoblots for the multidomain proapoptotic Bcl-2 family proteins are shown in Figure 4.2a. Bax and Bak did not consistently change in level after

CDDP treatment. The BH3-only proteins are shown in Figure 4.2b. Bad, Bid, Bim, Noxa, Hrk and Bmf did not increase in level after CDDP treatment. However, the BH3-only protein, Bik, showed a decrease in the full length 32 kDa band at 16 and 24 hours after CDDP addition whereas a smaller band of approximately 23 kDa appeared after 16 hours of CDDP treatment and increased in level at 24 hours of CDDP treatment. Formation of a smaller form of Bik, by proteolytic cleavage for example, might alter its properties or subcellular localisation. The change in the Bik protein was also examined with ZVAD-fmk-treated SH-SY5Y cell extracts and the results indicate that the decrease in full length Bik required caspase activity (**Figure 4.3**). This therefore suggests that the change in Bik is unlikely to be one of the key events regulating cytochrome c release.

4.2.2 PUMA protein levels increase in CDDP-treated SH-SY5Y cells and this is independent of caspase activity

Another BH3-only protein, PUMA (p53 upregulated modulator of apoptosis), which is a direct transcriptional target of p53, was also analysed by immunoblotting. The PUMA antibody used recognises the BH3 domain of the PUMA protein. In the immunoblot shown in **Figure 4.4a**, it can be seen that the PUMA antibody recognises two bands. The higher molecular weight band increased in level during CDDP treatment but did not change with TDDP. This could either be PUMA-α or PUMA-β which both contain the BH3 domain. The lower molecular band did not increase in level during CDDP or TDDP treatment and may be non-specific.

To identify which PUMA proteins these bands correspond to, expression vectors for the FLAG-tagged PUMA-α and -β isoforms were transfected into Cos-7 cells in duplicate. Protein extracts were prepared, separated by SDS-PAGE and transferred to nitrocellulose. Protein samples prepared from SH-SY5Y cells treated with CDDP for 8 hours and TDDP for 16 hours were run alongside the overexpressed PUMA protein samples. The blot was incubated overnight with the PUMA antibody and proteins were detected using ECL reagents. This blot (Figure 4.4.b) shows that the higher molecular weight band most likely corresponds to the 26 kDa PUMA-α protein and the lower molecular weight band

Figure 4.1 Immunoblotting analysis of antiapoptotic Bcl-2 family proteins in SH-SY5Y neuroblastoma cells

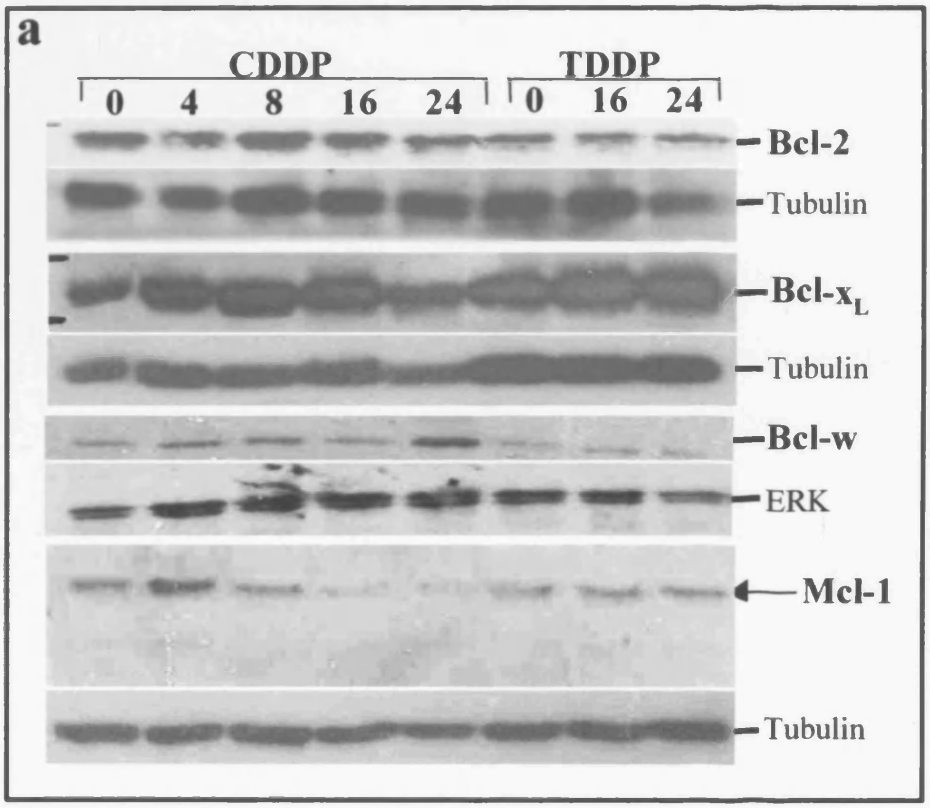

(a) Pattern of expression of antiapoptotic Bcl-2 family proteins in CDDP-treated SH-SY5Y cells

SH-SY5Y cells (6.5 X 10^5) were grown in 10 cm dishes until 80-100% confluent. Cells were treated with CDDP (10μg/ml) for 0, 4, 8, 16 and 24 hours and TDDP (10μg/ml) for 0, 16 and 24 hours. The pattern of expression of the Bcl-2 family members was investigated by performing immunoblotting experiments with protein extracts from SH-SY5Y cells. Representative immunoblots are shown in **(a),** together with their tubulin or ERK loading controls (as indicated). Each experiment was performed more than once.

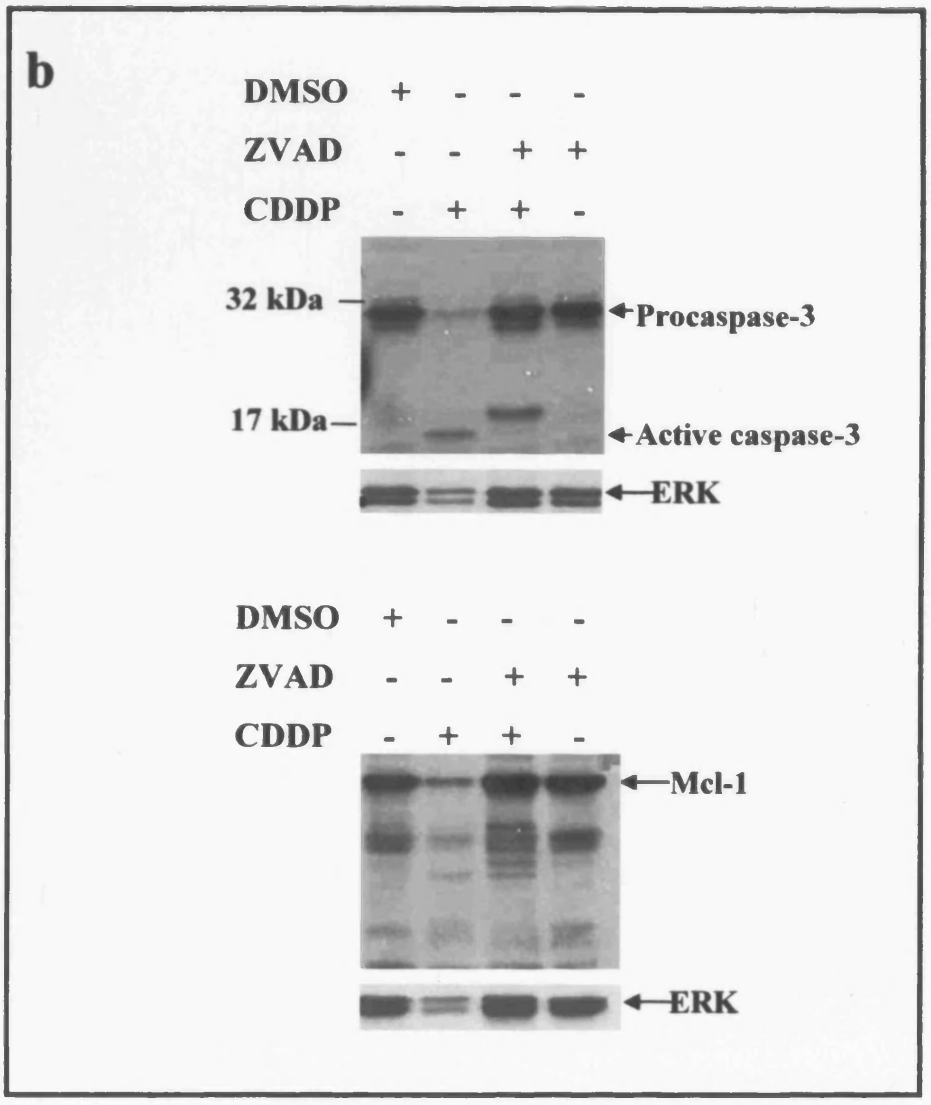

(b) Mcl-1 expression in cells treated with ZVAD-fmk and CDDP

Caspase-3 was used as a control for the effect of ZVAD-fmk. The level of Mcl-1 decreased after CDDP treatment, but in cells treated with the caspase inhibitor ZVAD-fmk before and during CDDP treatment, Mcl-1 levels were similar to the controls (DMSO or ZVAD-fmk alone). This indicates that the change in the level of Mcl-1 protein is a result of caspase activity and rules out Mcl-1 as a key regulator of cytochrome c release, which occurs in a caspase-independent manner in CDDP-treated SH-SY5Y cells.

Figure 4.2 Pattern of expression of proapoptotic Bcl-2 family proteins in CDDP and TDDP-treated SH-SY5Y cells

SH-SY5Y cells were treated with 10 μg/ml of CDDP or TDDP for the times (hours) indicated. Protein extracts were prepared at each timepoint and immunoblots were performed with antibodies specific for each proapoptotic Bcl-2 family protein (as indicated). Ponceau S staining or an ERK antibody were used to assess protein loading.

(a) The multidomain proapoptotic proteins

Bax and Bak did not change in level during CDDP and TDDP treatment of SH-SY5Y cells. Representative immunoblots are shown. Bax and Bak were probed on the same membrane following stripping. Tubulin is used as the loading control.

(b) The BH3-only proteins

Representative immunoblots are shown together with their corresponding loading controls (Tubulin, ERK or Ponceau S). Bad, Bid, Bim, Noxa, Hrk and Bmf did not consistently increase in level following CDDP or TDDP treatment. However, Bik showed a decrease in a 32 kDa band after 16 and 24 hours of CDDP treatment whereas a band of approximately 23 kDa appeared after 16 hours of CDDP treatment and increased in level at 24 hours of CDDP treatment.

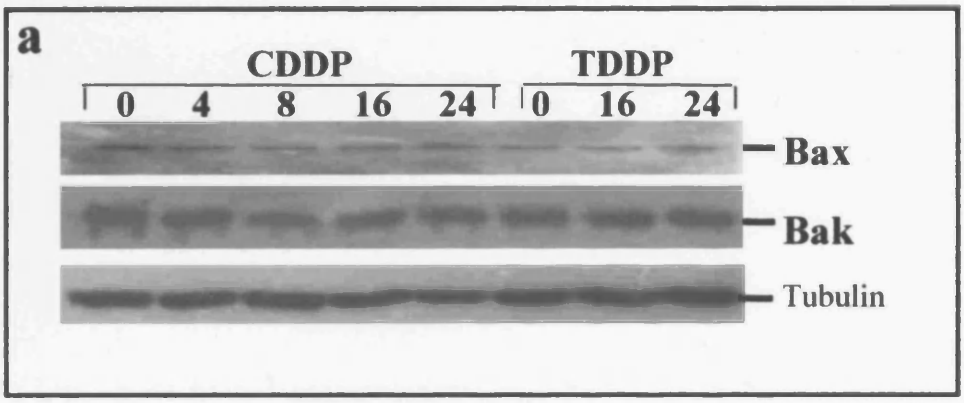
a
CDDP
TDDP
0 4 8 16 24
0 16 24
Bax
Bak
Tubulin

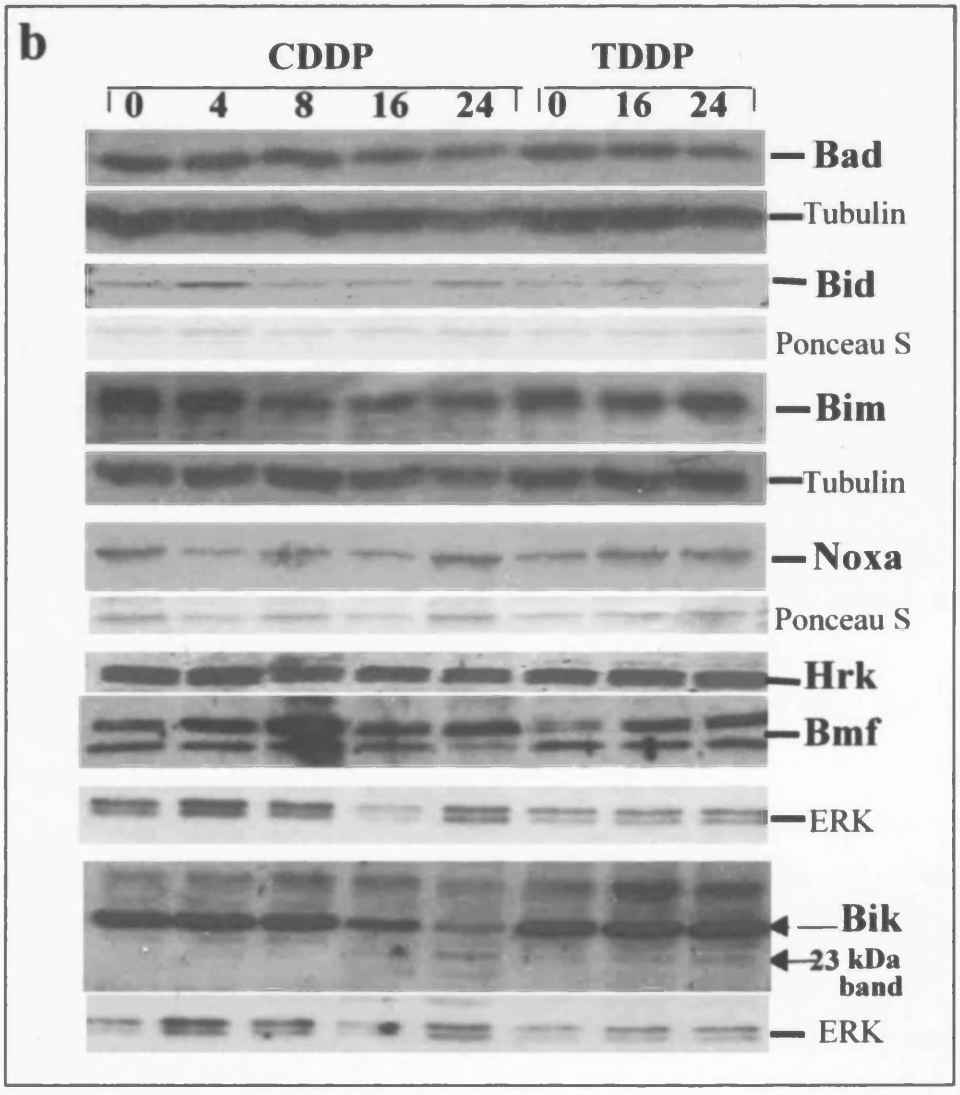
b
CDDP
TDDP
0 4 8 16 24
0 16 24
Bad
Tubulin
Bid
Ponceau S
Bim
Tubulin
Noxa
Ponceau S
Hrk
Bmf
ERK
Bik
23 kDa band
ERK

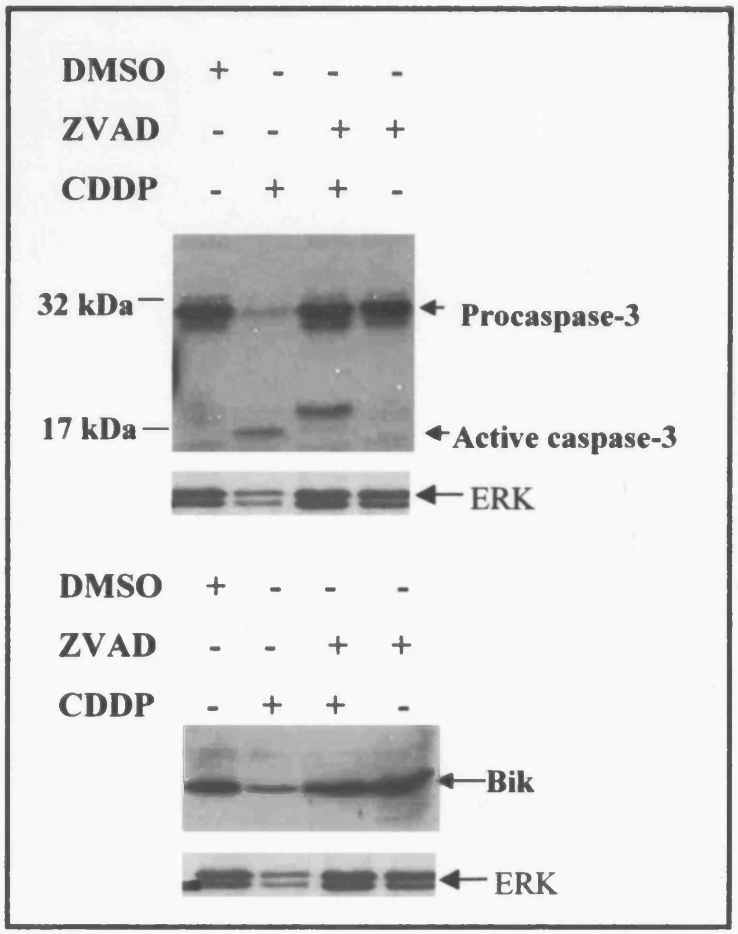

Figure 4.3 The CDDP-induced decrease in the level of full length Bik requires caspase activity

SH-SY5Y cells were treated with DMSO, 10μg/ml of CDDP, 100 μM ZVAD-fmk or CDDP together with ZVAD-fmk. Protein extracts were prepared after 16 hours and immunoblots were performed with antibodies specific for caspase-3 or Bik. Bik level decreased after CDDP treatment, but in cells treated with the caspase inhibitor ZVAD-fmk before and during CDDP treatment, Bik levels were similar to the controls. This indicates that the change in the level of Bik protein is caspase dependent and thus may not play a role in regulating cytochrome c release during CDDP-induced apoptosis in SH-SY5Y cells. Caspase-3 cleavage was studied in the same protein extracts as a control for the effect of ZVAD-fmk.

Figure 4.4 PUMA-α protein levels increase in CDDP-treated SH-SY5Y cells

(a) SH-SY5Y cells were treated with 10 μg/ml of CDDP or TDDP and protein constructs were prepared at the times indicated (up to 24 hours). Immunoblotting was performed with an antibody that recognises PUMA-α and -β. A representative PUMA immunoblot is shown. The PUMA antibody detected two bands. One of these increased in level from 8 hours of CDDP treatment whereas the other band did not reproducibly change in level. No change was detected in either band following TDDP treatment. Tubulin was used as loading control and this showed that the amount of protein loaded in each lane was relatively equal.

(b) Identification of the PUMA-α band in SH-SY5Y cells. Expression vectors for FLAG-tagged PUMA-α and PUMA-β were transfected into Cos-7 cells. CMV-Neo was transfected as a negative control. Protein extracts were prepared and run alongside extracts from SH-SY5Y cells treated with CDDP (10 μg/ml) for 8 hours (C8) or TDDP (10 μg/ml) for 16 hours (T16). The proteins were then transferred to nitrocellulose and immunoblotting was performed with the anti-PUMA antibody. The higher molecular weight band detected in the SH-SY5Y cells extracts is likely to be PUMA-α. The lower molecular weight band is larger than FLAG-tagged PUMA-β and is therefore non-specific.

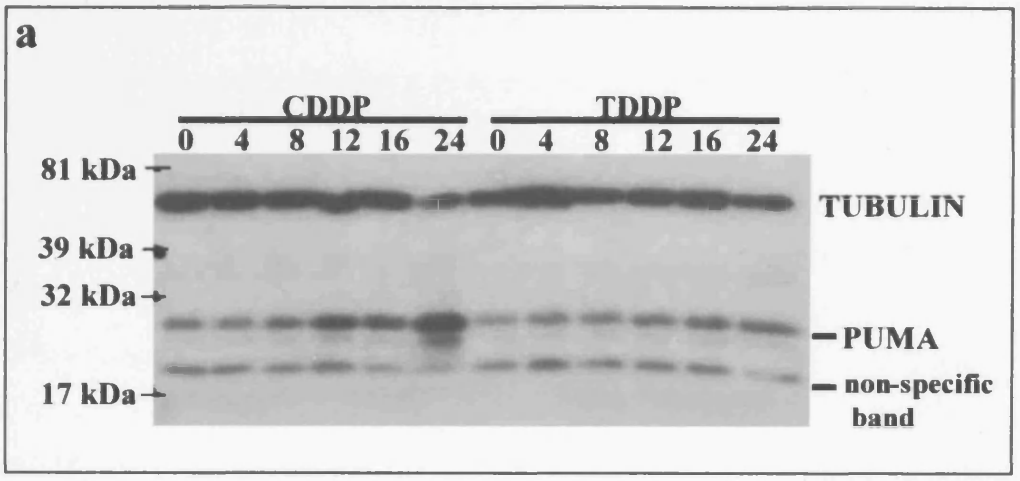
a
CDDP
TDDP
0 4 8 12 16 24 0 4 8 12 16 24
81 kDa
39 kDa
32 kDa
17 kDa
TUBULIN
PUMA
non-specific band

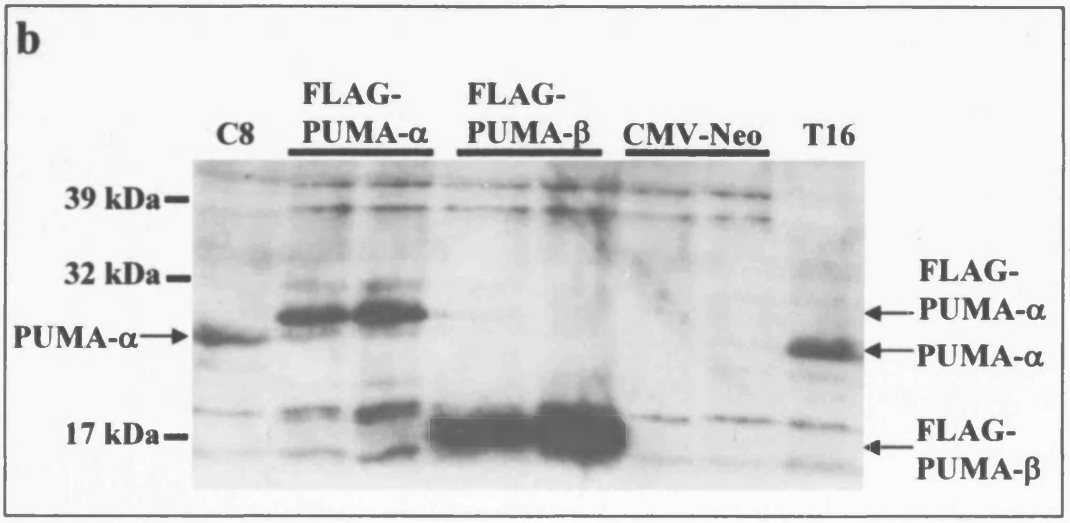
b
C8
FLAG-PUMA-α
FLAG-PUMA-β
CMV-Neo
T16
39 kDa
32 kDa
PUMA-α
17 kDa
FLAG-PUMA-α
PUMA-α
FLAG-PUMA-β

is probably non-specific since it was larger than the FLAG-tagged 18 kDa PUMA-β protein. So, PUMA-α increases in level in SH-SY5Y cells treated with CDDP starting between 8 to 12 hours (Figure 4.4a).

I next investigated whether the increase in PUMA-α levels was independent of caspase activity (**Figure 4.5a**). SH-SY5Y cells treated with CDDP with or without ZVAD-fmk were used to prepare protein extracts for immunoblotting experiments, with antibodies specific for p53 and its target PUMA. The proteins were detected using ECL reagents and there was no difference in pattern between the CDDP-treated and CDDP with ZVAD-fmk-treated cells. This indicates that changes in the level of both p53 and PUMA are upstream of caspase activation. PUMA could therefore play a role in regulating cytochrome c release, which leads to caspase activation in CDDP-treated SH-SY5Y cells.

Three independent PUMA immunoblots were quantitated on a densitometer and PUMA-α levels were normalised to the tubulin loading control to determine the relative level of PUMA protein at various times during CDDP and TDDP treatment. The average values and their standard error of the mean (SEM) were plotted (**Figure 4.5b**). The level of PUMA-α protein increased up to 6-fold on average in CDDP-treated cells whereas there was no significant change in its level following TDDP treatment.

4.2.3 *PUMA* mRNA levels increase during CDDP-induced apoptosis in SH-SY5Y cells

To determine whether the increase in the level of the PUMA protein was due to an increase in the level of *PUMA* mRNA, RT-PCR experiments were performed with total RNA extracted from SH-SY5Y cells treated with CDDP and TDDP and primers specific for PUMA. The structure of the human PUMA gene is shown in **Figure 4.6a**. As a result of alternate splicing several different transcripts are produced which encode the proteins PUMA-α, -β and -δ. PUMA-α and -β are BH3-only proteins. The position of the RT-PCR primers used is indicated. These primers can detect the three transcripts which encode PUMA-α, β and δ. In the case of SH-SY5Y cells several PCR products were observed on agarose gels (**Figure 4.6b**). The different bands were extracted from the gel,

Figure 4.5 The change in the level of PUMA-α protein is caspase-independent and PUMA increases in level by up to 6-fold after CDDP treatment.

(a) Induction of p53 and PUMA by CDDP is caspase independent

p53 and PUMA-α protein levels in cells treated with DMSO (**D**), 10μg/ml of CDDP (**C**) or CDDP (10μg/ml) and ZVAD-fmk (**CZ**) were analysed by immunoblotting. No change was observed between CDDP treatment and treatment with both ZVAD-fmk and CDDP. This indicates that the changes in p53 and PUMA-α protein levels are independent of caspase activity. Representative immunoblots are shown.

(b) Quantification of PUMA induction

The level of PUMA-α protein was measured on a densitometer and normalised to the level of tubulin. PUMA-α increases in level by up to 6-fold during CDDP treatment whereas there is no significant increase with TDDP treatment in SH-SY5Y cells. The results shown are the average of three independent experiments ± SEM. The level of PUMA-α protein was significantly higher in cells that had been treated with CDDP for 24 hours compared to time zero. * $p<0.05$, Student's t-test. In the case of cells treated with TDDP for 24 hours the level of PUMA-α was not significantly different to the level at time zero. $p=0.792$, Student's t-test.

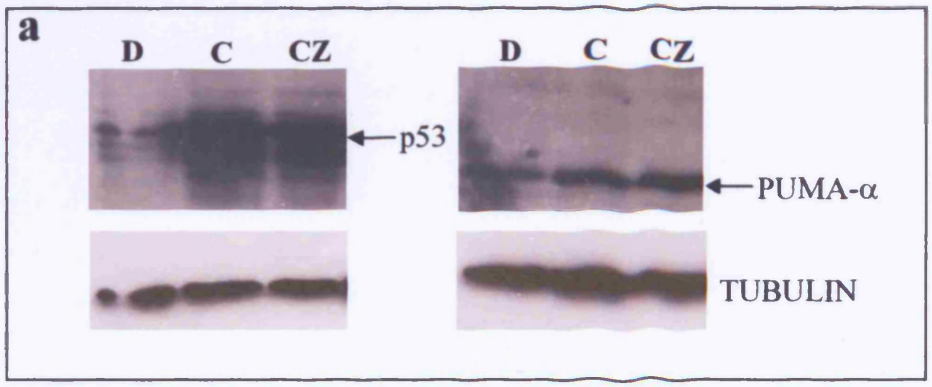
a
D
C
CZ
D
C
CZ
p53
PUMA-α
TUBULIN

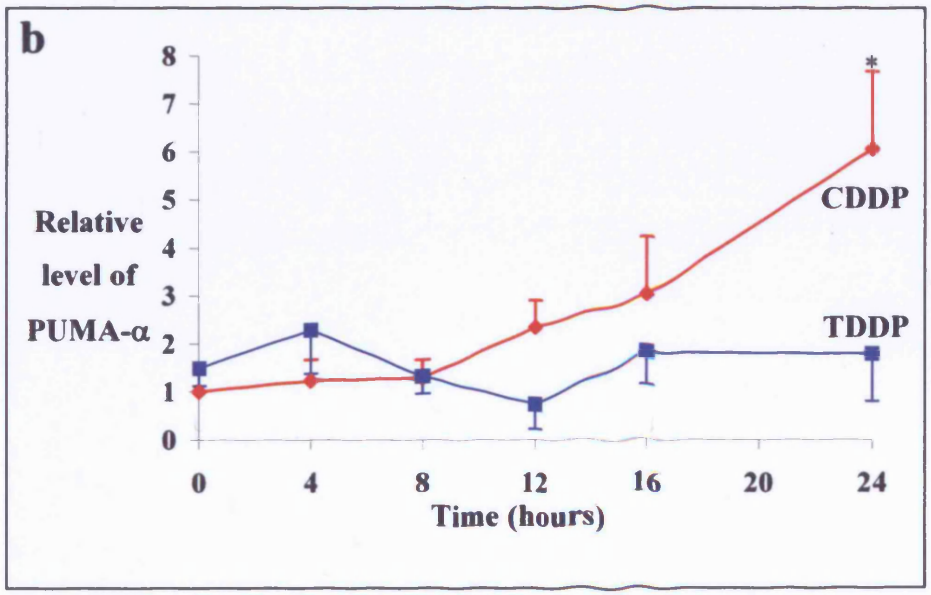
b
Relative level of PUMA-α
8
7
6
5
4
3
2
1
0
*
CDDP
TDDP
0
4
8
12
16
20
24
Time (hours)

Figure 4.6 Characterisation of PUMA transcripts in CDDP-treated SH-SY5Y cells.

(a) Structure of the human PUMA gene

Alternate splicing of the PUMA mRNA generates the three transcripts shown, which encode PUMA-α, β and δ as indicated as found by Nakano and Vousden, (2001) and transcript 4 was identified by Yu *et al.* (2001) to also encode PUMA-α. Exons are shown as orange boxes. The position of the RT-PCR primers used in my experiments is shown on Exon 1b and Exon 4 (red arrows). Transcript 1 is the longest transcript containing two long open reading frames: one ORF starts in Exon 2 and encodes PUMA-α, the BH3 domain is in Exon 3 and the other initiates at exon 1b to encode a protein with no known homology, PUMA-γ. The other BH3-domain containing protein, PUMA-β is encoded by transcript 2 with its initiation codon in Exon 1b. Transcript 4 described by Yu *et al.* (2001) to encode PUMA-α contains Exon 1a and not Exon 1b (as with Nakano and Vousden, 2001). The position of a p53 binding site in the PUMA gene is indicated. Transcript 3 contains Exons 1b and 4 and encodes the PUMA-δ protein initiating from exon 1b with no BH3 domain. This figure is based on Figure 1 in Nakano and Vousden, 2001.

(b) PUMA transcripts in CDDP-treated SH-SY5Y cells

RT-PCR was performed using PUMA-specific primers and total RNA extracted from CDDP-treated SH-SY5Y cells. The PCR products were run on a 1.5% agarose gel. The bands observed were extracted from the gel, cloned into the pGEM-T Easy vector and sequenced. The positions of the PUMA-α, -β and -δ transcripts are indicated.

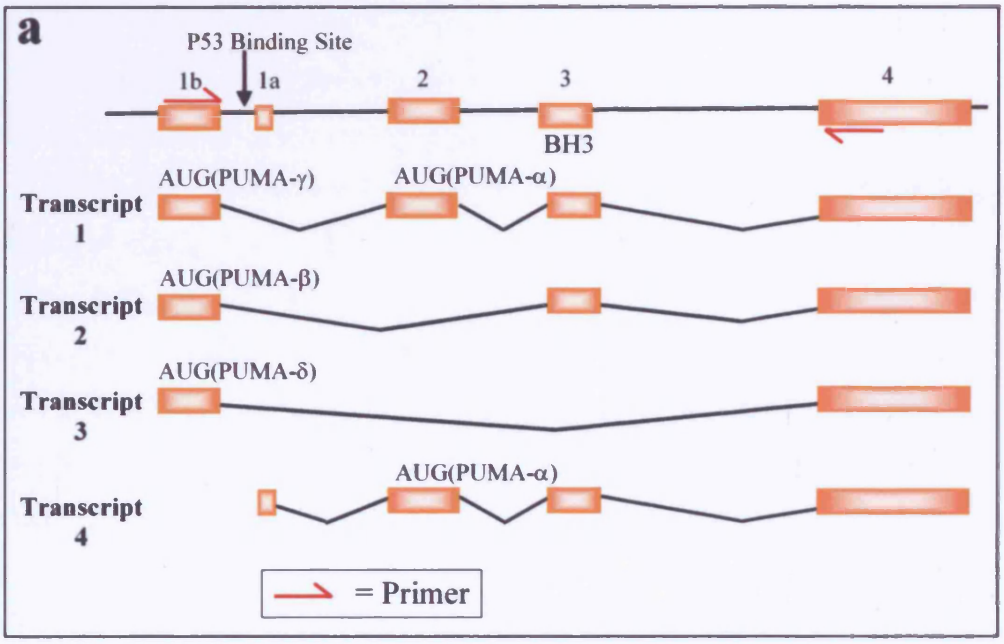
a
P53 Binding Site
1b
1a
2
3
4
BH3
AUG(PUMA-γ)
AUG(PUMA-α)
Transcript 1
AUG(PUMA-β)
Transcript 2
AUG(PUMA-δ)
Transcript 3
AUG(PUMA-α)
Transcript 4
= Primer

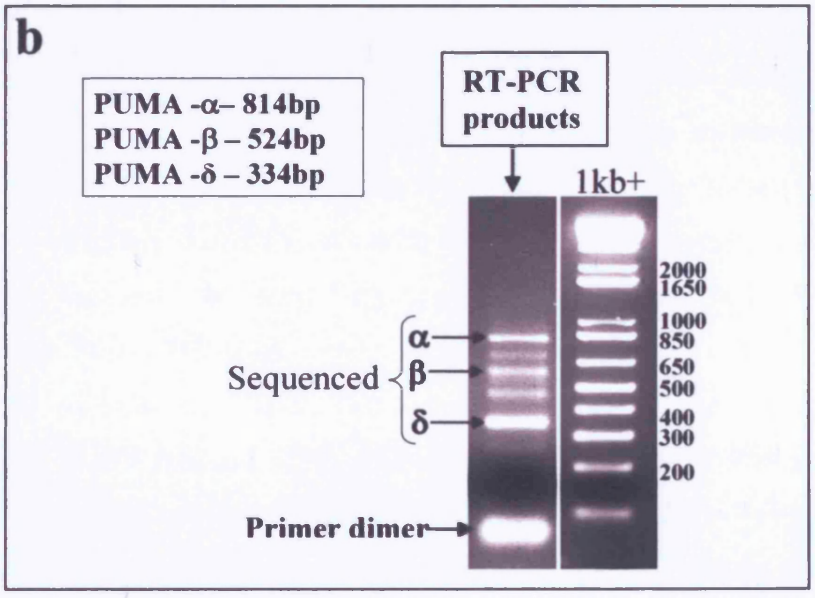
b
PUMA -α– 814bp
PUMA -β – 524bp
PUMA -δ – 334bp
RT-PCR products
1kb+
2000
1650
1000
850
650
500
400
300
200
Sequenced
α
β
δ
Primer dimer

cloned and sequenced to determine their identity. **Figure 4.6b** shows which of the bands correspond to the three PUMA transcripts that encode PUMA-α, -β and -δ. The other bands between these PCR products varied in intensity from experiment to experiment and were usually less abundant. When cloned and sequenced, they were found to contain some regions of homology to PUMA but it was not possible to conclude whether they were artefacts of the PCR conditions used or genuine alternative transcripts present in SH-SY5Y cells.

Timecourse experiments were performed to determine whether the PUMA transcripts changed in level in SH-SY5Y cells treated with CDDP and TDDP (**Figure 4.7**). The PUMA-α transcript increased in level in CDDP-treated cells (**Figure 4.7a**). Three independent experiments were performed and the relative level of the PUMA-α transcript was determined (**Figure 4.7b**). The PUMA-α transcript increased within the first 8 hours after CDDP treatment and reached a peak after 16 hours. There was only a minor change in its level in TDDP-treated cells.

4.2.4 Overexpression of PUMA-α promotes apoptosis in SH-SY5Y cells

Since PUMA-α increased in level after CDDP treatment, I investigated whether overexpression of PUMA-α was sufficient to induce apoptosis in SH-SY5Y cells and whether the BH3 domain was required for this. To answer these questions, I transfected SH-SY5Y cells with a GFP expression vector, to mark the transfected cells, and the other expression vectors were pCMVneoBam, pCMVneoBam-FLAG-PUMA-α and pCMVneoBam-FLAG-ΔLRR-PUMA-α (provided by K.Vousden, CRUK; Nakano and Vousden, 2001). Cells were transfected at a 1:3 ratio of GFP: PUMA expression vector (**Figure 4.8a**). Representative images are shown in **Figure 4.8a** showing that the cells transfected with the Flag-tagged expression vector also co-express the GFP protein. Since the two proteins were co-expressed in transfected cells, I was able to simplify the cell staining procedure by omitting the incubation step with the FLAG antibody and its secondary mouse antibody. Consequently, I only counted the cells expressing GFP. In experiments to block caspase activity, ZVAD-fmk was added to the SH-

Figure 4.7 RT-PCR analysis of *PUMA* mRNA induction in SH-SY5Y cells

(a) RT-PCR analysis of *PUMA* mRNA levels in CDDP-treated SH-SY5Y cells

Representative RT-PCR timecourse showing that *PUMA* mRNA levels increase in SH-SY5Y cells during CDDP-induced apoptosis. *PUMA* mRNA was amplified using the PCR primers specific for Exon 1b and Exon 4 of the PUMA gene. PCR products were run on a 1.5% agarose gel alongside the 1 kb^+ DNA ladder. RT-PCR reactions were also performed with GAPDH-specific primers as a control. The position of the PUMA-α transcript (transcript 1) is indicated.

(b) Relative level of the PUMA-α transcript compared to GAPDH in SH-SY5Y cells treated with CDDP and TDDP

The PUMA-α transcript at each timepoint was quantitated using the gel image (**Figure 4.7a**) and by setting the level of the most saturated PUMA-α band as the level to which the bands at other timepoints were compared. The values were normalised to the amount of GAPDH to give the relative level. The relative level of *PUMA-α* mRNA was then plotted against time after addition of CDDP and TDDP. The PUMA-α transcript increases up to 8-fold peaking at 16 hours of CDDP treatment. The graph represents the average of at least three independent RT-PCR experiments ± SEM.

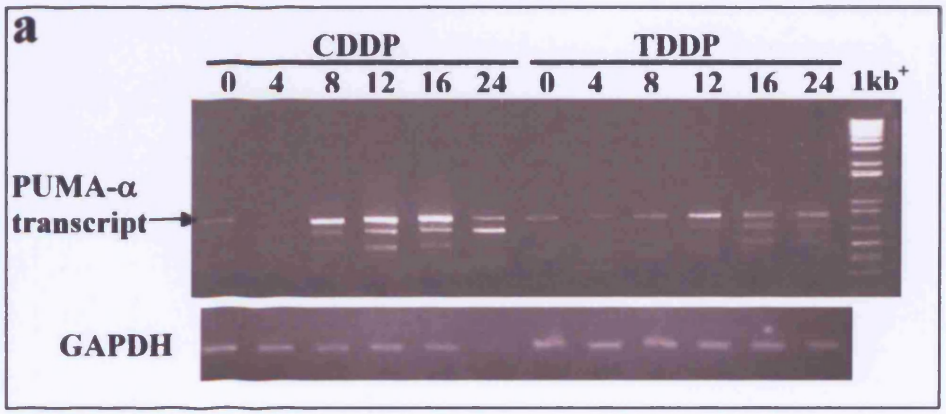
a
CDDP
TDDP
0 4 8 12 16 24 0 4 8 12 16 24 1kb+
PUMA-α transcript
GAPDH

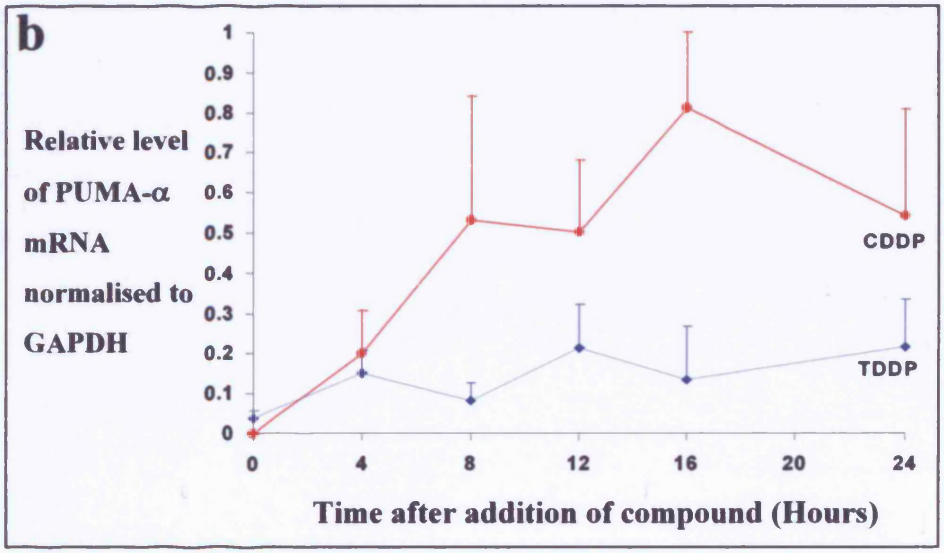
b
Relative level of PUMA-α mRNA normalised to GAPDH
1
0.9
0.8
0.7
0.6
0.5
0.4
0.3
0.2
0.1
0
0 4 8 12 16 20 24
CDDP
TDDP
Time after addition of compound (Hours)

SY5Y medium at a concentration of 100 μM after the transfection medium had been aspirated.

At 16 hours after transfection, the number of transfected GFP-expressing cells (green cells) was determined by counting green cells in ten fields of view along each coverslip. This corresponded to 500-600 green cells on average for the empty pCMVneoBam vector (**Figure 4.8b**). Cells were then prepared for immunofluorescence and stained with Hoechst dye to visualise nuclear morphology. Around 200 GFP expressing cells were counted per coverslip and their nuclear morphology was recorded to calculate the percentage of *attached* transfected cells undergoing apoptosis (**Figure 4.8c**).

At first, it seemed as if the PUMA-α expression vector had a low transfection efficiency because the number of GFP positive cells in 10 fields was approximately 100 times less than in the pCMVneoBam-FLAG-ΔLRR-PUMA-α and pCMVneoBam transfections. However, treatment with ZVAD-fmk showed that this low number of GFP positive cells is due to cells being lost through caspase-dependent apoptosis, which ZVAD-fmk rescued (**Figure 4.8b**). The percentage of apoptotic and normal nuclei in 200 of the transfected cells was also determined and the average of three independent experiments was plotted (**Figure 4.8c**). The results suggest that overexpression of PUMA-α tends to increase the percentage of pyknotic nuclei compared to the control vector and this is reversed by ZVAD-fmk. Furthermore the BH3-domain was essential, as a construct expressing the BH3 mutant of PUMA-α did not induce an increase in the percentage of pyknotic nuclei or cell death in SH-SY5Y cells compared to the empty vector control. The number of cells transfected with the FLAG-PUMA-α vector that had apoptotic nuclei was higher than the controls, this difference was not significant (Student's t-test) as might be expected. This could be due to the cell staining procedure which involves a number of washing steps during which it is possible that many cells at advanced stages of apoptosis were washed off.

4.2.5 Construction and characterisation of PUMA siRNA expression vectors

It will be important to determine whether PUMA-α is essential for CDDP-induced apoptosis in SH-SY5Y cells. As a tool for such studies I constructed

Figure 4.8 Overexpression of FLAG-PUMA-α in SH-SY5Y cells induces caspase-dependent cell death and this requires a functional BH3-domain

SH-SY5Y cells were transfected with a GFP expression vector together with pCMVneoBam, pCMVneoBam-FLAG-PUMA-α or pCMVneoBam-FLAG-ΔLRR-PUMA-α. Cells were transfected at a 1:3 ratio of GFP: PUMA expression vector. ZVAD-fmk was added to the SH-SY5Y medium at a concentration of 100 μM to block caspase activity, as indicated.

(a) SH-SY5Y cells were transfected with the GFP expression vector and pCMVneoBam-FLAG PUMA-α and were fixed at 16 hours after transfection and stained with the FLAG-specific M2 monoclonal antibody and Rhodamine-conjugated anti-mouse antibody followed by Hoechst dye, as described in the Methods section. Representative images are shown of transfected SH-SY5Y cells expressing FLAG-PUMA-α **(A)** and EGFP **(B)** and stained with Hoechst to reveal nuclear morphology **(C).** The arrow indicates a transfected cell co-expressing the Flag-tagged PUMA protein and EGFP **(D).** It has a pyknotic nucleus **(C).**

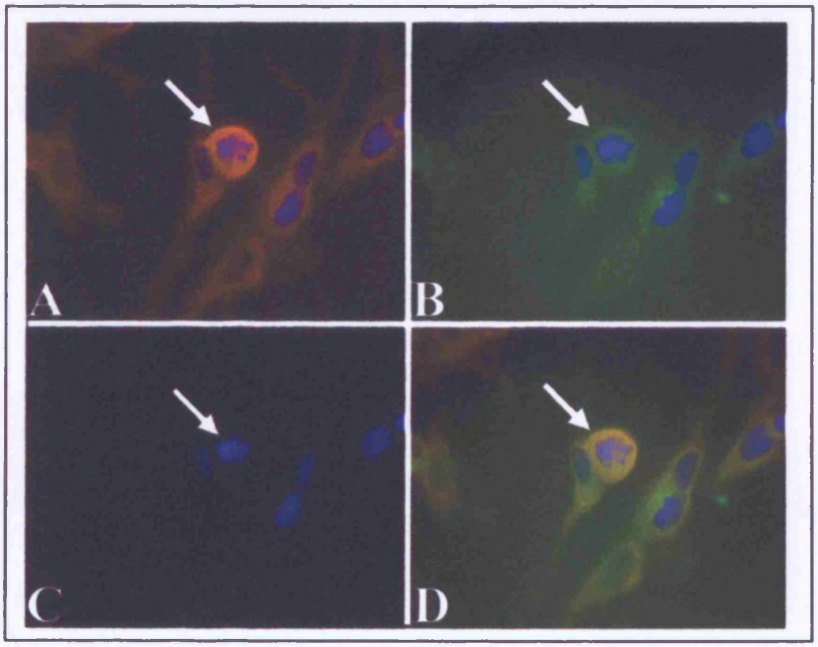

Figure 4.8 (continued)

(b) At 16 hours after transfection, the number of green GFP-expressing transfected cells was determined in ten fields of view along each coverslip. In the case of cells transfected with the empty vector pCMVneoBam or the BH3 mutant expression vector (FLAG-ΔLRR-PUMA-α) there were 500-600 GFP positive cells per field. However, when cells were transfected with the PUMA-α expression vector there were 100 X fewer GFP positive cells. ZVAD-fmk treatment rescued nearly all of the cells transfected with the PUMA-α expression vector. The average ± SEM for three independent experiments is shown.

(c) After the number of GFP expressing cells had been determined, the cells were prepared for immunofluorescence and stained with Hoechst dye to reveal nuclear morphology. Around 200 cells per coverslip were counted and their nuclear morphology was recorded to calculate the percentage undergoing apoptosis. The number of apoptotic and normal nuclei in 200 of the transfected cells was determined and the average values for three independent experiments were plotted with the SEM. The figure shows that overexpression of PUMA-α induces a caspase-dependent increase in the percentage of pyknotic nuclei and this effect requires the PUMA BH3 domain. Even though the trend is towards an increase in pyknotic nuclei with PUMA-α overexpression but with the average of three experiments, this difference is not significant and more experiments are necessary.

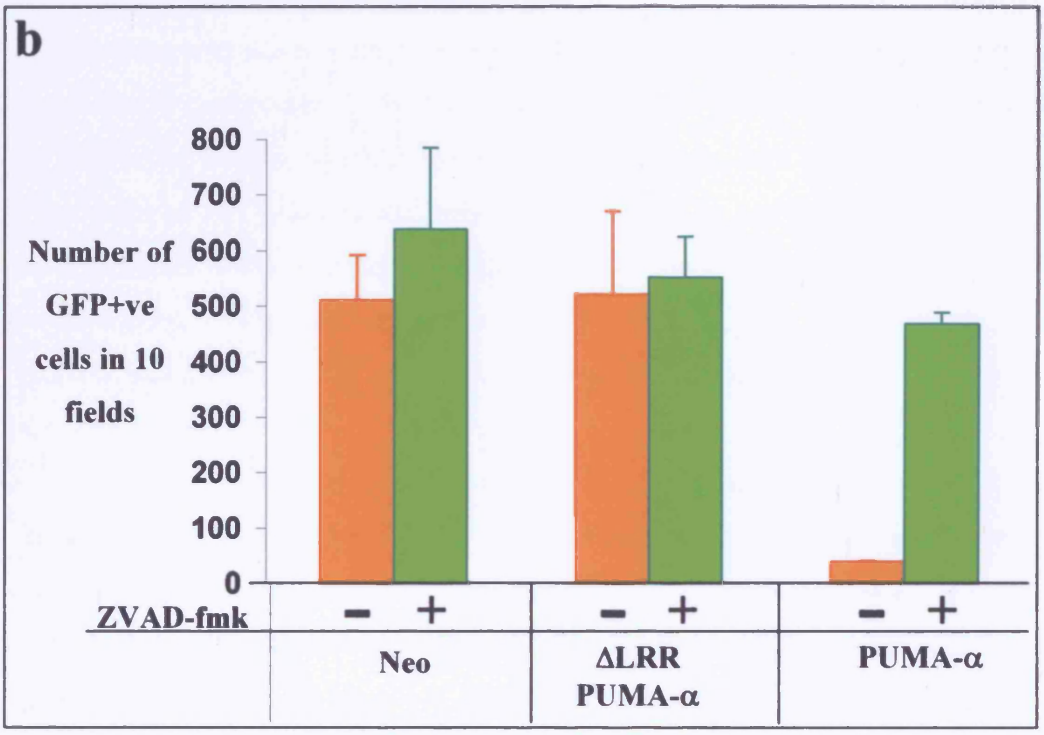
b
800
700
Number of 600
GFP+ve 500
cells in 10 400
fields 300
200
100
0
ZVAD-fmk
- + - + - +
Neo
ΔLRR
PUMA-α
PUMA-α

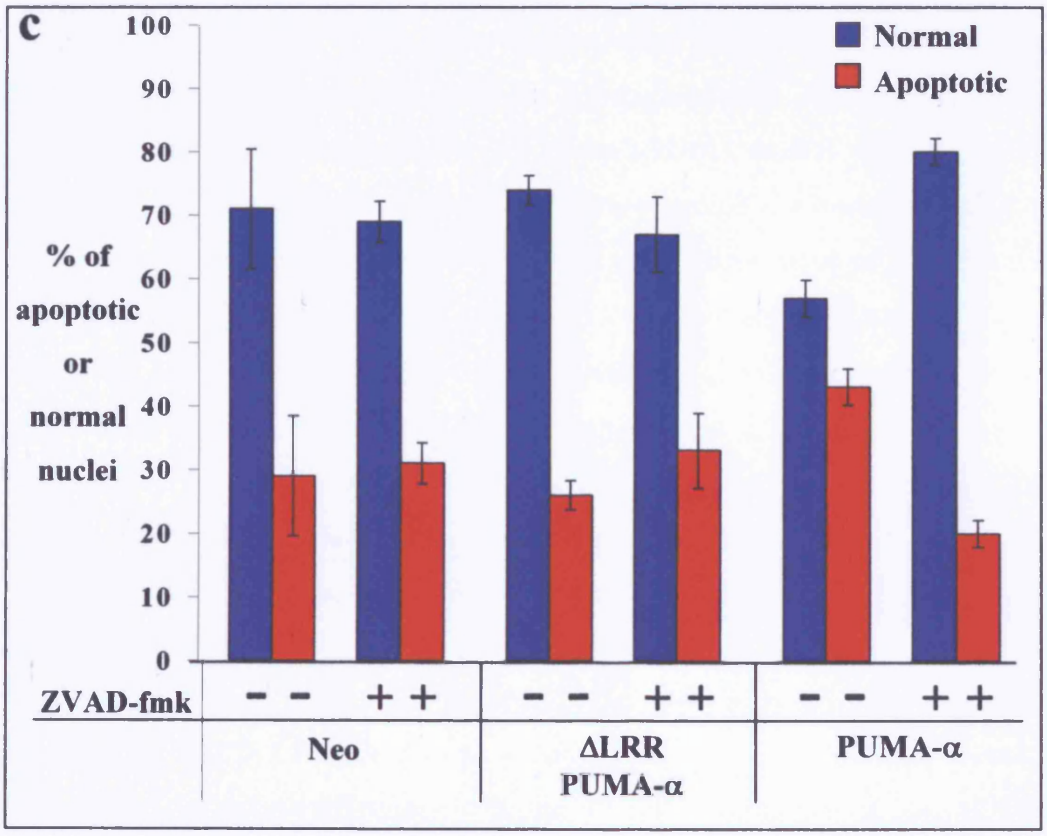
c
100
90
80
70
% of 60
apoptotic 50
or
normal 40
nuclei 30
20
10
0
Normal
Apoptotic
ZVAD-fmk
- - + + - - + + - - + +
Neo
ΔLRR
PUMA-α
PUMA-α

expression vectors for siRNAs specific for human PUMA-α. Using Oligoengine software, 64 nucleotide double stranded oligonucleotides were designed and cloned into pSUPER digested with BglII and HindIII (**Figure 4.9a**). The 19 nucleotide targets were selected according to the following criteria: to not contain stretches of four or more consecutive T or A residues, to have 30 –70% overall GC content, to lie within the coding sequence of the target, to begin with a G or C residue, to begin after an AA dimer in the 5' flanking sequence, to end just prior to a TT, TG or GT doublet in the 3' flanking sequence, to not contain *XhoI* or *EcoRI* restriction enzyme sites, to share minimal sequence identity with other genes (assessed by a BLAST search) and to not overlap with other 19 nucleotide targets selected from the same target sequence.

Plasmids with inserts were identified by digesting the miniprep DNA with EcoRI and HindIII (**Figure 4.9b**). The constructs were then sequenced using the T3 and T7 primers to identify inserts with the correct DNA sequence. In order to find the most efficient siPUMA construct, initial experiments involved transfecting SH-SY5Y cells with the FLAG-PUMA-α expression vector and either pSUPER or the pSUPER siPUMA constructs for 16 hours with 50 μM ZVAD-fmk (to reduce PUMA-induced death). At 16 hours after transfection, protein was extracted and immunoblotting was performed using the PUMA antibody. **Figure 4.9c** shows a representative PUMA immunoblot. All of the siPUMA constructs tested reduced the level of the over-expressed FLAG-PUMA-α protein. Constructs 452.1 and 518.1 appeared to be the most effective and reduced the level of overexpressed PUMA-α by 67% (**Figure 4.9d**). Although I was not able to completely knock down the level of overexpressed PUMA-α with the siPUMA constructs in these pilot experiments the siPUMA vectors might have a greater effect on the endogenous PUMA-α, which is present at much lower levels during CDDP treatment. This could be investigated by co-transfecting SH-SY5Y cells with a GFP expression vector and pSUPER or the siPUMA constructs. The transfected cells would then be treated with or without CDDP for 16 hours to induce the endogenous PUMA protein and the transfected GFP expressing cells would be isolated by FACS. PUMA protein levels in the GFP positive cells would be determined by immunoblotting with the PUMA antibody. If the siPUMA constructs effectively knock down the level of the endogenous PUMA protein their

effect on CDDP-induced death could be investigated using the GFP co-transfection assay described in **Figure 4.8**.

Figure 4.9 Construction and preliminary characterisation of siPUMA expression vectors.

(a) Overview of how functional siRNA is produced by the pSUPER RNAi system

The silencing of a specific gene can be carried out by cloning a 64 nucleotide (nt) double stranded oligonucleotide, that contains a unique 19-nucleotide sequence derived from the mRNA transcript of the targeted gene, followed by a spacer and the inverse 19 nt sequence into the pSUPER vector between the unique BglII and HindIII enzyme sites. In this position, the oligo is downstream of the H1 promoter and is transcribed to generate a transcript that can form a short hairpin structure with a 19 base-pair double-stranded region and a short loop formed by the spacer region. The hairpin has been designed to be an optimal substrate for the enzyme Dicer, which cleaves the hairpins to generate the short double-stranded siRNA.

(b) Screening for siPUMA constructs by restriction enzyme digestion

Plasmids with inserts of 285 bp were identified by digesting miniprep DNA with EcoRI and HindIII and then running the digested DNA on a 2% agarose gel alongside the 1 kb DNA ladder. Eight DNA samples of each of the three siPUMA constructs (**437**, **452** and **518**) were selected for restriction enzyme digest. The pSUPER construct (**P**) was digested with EcoRI and HindIII to release a 227 bp band (indicated by ✱) and run alongside the miniprep DNA as a control.

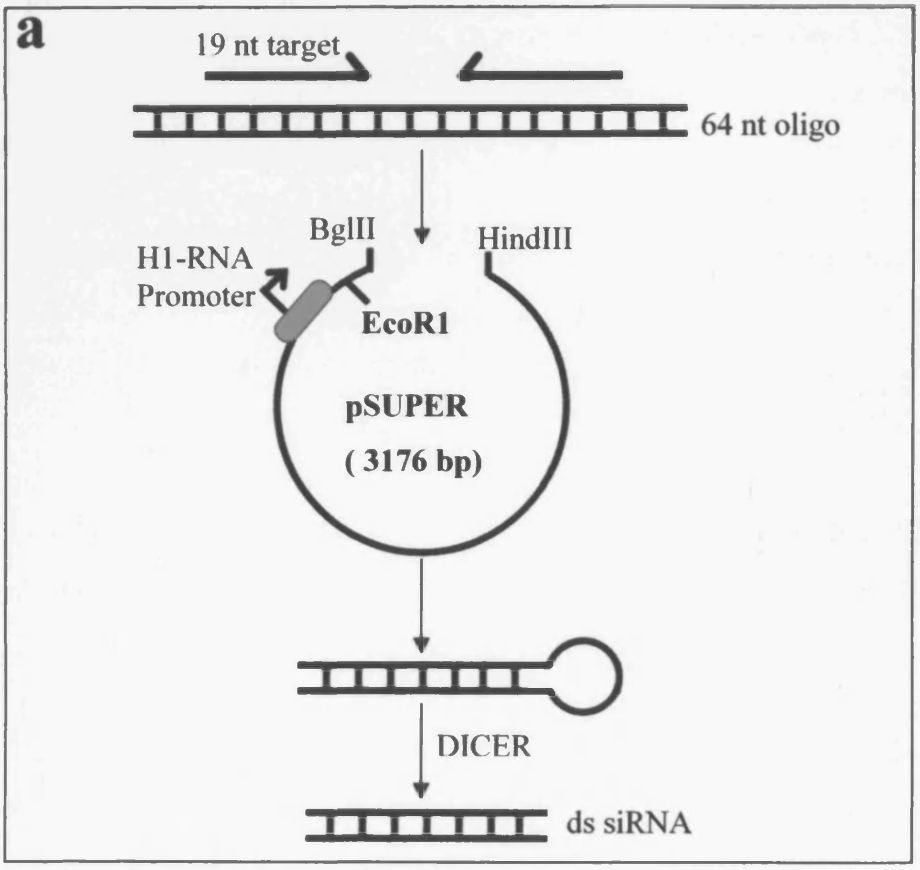
a
19 nt target
64 nt oligo
BglII
HindIII
H1-RNA
Promoter
EcoR1
pSUPER
(3176 bp)
DICER
ds siRNA

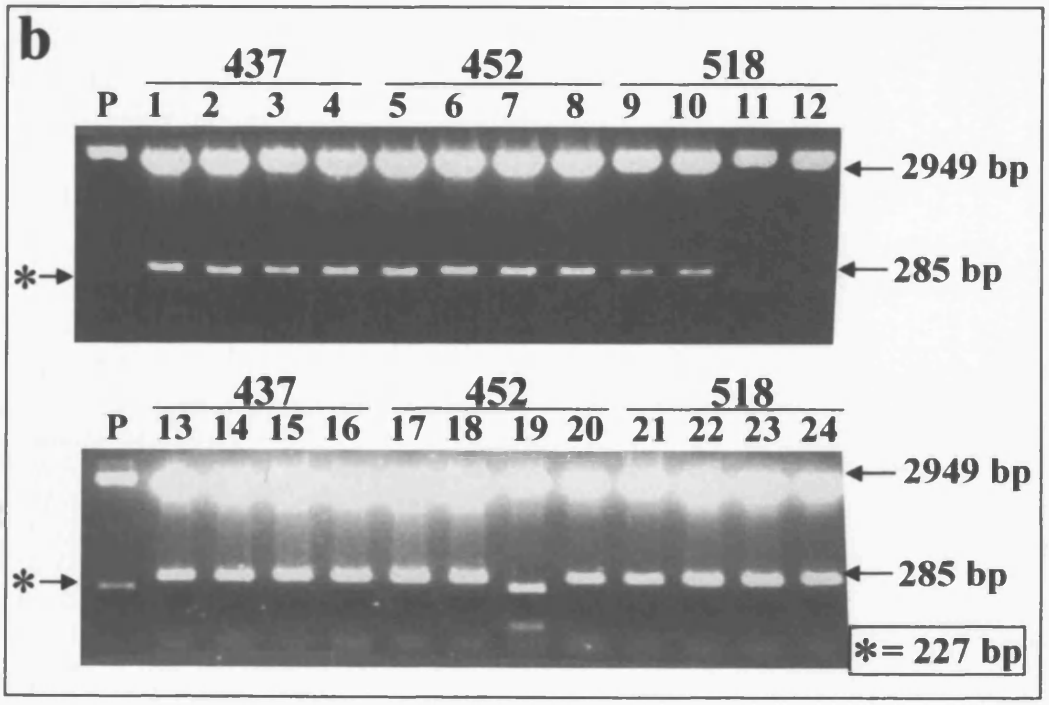
b
437
452
518
P 1 2 3 4 5 6 7 8 9 10 11 12
2949 bp
285 bp
437
452
518
P 13 14 15 16 17 18 19 20 21 22 23 24
2949 bp
285 bp
*= 227 bp

Figure 4.9 (continued)

(c) PUMA-α protein expression in co-transfected SH-SY5Y cells

SH-SY5Y cells were transfected with the FLAG-PUMA-α expression vector and either pSUPER or the pSUPER siPUMA constructs as indicated. The transfected cells were treated with 50 μM ZVAD-fmk to reduce PUMA-induced cell death. At 16 hours after transfection, protein extracts were prepared and immunoblotting was performed with antibodies specific for PUMA or tubulin. The representative immunoblot shows a reduction in PUMA-α expression with the siPUMA constructs.

(d) Average level of PUMA-α protein

PUMA-α protein levels were determined by scanning immunoblots on a densitometer and were normalised to the level of tubulin. The average level of PUMA-α protein was calculated for three independent experiments. The siPUMA constructs 452.1 and 518.1 reduced FLAG-PUMA-α levels by 67%. The average ± SEM for three independent experiments is shown.

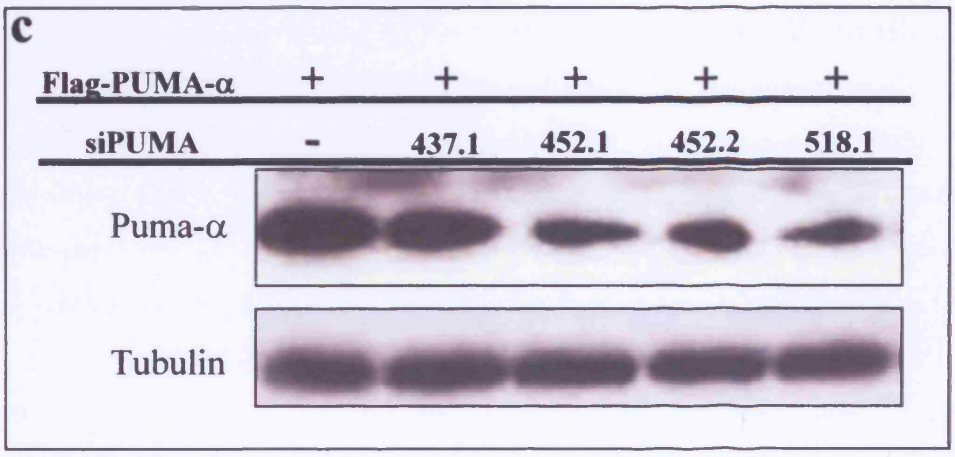
c
Flag-PUMA-α + + + + +
siPUMA - 437.1 452.1 452.2 518.1
Puma-α
Tubulin

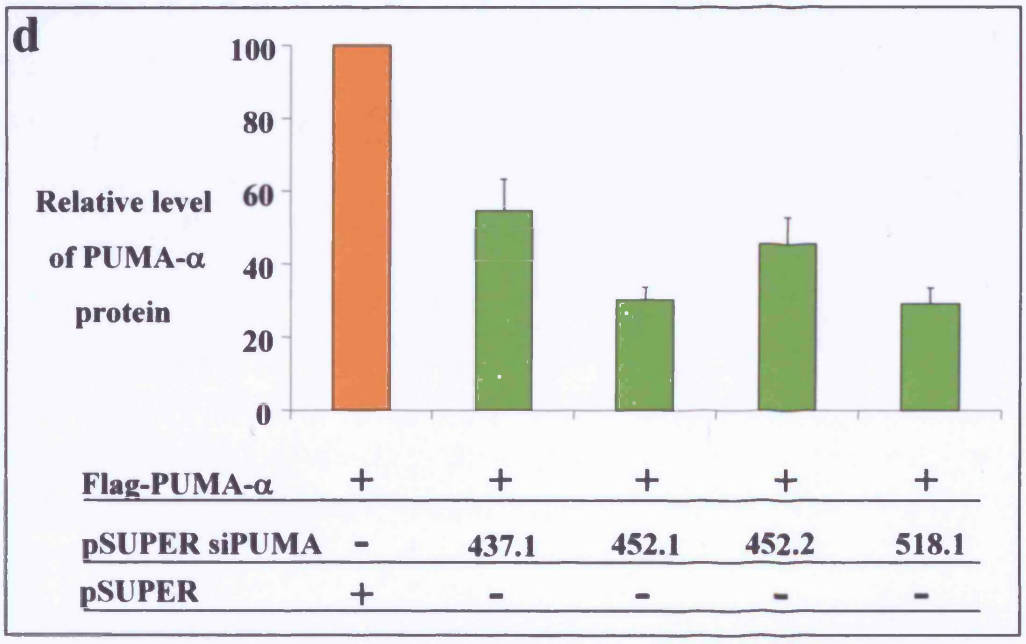
d
Relative level of PUMA-α protein
100
80
60
40
20
0
Flag-PUMA-α + + + + +
pSUPER siPUMA - 437.1 452.1 452.2 518.1
pSUPER + - - - -

4.4 Discussion

Bcl-2 family proteins regulate the release of cytochrome c and other proapoptotic molecules from the mitochondria. In this chapter, I investigated which members of the Bcl-2 family might play a role in the regulation of mitochondrial permeability during CDDP-induced apoptosis of SH-SY5Y cells. Western blotting was performed to determine whether any changes occur in the pattern of expression of Bcl-2 family proteins. The antiapoptotic Bcl-2 family members Bcl-2, Bcl-x_L and Bcl-w, did not consistently change in level but Mcl-1 levels decreased reproducibly after 8 hours of CDDP treatment. This change in the level of Mcl-1 protein is a result of caspase activity since it was prevented by ZVAD-fmk. However, we did not observe any of the Mcl-1 fragments generated by caspase cleavage that had been previously reported (Clohessy *et al.*, 2004; Weng *et al.*, 2005). There are two caspase cleavage sites in the human Mcl-1 protein, which results in the formation of three fragments. The three fragments are an N-terminal fragment from amino acids 1 to 127, a long C-terminal fragment from amino acids 128-350 (Δ127) and a shorter C-terminal fragment from amino acids 158-350 (Δ157). The Mcl-1 antibody used by the two groups is Santa Cruz sc-19, which was raised against a peptide from amino acid 121-139 in human Mcl-1 and which can detect the Δ127 fragment but not Δ157 fragment. However, in SH-SY5Y cells, Δ127 was not observed, even at longer exposure. This suggests that the caspase-regulated cleavage of Mcl-1 in CDDP-treated SH-SY5Y cells occurs by a mechanism different to that previously observed with other cell types. The decrease in Mcl-1 is unlikely to cause cytochrome c release because the latter is caspase-independent in CDDP-treated SH-SY5Y cells as shown by treatment with ZVAD-fmk.

The multidomain proapoptotic proteins Bax and Bak did not change in level in CDDP-treated cells. Bax has previously been reported to be a transcriptional target of p53 but this does not appear to be the case in SH-SY5Y cells. However, it would be interesting to investigate whether Bax translocates from the cytosol to the mitochondrial outer membrane by performing subcellular fractionation followed by immunoblotting or by immunocytochemistry. Indeed, Makin *et al.*, (2001) demonstrated that CDDP induced translocation of Bax and exposure of the N-

terminus of Bax in SH-SY5Y cells, even though Bax expression did not change under these conditions.

The BH3-only proteins Bad, Bid, Bim, Noxa, Hrk and Bmf did not show any consistent change during CDDP treatment in SH-SY5Y cells. It cannot be excluded that Bad phosphorylation changes during CDDP treatment and this would need to be assessed using appropriate phospho-Bad-specific antibodies. This is possible because it has previously been shown that p53 can activate the transcription of PTEN, a phosphatase that inhibits PI3K-Akt signalling (Stambolic *et al.*, 2001). Bid did not increase during CDDP treatment and did not appear to be cleaved, which is consistent with the data presented in the previous chapter showing that SH-SY5Y cells do not express caspase-8.

A recent study suggests that Bik induction is required to initiate early release of Ca^{2+} from the endoplasmic reticulum, mitochondrial fragmentation, and activation of the mitochondrial cytochrome c release pathway (Mathai *et al.*, 2005). In SH-SY5Y cells, the level of Bik protein decreased after 8 hours of CDDP treatment but remained constant during TDDP treatment. A smaller molecular weight band appeared after 16 hours and this increased in level at 24 hours of CDDP treatment. Human Bik is a phosphoprotein that migrates as a doublet at 24-25 kDa in immunoblots (Verma *et al.*, 2001). When SH-SY5Y cells were treated with both CDDP and ZVAD-fmk there was no decrease in Bik level suggesting that the CDDP-induced change in Bik depends upon caspase activity and thus Bik may not be a key regulator of cytochrome c release during CDDP-induced apoptosis in SH-SY5Y cells. I checked the human Bik protein sequence for the presence of potential caspase cleavage sites. Thirteen Asp residues were identified in the sequence and the three residues N-terminal to Asp were examined to identify any homology to known caspase cleavage sites (Thornberry *et al.*, 1997). I identified three possible candidates ($SEED^{38}$, $DEMD^{69}$ and $DIRD^{102}$) with some similarity to the caspase-3 cleavage site DEVD. Future work could involve identifying which of these possible caspase cleavage sites may be involved in the down regulation of Bik during CDDP treatment in SH-SY5Y cells.

Since the aim of my work was to identify the Bcl-2 family member that regulates the release of cytochrome c, the role of Mcl-1 and Bik was not pursued further since their downregulation was reversed by ZVAD-fmk. Nevertheless, to

have a complete understanding of the mechanism by which CDDP induces apoptosis in SH-SY5Y cells, it would be interesting to understand why Mcl-1 and Bik downregulation occurs. For example, does this contribute to the feed-forward amplification of the apoptotic signal once caspases are activated (clohessy, bjh, 2004, weng, jbc, 2005)?

PUMA, another BH3-only protein and a direct transcriptional target of p53, increased in level by up to 6-fold during CDDP treatment but did not increase during TDDP treatment. *PUMA-α* mRNA levels increased within the first 8 hours after CDDP treatment and reached a peak after 16 hours. PUMA was initially identified as a gene activated by p53 in cells undergoing p53-induced apoptosis (Nakano and Vousden, 2001; Yu *et al.*, 2001) and as a protein interacting with Bcl-2 (Han *et al.*, 2001). The *PUMA* gene contains a p53 binding site in its first intron and rapid induction of *PUMA* mRNA showed *PUMA* to be a direct transcriptional target of p53. Nakano and Vousden, (2001) described four PUMA transcripts, whereas Yu *et al.* (2001) reported only one. Yu *et al.* describe their transcript to contain exon 1a and not exon 1b (as with Nakano and Vousden, 2001) (**Figure 4.6a**). The exon 1a-containing transcript encodes the protein that Vousden and Yu name PUMA-α, which is functionally identical to PUMA-β. However, both groups identify the same p53 binding site so p53 dependent activation will lead to expression of a pro-apoptotic BH3 domain protein regardless of which first exon is used. Expression of the PUMA locus is complex due to extensive splicing and the presence of alternative open reading frames. Only PUMA-α and PUMA-β contain the BH3 domain, interact with Bcl-2 and Bcl-x_L, and localise to the mitochondria. However, this localisation is not dependent on the presence of the BH3 domain. The BH3 domain is essential for the efficient induction of apoptosis by both PUMA-α and PUMA-β. PUMA-δ does not contain the BH3 domain, does not interact with Bcl-2 and has no growth-inhibitory or apoptotic activity. Yu *et al.* (2003) showed using colorectal cancer cells that PUMA-induced apoptosis depends on the presence of Bax, which undergoes multimerisation when PUMA is induced.

Overexpression of PUMA-α shows a trend towards an increase in apoptotic nuclei when compared to the normal and BH3-mutated constructs (Figure 4.8c). However, this increase is not significant and more experiments will be required. SH-SY5Y cells detach when they undergo apoptosis, so many of these dying cells

would have been lost when counting the number of normal and apoptotic nuclei in PUMA-α overexpression without ZVAD-fmk. However, cells protected by ZVAD-fmk, will be attached and show normal nuclei even though PUMA-α overexpression may have already initiated apoptosis by cytochrome c release. This overexpression study needs to be supported by analysing cytochrome c release as shown in section 3.2.6.2.

Inhibition of PUMA expression will lead to a more comprehensive understanding of the role of PUMA-α in CDDP-induced apoptosis in SH-SY5Y cells. *PUMA* knockout mice replicate a majority of the apoptotic deficiencies observed in *p53* knockout mice. Apoptosis induced by DNA-damaging drugs and γ-irradiation (models for p53-induced apoptosis) were reduced by an extent similar to that observed in *p53* knockout mice (Jeffers *et al.*, 2003; Villunger *et al.*, 2003). The similar phenotypes of *PUMA* knockout mice and *p53* knockout mice suggest that PUMA is an essential p53 effector during apoptosis under some conditions. I aimed to study whether PUMA was essential for CDDP-induced apoptosis in SH-SY5Y cells by using RNA interference to suppress PUMA-α expression. I found that two of the four siPUMA constructs that I had designed and transfected into PUMA-α-overexpressing SH-SY5Y cells knocked down PUMA-α expression by two-thirds. The aim of future experiments will be to transfect one of these efficient siPUMA constructs into SH-SY5Y cells together with a GFP expression vector and then treat the cells with CDDP or DMSO. GFP-expressing transfected cells would be isolated by FACS and PUMA protein levels would be analysed by immunoblotting. If the siPUMA construct reduces the induction of PUMA-α by CDDP, I will investigate its effect on CDDP-induced death using the co-transfection assay described in section 4.2.5.

Another important question is to determine whether induction of PUMA in SH-SY5Y cells requires p53. RNAi technology could be used to suppress p53 expression in SH-SY5Y cells using the previously characterised pSUPERp53 construct developed by Agami *et al.*, (2002). Studies involving the suppression of p53 expression to determine whether PUMA levels increase in CDDP-treated SH-SY5Y cells would answer whether PUMA is a direct transcriptional target of p53 or whether as Melino *et al.* (2004) found in SAOS and HeLa cells, p73 contributes to PUMA induction and subsequent Bax translocation and cytochrome c release.

It is possible that p53 activates the transcription of other proapoptotic genes in CDDP-treated SH-SY5Y cells. In the experiments described in the next chapter, I attempted to acquire some information about what other genes could possibly play a role in CDDP-induced death of SH-SY5Y cells by using Affymetrix microarrays to analyse the expression of a large number of genes in SH-SY5Y cells treated with DMSO, TDDP and CDDP. See summary of results thus far (**Figure 4.10**).

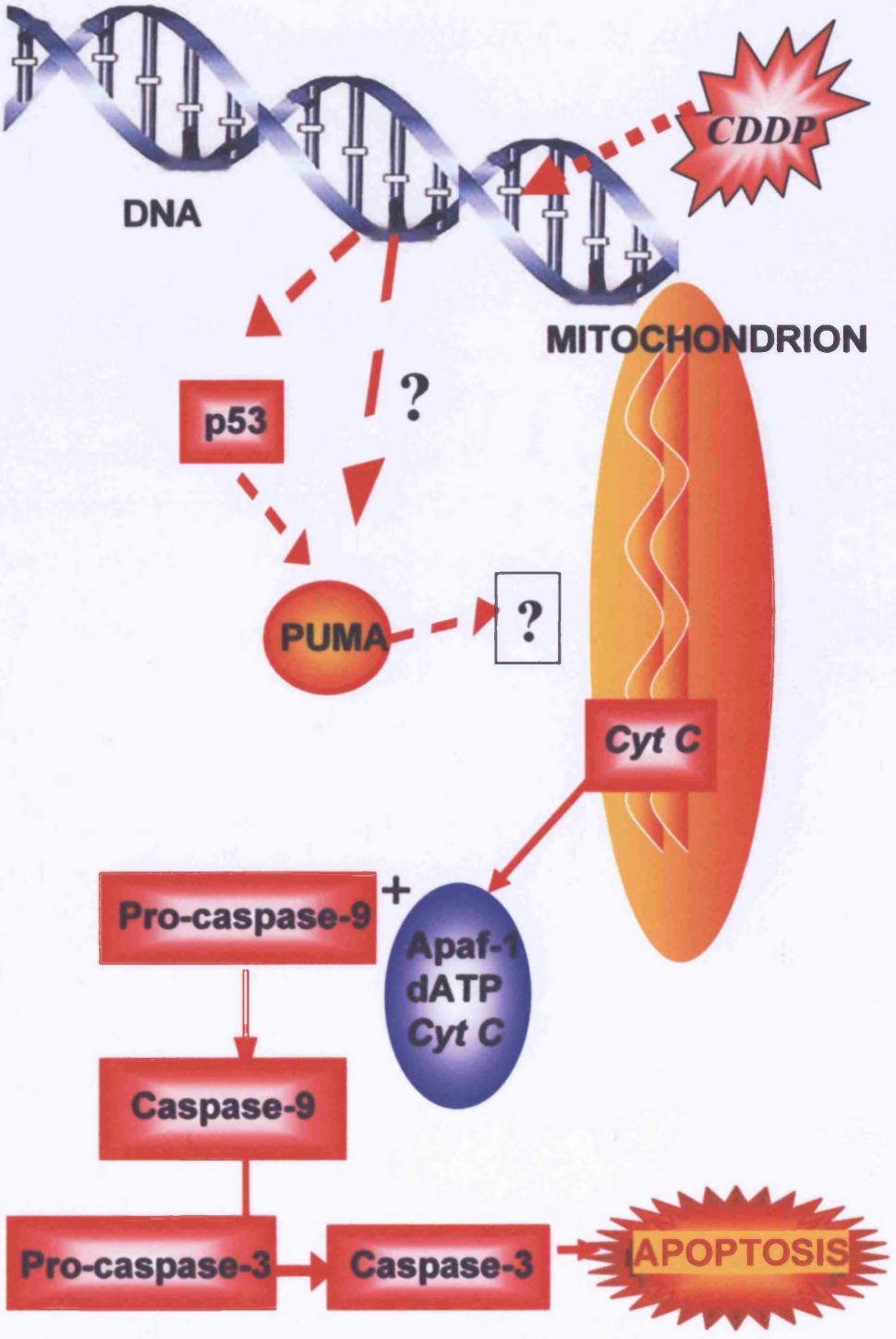

Figure 4.10 Hypothetical model of CDDP-induced death incorporating the results of chapter 4

Dotted lines indicate unknown mechanisms and future work.

Chapter 5: Microarray analysis of CDDP-induced apoptosis in SH-SY5Y cells

5.1 Introduction

I have shown in the previous chapters that CDDP induces apoptosis in SH-SY5Y cells via the intrinsic mitochondrial pathway with the release of cytochrome c leading to procaspase-9 cleavage and caspase-3 activation. I have also found an increase in the level of p53 protein during CDDP and TDDP treatment but to a much greater extent with the former. In the previous chapter, I described how PUMA-α RNA and protein levels increase during CDDP treatment and that overexpression of PUMA-α was sufficient to induce apoptosis in SH-SY5Y cells.

In this chapter, I describe experiments in which I used the Human Genome U133A microarray containing over 22,000 probe sets bound to a solid surface, each representing a single gene, splice variant, or other DNA element to study the gene expression profile of over 14,000 genes during treatment of SH-SY5Y cells with DMSO, TDDP and CDDP. The aim was to determine which mRNAs change significantly in level with CDDP but not with TDDP and DMSO treatment that could play a role in the apoptotic response in SH-SY5Y cells. Each high-density array provides multiple, independent measurements for each transcript. The multiple probes offer a complete data set with accurate, reliable, reproducible results from every experiment.

5.2 Results

5.2.1 Cell preparation for microarray analysis

SH-SY5Y cells were grown in three 10 cm dishes and prepared as described in section 2.2.7.1. When 90% confluent, the cells were treated with DMSO, CDDP and TDDP for 12 hours before RNA was extracted as described in section 2.2.9.1. Since I required a triplicate set of RNA samples for microarray analysis, cells from three different passages were grown and treated with DMSO, CDDP or TDDP when confluent (**Figure 5.1**). RNA was extracted using Trizol and following the chloroform step, the RNA pellets from each cell passage were stored under 75% ethanol at -20°C until all the RNA from triplicate experiments had been collected. I then continued to process the RNA samples from the triplicate experiments all together to limit variability in the experiments as described in section 2.2.9.1, except that RNA prepared for microarray analysis was not treated with DNase I nor was glycogen used as a carrier.

RNA concentration was determined by measuring the absorbance at 260 nm (A260) in a spectrophotometer using a quartz cuvette. A solution of RNA whose A_{260} = 1 contains approximately 40 μg of RNA per ml. RNA integrity was assessed by denaturing gel electrophoresis and ethidium bromide staining. The gel was run at 70 V in 1 X MOPS running buffer and viewed using a transilluminator (**Figure 5.2a**). In undegraded RNA preparations, the 28S ribosomal RNA band should appear twice as intense as the 18S ribosomal RNA band. If the RNA is degraded, this would appear as a smear of smaller sized RNAs or the 28S and 18S ribosomal RNA bands will show equal intensities. The figure clearly shows that the RNA prepared for microarray analysis was undegraded. This was also confirmed by running the RNA on a Bioanalyser chip (data not shown). In addition, the RNA was used for RT-PCR with the PUMA-α primers to confirm that the quality of the RNA was good. **Figure 5.2b** shows that following CDDP treatment the transcript encoding PUMA-α was present at higher concentrations than during TDDP treatment.

Figure 5.1 Experimental Design

The aim of the experiments described in this chapter was to use Affymetrix GeneChip® arrays to identify genes that change greatly in expression during CDDP treatment of SH-SY5Y cells and slightly or not at all with TDDP and DMSO treatment and then to go on to identify any functional role such genes may play in CDDP-induced apoptosis of SH-SY5Y cells. Cells were grown until 90% confluent then treated with CDDP, TDDP and DMSO for 12 hours prior to the extraction of total RNA for microarray analysis. RNA integrity was assessed by denaturing gel electrophoresis and also by running the RNA on a Bioanalyser chip. RT-PCR was also carried out on the RNA with primers for PUMA. After verifying that the RNA was of good quality, it was processed for Affymetrix Genechip Hybridisation (the picture in **Figure 5.2.1** is taken from www.affymetrix.com) and the data was analysed for changes in gene expression during CDDP induced-apoptosis in SH-SY5Y cells compared to TDDP and DMSO treatment.

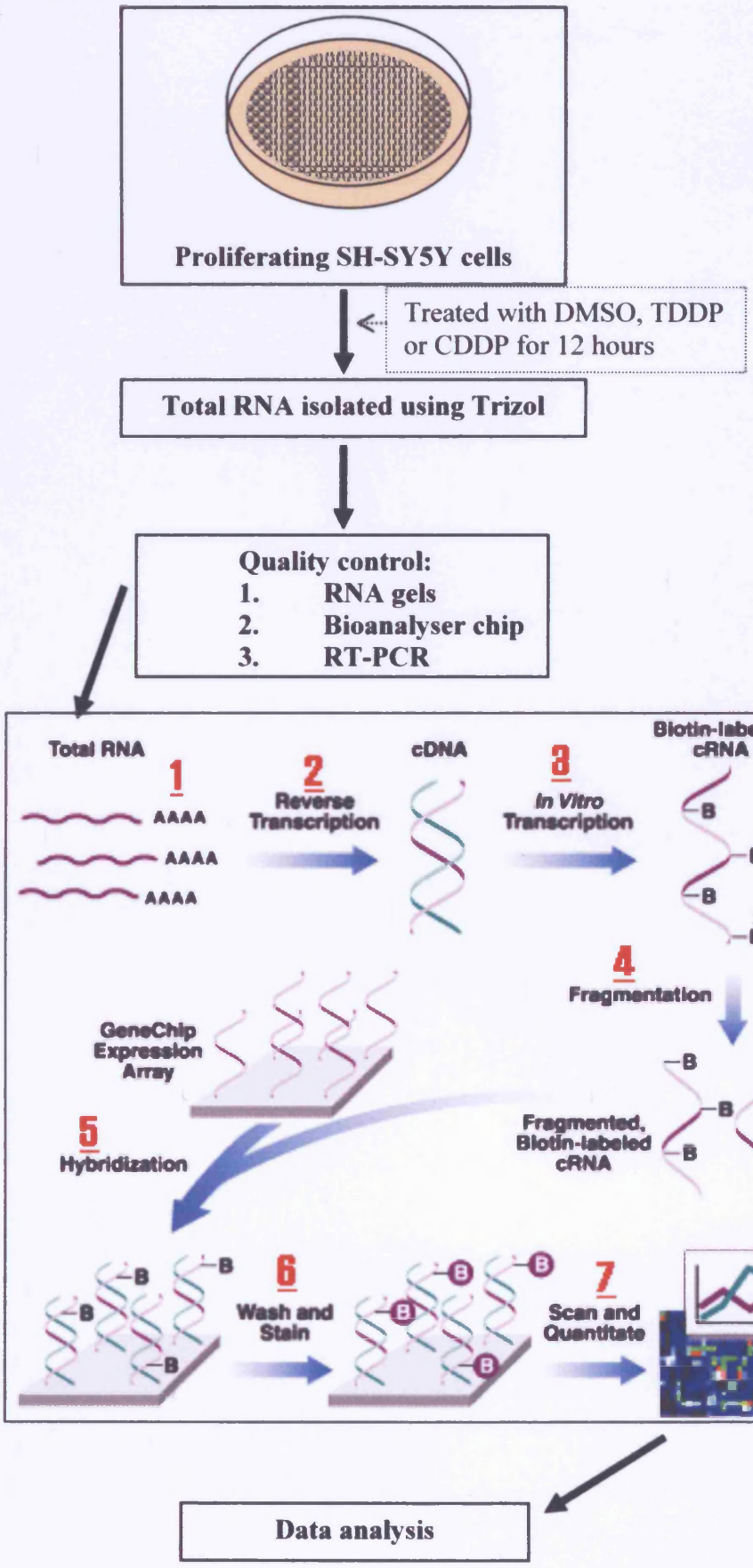
Proliferating SH-SY5Y cells
Treated with DMSO, TDDP or CDDP for 12 hours
Total RNA isolated using Trizol
Quality control:
1. RNA gels
2. Bioanalyser chip
3. RT-PCR
Total RNA
1
AAAA
AAAA
AAAA
2
Reverse Transcription
cDNA
3
In Vitro Transcription
Biotin-labeled cRNA
4
Fragmentation
Fragmented, Biotin-labeled cRNA
GeneChip Expression Array
5
Hybridization
6
Wash and Stain
7
Scan and Quantitate
Data analysis

Figure 5.2 Assessment of RNA integrity & quality

(a) Analysis of RNA integrity

RNA was run on a denaturing gel with ethidium bromide and analysed for degradation. Undegraded RNA shows a 2:1 ratio of the 28S: 18S ribosomal bands. Degraded RNA would appear as a smear of smaller sized bands or 28S and 18S would show similar intensities. The gel photo shows the integrity of the RNA from SH-SY5Y cells treated with CDDP (**C**), TDDP (**T**) or DMSO (**D**) in the triplicate set of experiments (**I**, **II** and **III**).

(b) *PUMA-α* mRNA expression

The level of the PUMA-α mRNA was greatly increased in the RNA samples prepared from CDDP (**C**) treated SH-SY5Y cells but was much lower following TDDP (**T**) or DMSO (**D**) treatment.

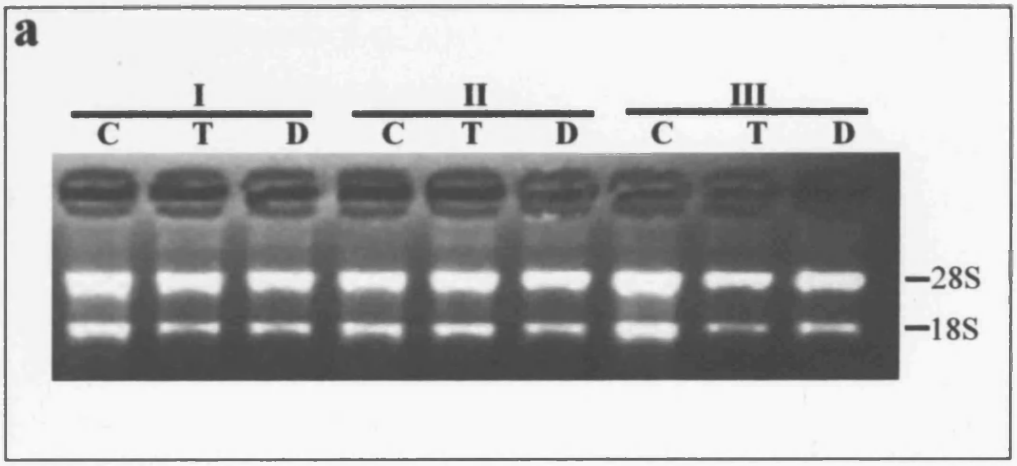
a
I
II
III
C T D C T D C T D
28S
18S

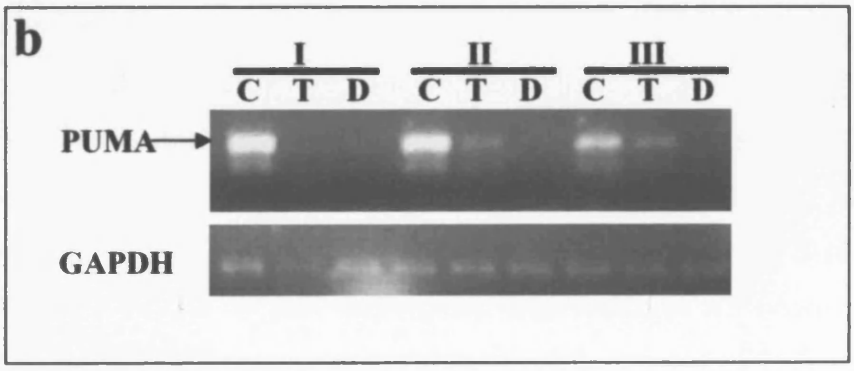
b
I
II
III
C T D C T D C T D
PUMA
GAPDH

5.2.2 Affymetrix GeneChip® Hybridisation

Biotin-labelled cRNA was prepared from the total RNA using a T7-$(dT)_{24}$ primer and the Superscript Choice system (Gibco), and BioArray™ HighYield™ RNA Transcript labelling kit (ENZO) and then purified using Qiagen RNeasy columns. The purified labelled cRNA was fragmented and hybridised to the Affymetrix Human Genome U133A Array, which contains 22,283 human gene cDNA probes. Three independent experiments were performed to assess array reproducibility. The procedure of processing total RNA for Affymetrix GeneChip® Hybridisation was performed by Danielle Fletcher as described in the Affymetrix GeneChip® Expression Analysis Manual.

5.2.3 Statistical analysis of microarray data

The data collected from the three independent experiments via Affymetrix GeneChip® Hybridisation was analysed using Genespring 5 software. All 22,283 genes found (**Figure 5.3a**) were normalised to the median within and across the arrays. Genes detected in at least one treatment condition (DMSO, CDDP or TDDP) are shown in **Figure 5.3b**. 3,312 genes showed a greater than 1.5 fold change and PUMA was included in this (**Figure 5.3c**). However, in order to reduce the number of genes for analysis, stringency was increased to detect genes that showed a greater than 2 fold change between TDDP and CDDP. 1014 genes were detected and 864 genes passed the MTC and Benjamini-Hochberg test (**Figure 5.3d**). These genes were analysed and classified according to their function and their average relative level during DMSO, TDDP and CDDP treatment. Some of the genes analysed are represented in **Figure 5.4**.

Figure 5.3 Analysis of the SH-SY5Y microarray data

(a) All 22,283 genes detected

All genes found on the Human Genome U133A micro arrays were normalised to the median fluorescence. The figure shows the log of the normalisation to the median of intensity per-chip and per-gene. Normalising per chip was done where the signal of each gene is divided by the median intensity of the chip to control variations between the arrays and normalisation per gene was done to account for the difference in detection efficiency of each probe. This also scales the relative gene expression levels for comparison. The y-axis represents normalised intensity (log scale).

(b) Genes detected in at least one treatment condition

The data is filtered to remove the genes that show no change in gene expression during the three treatment conditions. The graph shows the median expression of the triplicate experiments for each gene during DMSO, TDDP and CDDP treatment. The yellow lines represent the expression of each gene during the three treatment conditions. Some of the genes with high expression during CDDP treatment are shown (white lines). The y-axis represents normalised intensity (log scale).

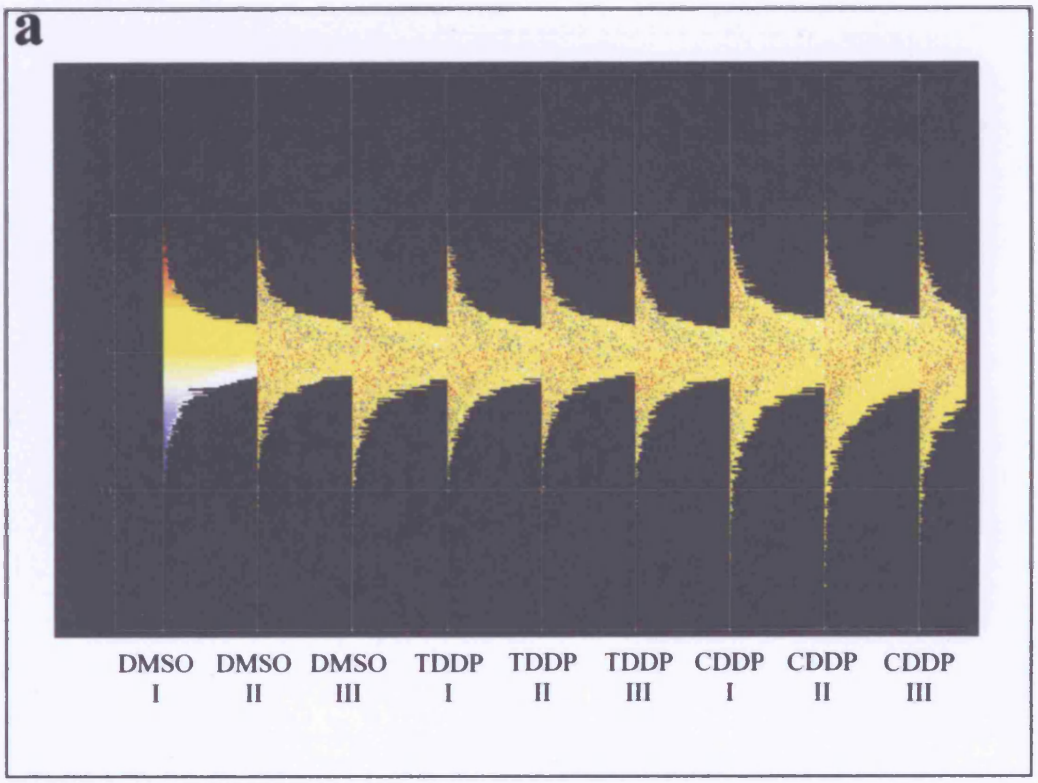
a
DMSO I
DMSO II
DMSO III
TDDP I
TDDP II
TDDP III
CDDP I
CDDP II
CDDP III

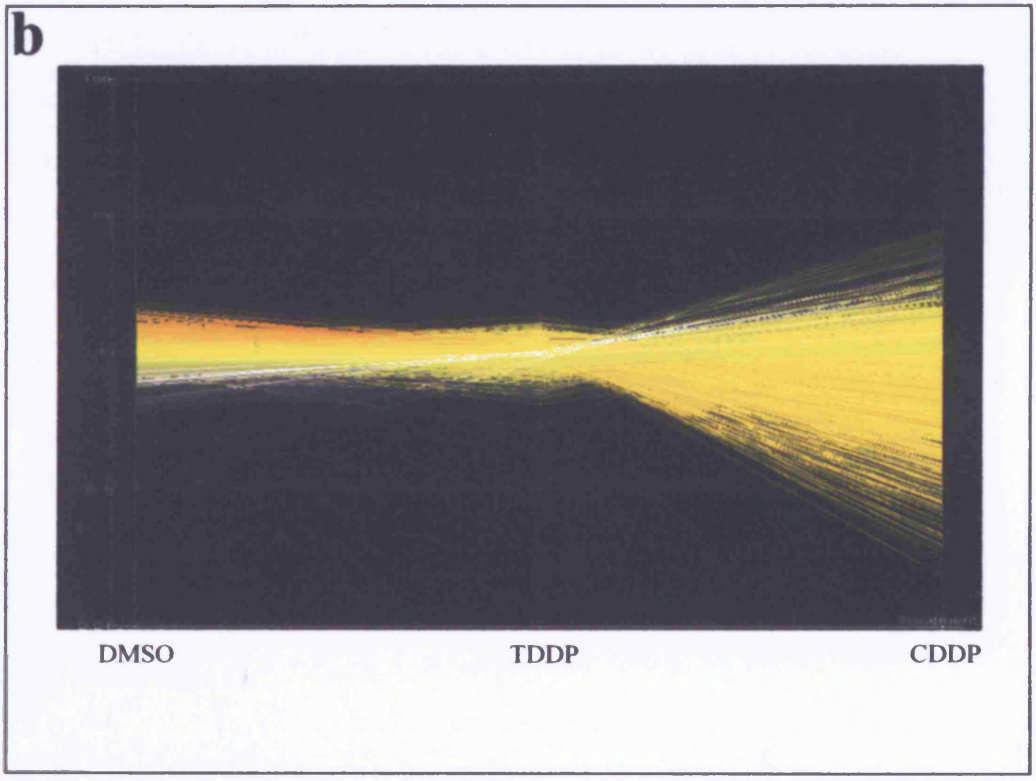
b
DMSO
TDDP
CDDP

(c) Genes showing greater than 1.5 fold change

3,312 genes showing a greater than 1.5 fold change in gene expression between TDDP and CDDP. PUMA expression is indicated by a red line. The y-axis represents normalised intensity (log scale).

(d) Genes showing greater than 2 fold change

All 22,283 genes found were normalised to the median within and across the arrays. The figure represents the intensity of 1,014 genes detected based on ANOVA and a 2-fold change in gene expression between TDDP and CDDP. White lines show some of the genes that are upregulated with CDDP treatment. 864 of these genes passed MTC and Benjamini-Hochberg tests. The y-axis represents normalised intensity (log scale).

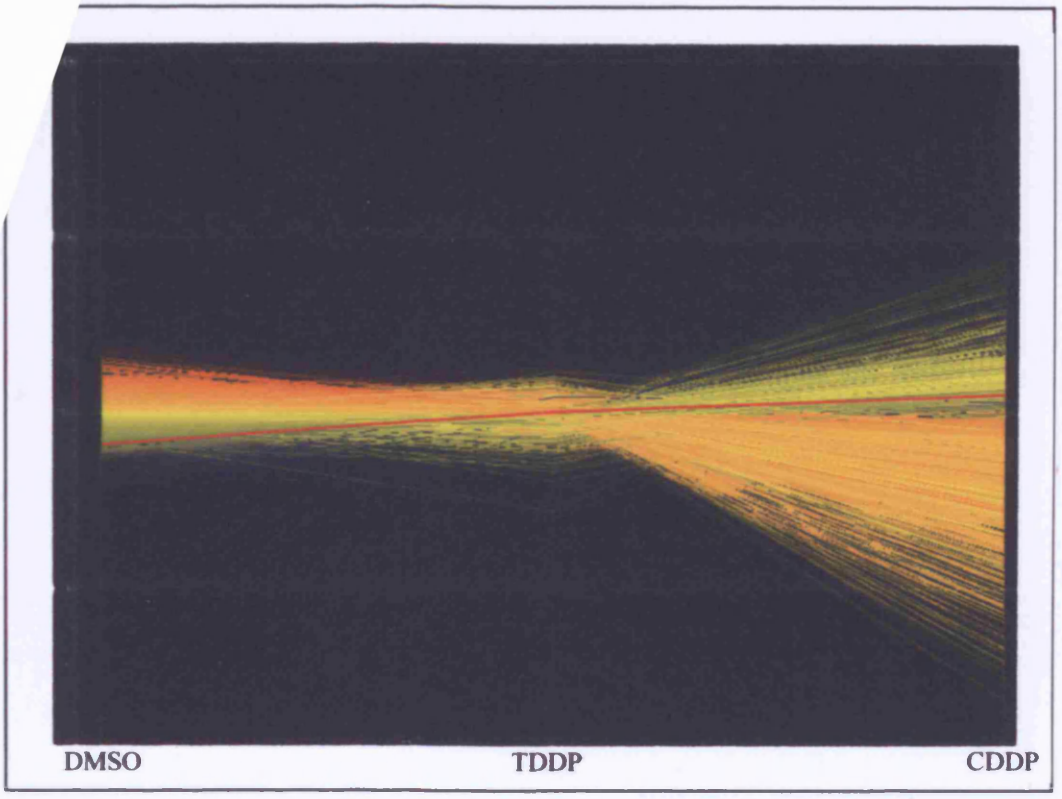
DMSO
TDDP
CDDP

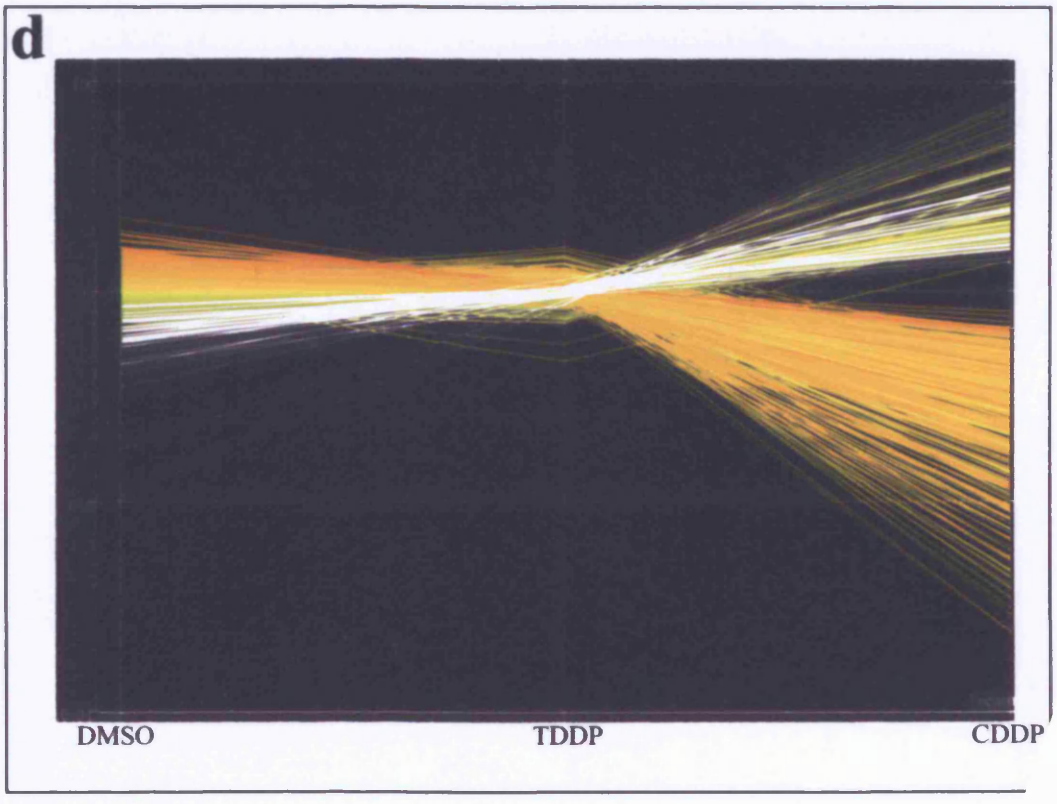
d
DMSO
TDDP
CDDP

Figure 5.4 Representative gene lists from microarray data

The data from the microarray experiments was organised into lists of genes that were upregulated **(a)** or downregulated **(b)** during CDDP treatment. The name of the gene, its function, Affymetrix identity number and the average relative value during DMSO, TDDP and CDDP treatment are shown.

(a) Representative list of upregulated genes

The genes are listed according to the degree of induction during CDDP treatment starting with the most highly upregulated.

(b) Representative list of down regulated genes

The genes are listed according to the degree of repression during CDDP treatment starting with the most highly downregulated.

(a) Representative list of upregulated genes				Average Relative Value of:		
Gene	**Name**	**Affy. I.D. No.**	**Function**	**DMSO**	**TDDP**	**CDDP**
SNK	Serum-inducible kinase	201939_at	ATP binding, protein-threonine kinase activity, cell cycle	1	1.8659	22.0712
PDF	Prostate differentiation factor	221577_x_at	downstream mediator of p53 function	1	8.2797	76.8777
SSAT	Spermidine/spermine N1-acetyltransferase	210592_s_at	role in apoptosis	1	1.1142	8.76014
HIS1	HMBA-inducible	202815_s_at	cyclin dependent protein kinase inhibitor activity, transcriptional repressor activity	1	1.4996	9.41317
ADXR	Ferredoxin reductase	207813_s_at	encodes a mitochondrial flavoprotein	1	1.5876	9.01499
NOXA	Phorbol-12-myristate-13-acetate-induced protein 1	204286_s_at	mediates p53-dependent apoptosis, BH3-only protein	1	1.1781	6.36109
p21	Cyclin-dependent kinase inhibitor 1A (p21, Cip1)	202284_s_at	cell cycle arrest	1	2.6943	14.4121
FAS	tumor necrosis factor receptor superfamily, member 6	204780_s_at	death receptor activated by FasL binding	1	2.3974	12.4014
ATF3	Activating transcription factor 3	202672_s_at	p53 target, bZip transcription factor	1	1.1156	5.75011
PLGF	Placental growth factor, vascular endothelial growth factor-related protein	209652_s_at	molecular marker for inflammation	1	1.491	7.20465
NOXA	Phorbol-12-myristate-13-acetate-induced protein 1	204285_s_at	mediator of p53-induced apoptosis	1	1.1852	5.3237
HEN2	Unknown helix loop helix 2	215228_at	DNA binding	1	1.6743	6.70879

PIG10	Ectodermal-neural cortex (with BTB-like domain)	201341_at	actin-binding, protein binding, p53 inducible gene	1	1.1587	4.56057
GADD45α	Growth arrest & DNA-damage-inducible, alpha	203725_at	mediates activation of p38/JNK pathway under stress	1	1.2894	4.86002
GCLM	Glutamate-cysteine ligase, modifier subunit	203925_at	cysteine metabolism	1	1.0563	3.71407
SBBI48	Immediate early response 5	218611_at	mediating the cellular response to mitogenic signals	1	1.3711	4.78518
TOB1	transducer of ERBB2, 1	202704_at	cell growth regulation	1	1.411	4.62197
PC3	BTG family, member 2	201236_s_at	antiproliferative properties	1	1.6708	5.4044
MDM2	Mouse double minute 2, human homolog of; p53-binding protein	217373_x_at	p53 target, negative regulation of cell proliferation	1	1.0565	3.01307
DDB2	Damage-specific DNA binding protein 2 (48 kD)	203409_at	required for DNA binding, NER	1	2.3317	6.50521
GNRH	Gonadotropin-releasing hormone 1 (leutinizing-releasing hormone)	207987_s_at	negative regulation of cell proliferation	1	0.8335	2.26512
PA26	P53 regulated PA26 nuclear protein	218346_s_at	responds to DNA damage stimulus, negative regulation of cell proliferation, cell cycle arrest	1	1.6569	4.32025
p57	Cyclin-dependent kinase inhibitor 1C (p57, Kip2)	219534_x_at	negative regulation of cell proliferation	1	0.8531	2.11076
DR5	Tumor necrosis factor receptor superfamily, member 10b	209295_at	Death receptor, regulation of apoptosis	1	1.6537	3.97002
PIM2	Pim-2 oncogene	204269_at	reverses BAD-induced cell death.	1	1.2526	2.94677

BTG1	B-cell translocation gene 1, anti-proliferative	200920_s_at	negative regulation of cell proliferation	1	1.1753	2.71482
RBBP6	Retinoblastoma-binding protein 6	205178_s_at	suppresses cell proliferation	1	0.9009	2.07273
CCNG	Cyclin G1	208796_s_at	p53 target	1	1.093	2.47884
TP53TG1	TP53 target gene 1	209917_s_at	DNA damage response	1	0.9844	2.15731
BAG-3	BCL2-associated athanogene 3	217911_s_at	anti-apoptotic role	1	1.0458	2.25734
DUSP4	Dual specificity phosphatase 4	204014_at	negative regulator of MAPK pathway	1	1.2688	2.68438
PIG8	Etoposide-induced mRNA	208289_s_at	immediate-early induction target of p53-mediated apoptosis	1	0.9923	2.06562
BAG1	BCL2-associated athanogene	202387_at	binds to & enhances anti-apoptotic effects of Bcl-2	1	1.0838	2.01442
WIP1	Protein phosphatase 1D magnesium-dependent, delta isoform	204566_at	induced in p53-dependent manner, negative regulation of cell proliferation	1	1.5316	2.80301
WIG-1	P53 target zinc finger protein	219628_at	p53 target, p53-dependent growth regulatory pathway	1	1.6197	2.55892
CART1	TNF receptor-associated factor 4	202871_at	p53-mediated proapoptotic signalling, oxidative activation of MAPK8/JNK	1	1.286	1.99849

(b) Representative list of downregulated genes				Average Relative Value of:		
Gene	**Name**	**Affy. I.D. No.**	**Function**	**DMSO**	**TDDP**	**CDDP**
MAD1	MAD1 (mitotic arrest deficient, yeast, homolog)-like 1	204857_at	inhibited by p53, cell cycle control, tumour suppression	1	0.846	0.019
ADCY9	Adenylate cyclase 9	204497_at	catalyses the formation of cyclic AMP from ATP	1	0.926	0.028
SYT	Synaptotagmin I	203998_s_at	Ca(2+) sensors in the process of vesicular trafficking & exocytosis	1	1.009	0.032
Mst2 /STK3	Mammalian STE20-like kinase 2/Serine/threonine kinase 3	204068_at	positive regulation of apoptosis, has caspase cleavage site	1	1.179	0.04
MYT1L	Myelin transcription factor 1-like	216672_s_at	regulation of transcription, DNA dependent	1	1.053	0.04
OATP-D	Solute carrier family 21 (organic anion transporter), member 11	219229_at	translocating prostaglandins	1	1	0.039
HFAF1	Fas (TNFRSF6) associated factor 1	218080_x_at	binds to FAS to initiate apoptosis or enhance apoptosis initiated by FAS antigen	1	0.877	0.041
TENS1	Tumor endothelial marker 6	217853_at	protein amino acid dephosphorylation	1	0.76	0.037
PARD3	Par-3 (partitioning defective 3, C.elegans) homolog	221527_s_at	establishment &/or maintenance of cell polarity	1	0.883	0.044
ITPR1	Inositol 1,4,5-triphosphate receptor, type 1	216944_s_at	target for cdc2/CycB during cell cycle progression.	1	0.802	0.04
STAG1	Stromal antigen 1	202293_at	transcriptional target for p53, mediates p53-dependent apoptosis.	1	0.803	0.054
FUT8	Fucosyltransferase 8 (alpha (1,6) fucosyltransferase)	203988_s_at	Contributes to cancer cell malignancy & their invasive & metastatic capabilities	1	1.117	0.078

CUTL1	cut-like 1, CCAAT displacement protein (Drosophila)	214743_at	DNA binding protein, regulate gene expression, morphogenesis, differentiation, cell cycle progession	1	0.914	0.065
PFTAIRE1	PFTAIRE protein kinase 1	204604_at	ATP binding, protein serine/threonine kinase activity	1	1.067	0.085
ROBO1	roundabout, axon guidance receptor, homolog 1 (Drosophila)	213194_at	axon guidance receptor activity	1	0.909	0.076
GRK5	G protein-coupled receptor kinase 5	204396_s_at	G-protein coupled receptor kinase activity	1	1.298	0.117
BACH2	BTB & CNC homology 1, basic leucine zipper transcription factor 2	221234_s_at	regulation of transcription, DNA dependent	1	0.993	0.096
ADK	Adenosine kinase	204119_s_at	catalyzes the transfer of the γ-phosphate from ATP to adenosine	1	1.104	0.113
ALK	Anaplastic lymphoma kinase (Ki-1)	208212_s_at	activates STAT3, protects from apoptosis	1	0.771	0.092
UNC5C	Unc5 (C.elegans homolog) c	206189_at	putative tumor suppressor controlling cell death commitment	1	1.315	0.167
MAP2K5	Mitogen-activated protein kinase kinase 5	211370_s_at	protein-tyrosine kinase activity, oncogenesis	1	0.931	0.13
GTC90	Golgi transport complex 1 (90 kDa subunit)	203630_s_at	intra-golgi transport	1	1.05	0.155
ABCC4	ATP-binding cassette, sub-family C (CFTR/MRP), member 4	203196_at	involved in multi-drug resistance, role in cellular detoxification as a pump for its substrate	1	1.035	0.162
SENP7	Sentrin/SUMO-specific protease	220735_s_at	protein sumoylation	1	1.041	0.166
FBXL7	F-box & leucine-rich repeat protein 7	213249_at	phosphorylation-dependent ubiquitination	1	1.083	0.178
PLXNA2	Plexin A2	213030_s_at	neuronal development	1	0.767	0.136
PTK2	PTK2 protein tyrosine kinase 2	208820_at	protein tyrosine-kinase activity	1	1.041	0.188
ELMO1	Engulfment & cell motility 1 (ced-12 homolog, C. elegans)	204513_s_at	promote phagocytosis & cytoskeletal rearrangements during apoptosis	1	0.967	0.175

NRCAM	Neuronal cell adhesion molecule	204105_s_at	CNS development	1	0.847	0.155
RSP5	Neural precursor cell expressed, developmentally down-regulated 4-like	212445_s_at	sodium channel regulator activity	1	1.098	0.205
ASAP1	Development & differentiation enhancing factor 1	221039_s_at	regulation of GTPase activity	1	0.968	0.181
SPAK	Ste-20 related kinase	202786_at	activates p38 pathway, has caspase cleavage site.	1	0.837	0.158
PDE4B	Phosphodiesterase 4B, cAMP-specific (dunce (Drosophila)-homolog phosphodiesterase E4)	211302_s_at	cAMP-specific phosphodiesterase activity, inhibitors promote apoptosis	1	0.935	0.18
ATBF1	AT-binding transcription factor 1	208033_s_at	neuronal differentiation	1	0.857	0.171
ADAM12	a disintegrin & metalloproteinase domain 12 (meltrin alpha)	213790_at	cell-cell & cell-matrix interactions including neurogenesis	1	0.675	0.135
ANK2	ankyrin 2, neuronal	202920_at	attach integral membrane proteins to cytoskeletal elements. Also bind to cytoskeletal proteins.	1	0.656	0.135
CHES1	Checkpoint suppressor 1	205022_s_at	suppression of sensitivity to DNA damage	1	0.877	0.182
NCAM1	neural cell adhesion molecule 1	212843_at	cell adhesion, cell-cell signalling	1	0.896	0.191
DAPK1	Death-associated protein kinase 1	203139_at	apoptosis induction	1	0.998	0.214
GULP1	GULP, engulfment adaptor PTB domain containing 1	215913_s_at	required for efficient engulfment of apoptotic cells by phagocytes	1	0.823	0.184
IGF1R	Insulin-like growth factor 1 receptor	203627_at	anti-apoptotic role	1	0.884	0.209
NAG	Neuroblastoma-amplified protein	202926_at	co-amplified with MYCN in neuroblastomas	1	0.903	0.232
NAIP	baculoviral IAP repeat-containing 1	204860_s_at	suppress apoptosis induced by various signals	1	1.055	0.291
FAK	PTK2 protein tyrosine kinase 2	207821_s_at	protein tyrosine-kinase activity	1	0.916	0.26
ATPIIA	ATPase, Class II, type 9A	212062_at	ATPase activity	1	0.841	0.24

ASK1	Mitogen-activated protein kinase kinase kinase 5	203837_at	induction of apoptosis by extracellular signals	1	1.014	0.294
SMAD6	MAD (mothers against decapentaplegic, Drosophila) homolog 6	207069_s_at	regulation of transcription, DNA-dependent	1	1.003	0.301
MAP4	Human microtubule-associated protein 4	243_g_at	major non-neuronal microtubule-associated protein promotes microtubule assembly	1	0.91	0.278
BCL2	B-cell CLL/lymphoma 2	203685_at	anti-apoptotic outer mitochondrial membrane protein	1	0.881	0.302
GPM6B	Neuronal membrane glycoprotein M6-b	209170_s_at	neurogenesis	1	1.344	0.476
TSSC1	Tumor suppressing subtransferable candidate 1	217968_at	Alterations in this region have been associated with many cancers	1	0.969	0.351
JNK3	c-Jun N-terminal kinase 3	204813_at	Phosphorylates & activates c-Jun	1	0.953	0.367
MAP3K1	mitogen-activated protein kinase kinase kinase 1	214786_at	proteinserine/threonine kinase activity	1	1.025	0.414
TNFAIP8	TNF-induced protein	210260_s_at	antiapoptotic molecule induced by the activation of the transcription factor NF-kappaB	1	0.864	0.369
CCND1	Cyclin D1 (PRAD1: parathyroid adenomatosis 1)	208712_at	Activates CDK4 & CDK6	1	0.884	0.397
E4	Ubiquitination factor E4B (homologous to yeast UFD2)	215533_s_at	strongest candidate neuroblastoma tumor suppressor gene	1	1.007	0.457
NOTCH2	Notch homolog 2 (Drosophila)	202443_x_at	anti-apoptotic	1	0.838	0.415
RSK	Ribosomal protein S6 kinase, 90kD, polypeptide 2	204906_at	controls cell growth & differentiation	1	0.922	0.477

5.2.4 Validation of microarray data

The results from the microarray data were validated by studying the protein levels of selected genes. The average relative level of mRNA of the p53 gene target, p21 was calculated and graphically represented (**Figure 5.5**) showing an approximately 7 times greater increase in expression during CDDP treatment compared to TDDP. In order to validate this mRNA data, p21 protein levels were analysed in immunoblotting experiments using protein extracts from SH-SY5Y cells treated for up to 24 hours with CDDP and TDDP. Protein extracts were prepared at various times during treatment, separated by SDS-PAGE and then transferred to nitrocellulose. Following blocking and overnight incubation with the p21 antibody, the proteins were detected using ECL reagents. A single immunoblot is shown alongside the tubulin loading control (**Figure 5.6**). In this experiment, p21 protein levels increased following CDDP treatment. Further experiments will need to be performed to determine how reproducible this result is.

p21	EXP 1	EXP 2	EXP 3	MEAN	SEM
DMSO	1	1	1	1	0
TDDP	2.861	2.7882	2.452	2.7	0.126
CDDP	13.97	18.713	11.451	14.71	2.129

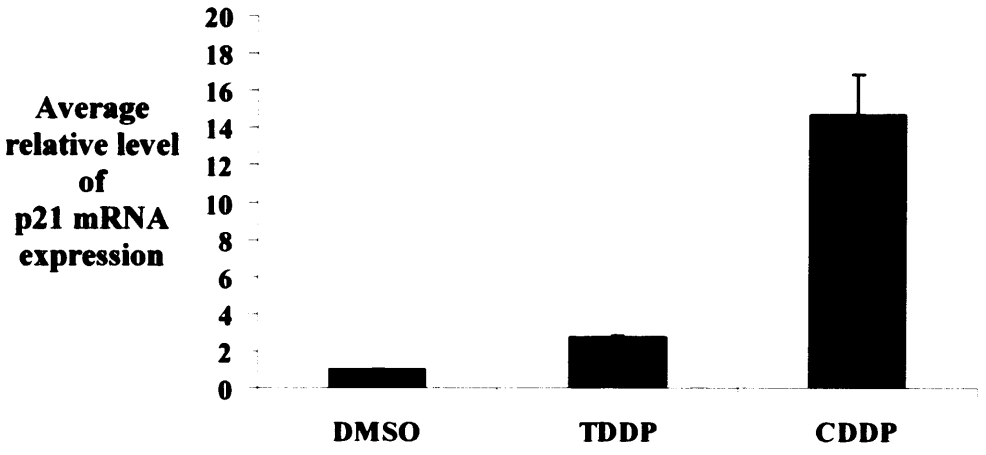

Figure 5.5 Microarray data for the p21 mRNA during CDDP-treatment in SH-SY5Y cells

The graph shows the average relative level of the p21 mRNA calculated from the triplicate microarray experiments. The SEM is also shown.

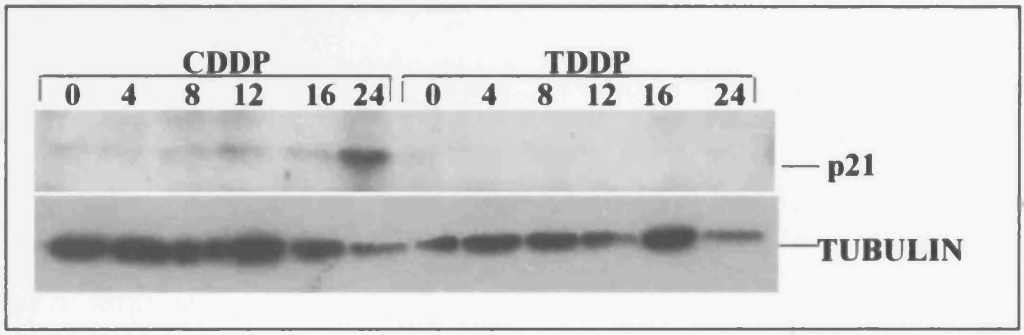

Figure 5.6 Validation of microarray data by immunoblotting

p21 protein expression in CDDP- and TDDP- treated SH-SY5Y cells

SH-SY5Y cells were treated with CDDP for 0, 4, 8, 12, 16 and 24 hours and TDDP for 0, 16 and 24 hours. The pattern of p21 protein expression was investigated by performing immunoblotting experiments with protein extracts from SH-SY5Y cells. A representative p21 immunoblot is shown along with the tubulin loading control.

5.3 Discussion

Affymetrix microarrays allow mRNA expression to be assessed on a large scale, where the expression of thousands of genes can be analysed in a single experiment. In this chapter, I have described microarray experiments which were performed on SH-SY5Y cells treated with CDDP, TDDP and DMSO in order to identify mRNAs that may significantly change in level with CDDP treatment compared to TDDP and DMSO.

The experiments were carried out independently and in triplicate under the three treatment conditions (CDDP, TDDP and DMSO) in order to separate genes that are truly differentially expressed from random changes. The data generated from the three independent experiments via the Affymetrix Genechip® Hybridisation was analysed using Genespring 5 software. All 22,283 genes found on the Human Genome U133A microarray were normalised to the median. This normalisation process is the first analytical step prior to statistical analysis. Normalisation of data is required in order to obtain the most accurate data possible, to be able to differentiate between real (biological) variations in gene expression levels and variations due to the measurement process. Normalising per chip was done where the signal of each gene is divided by the median intensity of the chip to control for variations between the arrays and normalisation per gene was done to account for the difference in detection efficiency of each probe, also allowing comparison of relative changes in gene expression levels and this also scales the relative gene expression levels for comparison. The triplicate set of experiments per treatment condition showed extremely identical patterns of gene intensity (**Figure 5.2.3a**) indicating the high reproducibility of the experiments. The gene intensity between the TDDP and DMSO samples are very similar as observed in **Figure 5.2.3a** whereas CDDP treatment shows a great difference from the other two treatments. This indicates that CDDP treatment induces a greater change in levels of gene expression when compared to TDDP and DMSO. The change observed shows more downregulated genes during CDDP treatment than upregulation.

Following normalisation the data is filtered to remove the genes that show no change in gene intensity during the three treatment conditions. The genes detected that showed an intensity change greater than 1.5 fold between TDDP and CDDP were selected for. PUMA was one of the 3,312 genes identified in these conditions. The

low level of intensity observed with PUMA in the Affymetrix microarray experiments may be due to experimental anomalies or variability between some of the experiments that may have brought down the differences in intensity. Since there were still an enormous number of genes detected with a greater than 1.5 fold change, more stringent conditions were required.

Selecting for a two-fold change increased stringency. 1,014 genes showing a greater than two-fold change were detected. However, PUMA was not one of these. The question arises as to whether by being more stringent, we could lose or filter out important genes such as PUMA that may play a role in CDDP-induced apoptosis in SH-SY5Y cells. Prior to statistical analysis, filtering of unreliable genes needs to be done since multiple testing correction (MTC) is directly affected by the number of genes in the list. The Analysis of variance (ANOVA) test was used to determine whether drug treatment has a significant effect on gene expression behaviour and also these tests take away unwanted experimental effects. 864 genes passed both the MTC test, which keeps the error rate low, and the Benjamini-Hochberg false discovery rate test, which shows statistically significant differences in gene expression and protection against false positives.

Analysis of gene expression using microarrays has the potential to identify candidate genes involved in a variety of processes, to identify genes that are related, or to identify which genes cause disease. The microarray data showed that TDDP and DMSO had very similar gene intensities whereas in comparison, CDDP treatment induced a greater change in levels of gene expression. The data from the microarrays can be classified into functional groups such as genes involved in apoptosis, the cell cycle, cell survival, DNA damage response and p53 target genes. Many of the genes upregulated by CDDP treatment in SH-SY5Y cells were p53 target genes (e.g. SNK, p21, NOXA, PUMA, MDM2, ATF3, cyclin G1, PIG8, WIP1, GADD45α), DNA damage response (e.g. TP53, PA26, DDB2), negative regulators of cell growth/ proliferation (e.g. MDM2, GNRH) and cell cycle arrest genes (e.g. p21, PA26) (see **Figure 5.4a**). Interestingly, I observed that the BH3-only family member and p53 target gene, NOXA was induced by CDDP in the microarray experiments. However, in the immunoblotting experiments in chapter 4, I did not detect a change in NOXA protein levels in CDDP, and TDDP treated SH-SY5Y cells. Perhaps the NOXA antibody I used did not recognise the right protein and these immunoblotting

experiments will need to be repeated using better NOXA antibodies. A high level of expression of the death receptor FAS is also observed during CDDP treatment, however, we know that this is unlikely to play a role in SH-SY5Y cells because no caspase-8 expression was detected (**Figure 3**) in CDDP-treated SH-SY5Y cells.

A greater number of genes were downregulated during CDDP treatment of SH-SY5Y cells. Many of the down-regulated genes play a role in cell metabolism such as ATP binding genes, genes involved in calcium channel activity, protein-kinase activity, GTPase activity. SH-SY5Y cells undergoing apoptosis with CDDP lose mitochondrial function leading to matrix swelling and outer membrane ruptures and release of mitochondrial contents such as cytochrome c. It is possible that the loss of mitochondrial function might lead to a down regulation of genes responsible for maintaining cell metabolism, for example, ITPR1, ADCY9, OATP-D, PFTAIRE-1, ADK, etc (see **Figure 5.4b**). The gene showing the greatest level of downregulation with CDDP treatment is MAD1, which is inhibited by p53. Many genes that play a role in cell growth, cell cycle progression, and regulation of DNA-dependent transcription were also downregulated. Some genes involved in regulating apoptosis were also down regulated, for instance, anti-apoptotic Bcl-2, NOTCH2, TNFAIP8, CCND1 (reduced expression of which leads to apoptosis), and NAIP (an IAP family member).

Any genes of interest identified in these microarray experiments will need to be validated. p21 was the gene with the highest change in gene intensity during CDDP treatment and was used to validate the microarray data (**Figure 5.6**). Other genes of interest from these microarrays will be validated in a similar manner and their function investigated by overexpressing them in SH-SY5Y cells in the presence or absence of CDDP. The siRNA system could be used, as with PUMA (**Chapter 4**), to understand whether the genes of interest are essential for CDDP-induced apoptosis in SH-SY5Y cells. Validated microarray data has the potential for a variety of uses such as understanding the relationships between genes, their regulation and where they are in biochemical pathways.

Chapter 6: Conclusions

The aim of this thesis was to identify the signalling pathway by which CDDP triggers caspase activation and apoptosis in the SH-SY5Y neuroblastoma cell line (Cece *et al.*, 1995). Understanding the cellular responses to CDDP is critical for determining the mechanisms of drug resistance and for allowing the development of therapeutic approaches for increasing the effectiveness of CDDP treatment.

I have shown that CDDP treatment of SH-SY5Y neuroblastoma cells induces apoptosis via the intrinsic mitochondrial death pathway, in which the translocation of cytochrome c from the mitochondria to the cytoplasm triggers the cleavage of procaspase-9 leading to cleavage of the executioner caspase, caspase-3. This results in the apoptotic nuclear changes observed by TUNEL and Hoechst staining. CDDP also induced the upregulation of the p53 protein and its direct transcriptional target, PUMA. I showed that proapoptotic PUMA-α RNA and protein levels increase during CDDP treatment and that overexpression of PUMA-α was sufficient to induce apoptosis in SH-SY5Y cells. By using RNA interference to suppress PUMA-α expression, I aimed to study whether PUMA was essential for CDDP-induced apoptosis in SH-SY5Y cells. Another important question is to determine whether induction of PUMA in SH-SY5Y cells requires p53. This could be addressed by using RNAi technology to suppress p53 expression in SH-SY5Y cells.

Using the Human Genome U133A microarray, I attempted to acquire some information about what other genes could possibly play a role in CDDP-induced death of SH-SY5Y cells. Genes of interest from these microarrays will be studied further. The microarray analysis of the CDDP-sensitive SH-SY5Y cells could have been performed in parallel with a CDDP-resistant neuroblastoma cell line in order to compare and gain insights into the mechanisms of CDDP resistance in neuroblastoma. However, the use of data from a new experiment would introduce several experimental variables that would need to be considered during the statistical analysis of the data. With microarray analysis, it is best to minimise the variables at the beginning of the experiment rather than compensate statistically. The factors that play a role in the mechanisms of CDDP resistance differ between cancers and cell lines of the same disease. So even though there are commercially available CDDP-

resistant cell lines such as BM1R2, it would be better to develop a resistant cell line from the SH-SY5Y cells by repeated exposure to CDDP.

The use of CDDP is limited due to inherent resistance to the drug in the case of some patients and the acquisition of CDDP resistance by initially responsive patients. The development of resistance to CDDP affects approximately 10% of neuroblastoma patients undergoing chemotherapy. Several mechanisms are thought to be involved in CDDP resistance, such as decreased intracellular drug uptake and increased efflux, increased levels of cellular thiols, increased DNA repair, change in the expression of oncogenes and tumour suppressors and inhibition of apoptotic pathways.

A decrease in intracellular CDDP accumulation arising from a decrease in uptake or increased efflux of CDDP has been frequently observed in CDDP-resistant cell lines (Andrews *et al.*, 1990; Parker *et al.*, 1991). There is evidence to suggest that CDDP enters the cell via passive diffusion (Binks and Dobrota, 1990). CDDP accumulation is potassium dependent even though CDDP is not transported into the cells through the sodium-potassium pump, suggesting that accumulation depends on cell membrane potential (Andrews *et al.*, 1988). Recent studies show that there is a direct link between the cellular management of copper and platinum concentrations. Deletion mutations of the yeast CTR1 (high affinity copper transporter) gene resulted in increased CDDP resistance and reduction of platinum levels in yeast. Similarly, mouse cells lines lacking one or both mouse CTR1 alleles exhibit increased CDDP resistance and decreased CDDP accumulation (Ishida *et al.*, 2002). Decreased accumulation of CDDP may also occur due to increased efflux of the drug from cells. Copper-transporting p-type adenosine triphosphate (ATP7B), which has an important role in regulation of copper levels in cells, is associated with CDDP resistance *in vitro* and in various cancers (Komatsu *et al.*, 2000; Nakayama *et al.*, 2002).

Increased expression of p-glycoprotein (p-gp), an ATP-dependent efflux pump expressed by the *multidrug resistance -1 (MDR-1)* gene (Chan *et al.*, 1990; Kurowski and Berthold, 1998) is characteristic of multidrug resistance in chemotherapy of cancers. In neuroblastoma, the mechanism of multidrug resistance is thought to be associated with drug-pumping proteins such as P-glycoprotein encoded by the MDR-1 gene (Bourhis *et al.*, 1989), multidrug resistance-associated protein (MRP) (Bordow *et al.*, 1994), and canalicular multispecific organic anion transporter (cMOAT). In

adult breast and ovarian cancer cells, the breast cancer resistant protein (BCRP) and the ATP-binding cassette gene have been reported to be associated with multidrug resistance (Doyle *et al.*, 1998; Maliepaard *et al.*, 1999). Other MRP family members have been identified as multidrug resistance-related proteins that alter chemosensitivity to CDDP.

The *MDR-1* gene encodes a membrane-associated protein which belongs to the superfamily of ATP-binding cassette (ABC) transporters. The protein encoded by this gene is responsible for decreased drug accumulation in multidrug-resistant cells and often mediates the accumulation of resistance to anticancer drugs. Overexpression of another ABC transporter family member, ABCC2 (ATP binding cassette subfamily C2, also known as MDR2 or cMOAT) has been shown to enhance resistance to many chemotherapeutic drugs including CDDP where 10-fold resistance was seen (Cui *et al.*, 1999). In a recent study, the role of ABCC2 in platinum drug resistance was analysed using ovarian cancer cell lines, adrenocortical cell lines and melanoma cell lines (Materna *et al.*, 2005). The authors found that the use of anti-ABCC2 hammerhead ribozymes successfully downregulated the ABCC2-specific transcript and ABCC2 protein expression in these cell lines suggesting a potential gene therapy approach to overcome platinum-resistance in human cancers.

Another member of the same ABC transporter family, ABCC4 was identified as a down- regulated gene in my microarray data for SH-SY5Y neuroblastoma cells treated with CDDP (**Figure 5.4b**). *ABCC4* (*MDR4*) shows a 6-fold decrease in expression with CDDP treatment compared with TDDP and DMSO treatment in CDDP-sensitive SH-SY5Y cells (**Figure 5.4b**). ABCC4 has not previously been associated with resistance to drugs used to treat solid tumours. Analysis of expression of the multidrug resistance genes in human cancer cell lines showed that ABCC4, which is expressed at low levels in a few tissues, was not found to be overexpressed in multidrug / CDDP-resistant cell lines (Kool *et al.*, 1997). Expression of MDR-1 is currently a marker of poor prognosis in neuroblastoma but a very recent study suggests that ABCC4 can also be a marker of poor prognosis for the same type of tumour. Norris *et al.*, 2005 found that ABCC4 was frequently overexpressed in aggressive primary neuroblastoma and that high ABCC4 expression correlated with *MYCN* oncogene amplification and was significantly associated with poor clinical outcome (Norris *et al.*, 2005). In SH-SY5Y cells, there is no *MYCN* amplification and

my microarray result suggested that ABCC4 is downregulated during CDDP treatment. It would therefore be interesting to investigate whether, overexpression of ABCC4 would alter the sensitivity of these cells to CDDP.

Studies also suggest a role for the ATP-dependent glutathione S-conjugate export pump in effluxing CDDP that is covalently linked to glutathione and might be involved in reducing intracellular CDDP concentration in CDDP-resistant cells (Ishikawa *et al.*, 1993). Conjugation with glutathione inhibits the conversion of mono adducts to cross-links, thus reducing the cytotoxic potential of the adducts. Glutathione maintains the dNTP pool size required for DNA repair, so it has been found that depletion of glutathione inhibits repair in CDDP-resistant ovarian cancer cells (reviewed in Kartalou and Essigman, 2000). Elevated levels of glutathione have been found in some CDDP-resistant cell lines and inhibition of glutathione levels increased CDDP sensitivity in some cell lines and not others (Godwin *et al.*, 1992; Hromas *et al.*, 1987; Kartalou and Essigman, 2000). Many studies indicate that an increase in glutathione levels is a likely factor involved in CDDP resistance but it is not an absolute requirement (reviewed in Jamieson and Lippard, 1999).

Another intracellular thiol is metallothionein, which is from a cysteine rich protein family that has also been associated with CDDP resistance. Metallothioneins bind to CDDP and may affect drug sensitivity (Andrews *et al.*, 1987). Overexpression of metallothioneins sometimes leads to CDDP resistance but this is not a universal phenomenon.

An increase in DNA repair is another mechanism considered to play a part in CDDP resistance. Nucleotide excision repair (NER) is the main mechanism by which CDDP-DNA adducts are removed. The NER pathway is a network of many proteins that form the DNA repair system. The ERCC1 (excision repair cross complementing – group 1) gene has a key role in the NER pathway and has been associated with resistance to platinum compounds. Other DNA repair proteins including ERCC1 can be overexpressed in resistant cell lines (Koberle *et al.*, 1999). A number of studies have shown an increase in DNA repair in CDDP resistance cells such as human ovarian cancer cells lines, murine leukaemia cells, Chinese hamster ovary cells, cells found in human malignant glioma (Jamieson and Lippard, 1999). In my microarray study, an increase in the damage-specific DNA binding protein (DDB2) was observed in TDDP-treated cells but a three-fold greater increase was observed in CDDP-treated

SH-SY5Y cells. NER consists of two subpathways, transcription-coupled repair and global genomic repair (GGR). DDB2 transcription increases after DNA damage in a p53-dependent manner (Tang *et al.*, 2000) and enhances GGR. DDB2 is a direct transcriptional target of p53 (Tan and Chu, 2002).

As further studies into CDDP resistance take place using microarray technology (Deng *et al.*, 2002; Roberts *et al.*, 2005), this will provide a large pool of data to compare and analyse in the search to comprehend the mechanism of CDDP resistance. However, the amount of data presently available indicates that there are multiple mechanisms interconnected in a very complex way, which are responsible for CDDP resistance (Deng *et al.*, 2002).

CDDP triggers the induction of several cellular stress response signals. However, in my microarray experiments, the stress responsive kinases, apoptosis signal-regulating kinase (ASK) 1 and c-Jun N-terminal kinase 3 (JNK3) are both down-regulated. MAP kinase pathways can be activated by CDDP (sanchez-perez, oncogene, 1998). ASK1 activates the JNK and p38 MAP kinase cascades in response to environmental stress. Expression of JNK3 is mainly restricted to the nervous system and ASK1, JNKs and c-Jun promote apoptosis in sympathetic neurons following NGF withdrawal (Kanamoto *et al.*, 2000). However in CDDP-sensitive SH-SY5Y cells, downregulation of ASK1 and JNK3 occurs following CDDP treatment suggesting that they do not exhibit the same role in these cells, which are not postmitotic neurons.

Another gene of interest from the microarray data that could be a potential therapeutic target is the *focal adhesion kinase* (*FAK*). FAK, the substrate and binding partner of the src oncogene, is a tyrosine kinase protein that plays a role in cancer pathology. FAK contains binding sites for many signalling proteins, regulates normal and tumour cell proliferation, motility and invasion in culture. The *fak* gene shows an approximately 4-fold decrease in expression in CDDP-treated SH-SY5Y cells as compared with TDDP and DMSO treatment. Inhibition of FAK expression or signalling can induce apoptosis in cancer cells, but has little effect upon normal cells (Gabarra-Niecko *et al.*, 2003). This makes FAK a candidate therapeutic target.

In breast cancer cells, inhibition of FAK by antisense oligonucleotides increased the sensitivity to camptothecins (Satoh *et al.*, 2003). Oligonucleotides are

used to selectively target tumour-associated genes or mutated genes leaving normal genes unaltered, which is essential for anticancer drugs. Over the last few years, research efforts have been centred on developing new selective anticancer drugs with less cytotoxic side effects and work on antisense oligonucleotides looks hopeful. However, the uptake of antisense oligonucleotides by cells is inefficient and is not cell-type specific. To increase blood stability, cellular uptake and specificity of antisense oligonucleotides, lipid-based delivery systems are used.

Another alternative to overcome tumour resistance is to engineer BH3-only mimetics to promote apoptosis. If after further investigation, PUMA expression is found to be essential for CDDP to induce apoptosis in neuroblastoma cells, a BH3-mimetic drug for PUMA could be engineered to overcome acquired resistance to CDDP in neuroblastoma patients. David Huang reported that the BH3-only proteins, Bim and PUMA bind to Bcl-2, Bcl-X_L, Bcl-w, Mcl-1 and A1 making them potent killers compared to other BH3-only proteins which bound to fewer of these anti-apoptotic Bcl-2 family members (as presented at the 2004 Keystone Symposium on Programmed Cell Death).

The tumour suppressor, p53 is induced in SH-SY5Y cells treated with CDDP and many p53 target genes were found to be upregulated by CDDP treatment in my microarray analysis (**Figure 5.4a**). Experiments using a pSUPERp53siRNA expression vector could determine whether p53 is required for induction of p53 target genes by CDDP in SH-SY5Y cells. If p53 was not required, it would be important to determine whether another p53 family member, such as p73, or other transcription factors can substitute for p53. If p53 proves to be a key player in the CDDP-induced death of SH-SY5Y neuroblastomas cells, another potential therapeutic approach would be to interfere with the interaction between MDM2 using small molecule antagonists of MDM2 (Vassilev *et al.*, 2004). This would be predicted to lead to stabilisation of p53 and p53-dependent growth arrest / apoptosis. This would eliminate the need to use p53-inducing DNA damaging drugs, such as CDDP.

REFERENCES

Adams J.M., Harris A.W., Pinkert C.A., Corcoran L.M., Alexander W.S., Cory S., Palmiter R.D. and Brinster R.L. (1985) The c-myc oncogene driven by immunoglobulin enhancers induces lymphoid malignancy in transgenic mice. *Nature* **318,** 533-538.

Agami R. (2002) RNAi and related mechanisms and their potential use for therapy. *Curr.Opin.Chem.Biol.* **6,** 829-834.

Ajiro K. (2000) Histone H2B phosphorylation in mammalian apoptotic cells. An association with DNA fragmentation. *J.Biol.Chem.* **275,** 439-443.

Allan L.A., Morrice N., Brady S., Magee G., Pathak S. and Clarke P.R. (2003) Inhibition of caspase-9 through phosphorylation at Thr 125 by ERK MAPK. *Nat.Cell Biol.* **5,** 647-654.

Ambrosini G., Adida C. and Altieri D.C. (1997) A novel anti-apoptosis gene, survivin, expressed in cancer and lymphoma. *Nat.Med.* **3,** 917-921.

Andrews P.A., Murphy M.P. and Howell S.B. (1987) Metallothionein-mediated cisplatin resistance in human ovarian carcinoma cells. *Cancer Chemother.Pharmacol.* **19,** 149-154.

Andrews P.A., Velury S., Mann S.C. and Howell S.B. (1988) cis-Diamminedichloroplatinum(II) accumulation in sensitive and resistant human ovarian carcinoma cells. *Cancer Res.* **48,** 68-73.

Andrews P.A. and Howell S.B. (1990) Cellular pharmacology of cisplatin: perspectives on mechanisms of acquired resistance. *Cancer Cells* **2,** 35-43.

Appella E. (2001) Modulation of p53 function in cellular regulation. *Eur.J.Biochem.* **268,** 2763.

Appella E. and Anderson C.W. (2001) Post-translational modifications and activation of p53 by genotoxic stresses. *Eur.J.Biochem.* **268,** 2764-2772.

Arriola E.L., Rodriguez-Lopez A.M., Hickman J.A. and Chresta C.M. (1999) Bcl-2 overexpression results in reciprocal downregulation of Bcl-X(L) and sensitizes human testicular germ cell tumours to chemotherapy-induced apoptosis. *Oncogene* **18,** 1457-1464.

Azar C.G., Scavarda N.J., Reynolds C.P. and Brodeur G.M. (1990) Multiple defects of the nerve growth factor receptor in human neuroblastomas. *Cell Growth Differ.* **1,** 421-428.

Banelli B., Casciano I., Croce M., Di Vinci A., Gelvi I., Pagnan G., Brignole C., Allemanni G., Ferrini S., Ponzoni M. and Romani M. (2002) Expression and methylation of CASP8 in neuroblastoma: identification of a promoter region. *Nat.Med.* **8,** 1333-1335.

Barbacid M. (1994) The Trk family of neurotrophin receptors. *J.Neurobiol.* **25,** 1386-1403.

Barres B.A., Hart I.K., Coles H.S., Burne J.F., Voyvodic J.T., Richardson W.D. and Raff M.C. (1992) Cell death in the oligodendrocyte lineage. *J.Neurobiol.* **23,** 1221-1230.

Barres B.A., Hart I.K., Coles H.S., Burne J.F., Voyvodic J.T., Richardson W.D. and Raff M.C. (1992) Cell death and control of cell survival in the oligodendrocyte lineage. *Cell* **70,** 31-46.

Bennett M., Macdonald K., Chan S.W., Luzio J.P., Simari R. and Weissberg P. (1998) Cell surface trafficking of Fas: a rapid mechanism of p53-mediated apoptosis. *Science* **282,** 290-293.

Berridge M.J., Lipp P. and Bootman M.D. (2000) The versatility and universality of calcium signalling. *Nat.Rev.Mol.Cell Biol.* **1,** 11-21.

Biggs W.H., III, Meisenhelder J., Hunter T., Cavenee W.K. and Arden K.C. (1999) Protein kinase B/Akt-mediated phosphorylation promotes nuclear exclusion of the winged helix transcription factor FKHR1. *Proc.Natl.Acad.Sci.U.S.A* **96,** 7421-7426.

Binks S.P. and Dobrota M. (1990) Kinetics and mechanism of uptake of platinum-based pharmaceuticals by the rat small intestine. *Biochem.Pharmacol.* **40,** 1329-1336.

Bordow S.B., Haber M., Madafiglio J., Cheung B., Marshall G.M. and Norris M.D. (1994) Expression of the multidrug resistance-associated protein (MRP) gene correlates with amplification and overexpression of the N-myc oncogene in childhood neuroblastoma. *Cancer Res.* **54,** 5036-5040.

Bouillet P., Metcalf D., Huang D.C., Tarlinton D.M., Kay T.W., Kontgen F., Adams J.M. and Strasser A. (1999) Proapoptotic Bcl-2 relative Bim required for certain apoptotic responses, leukocyte homeostasis, and to preclude autoimmunity. *Science* **286,** 1735-1738.

Bouillet P., Cory S., Zhang L.C., Strasser A. and Adams J.M. (2001) Degenerative disorders caused by Bcl-2 deficiency prevented by loss of its BH3-only antagonist Bim. *Dev.Cell* **1,** 645-653.

Bouillet P., Purton J.F., Godfrey D.I., Zhang L.C., Coultas L., Puthalakath H., Pellegrini M., Cory S., Adams J.M. and Strasser A. (2002) BH3-only Bcl-2 family member Bim is required for apoptosis of autoreactive thymocytes. *Nature* **415,** 922-926.

Bourhis J., Benard J., Hartmann O., Boccon-Gibod L., Lemerle J. and Riou G. (1989) Correlation of MDR1 gene expression with chemotherapy in neuroblastoma. *J.Natl.Cancer Inst.* **81,** 1401-1405.

Bown N. (2001) Neuroblastoma tumour genetics: clinical and biological aspects. *J.Clin.Pathol.* **54,** 897-910.

Brenner S. (1974) The genetics of Caenorhabditis elegans. *Genetics* **77,** 71-94.

Brodeur G.M., Seeger R.C., Schwab M., Varmus H.E. and Bishop J.M. (1984) Amplification of N-myc in untreated human neuroblastomas correlates with advanced disease stage. *Science* **224,** 1121-1124.

Brummelkamp T.R., Bernards R. and Agami R. (2002) A system for stable expression of short interfering RNAs in mammalian cells. *Science* **296,** 550-553.

Brunet A., Bonni A., Zigmond M.J., Lin M.Z., Juo P., Hu L.S., Anderson M.J., Arden K.C., Blenis J. and Greenberg M.E. (1999) Akt promotes cell survival by phosphorylating and inhibiting a Forkhead transcription factor. *Cell* **96,** 857-868.

Cande C., Cecconi F., Dessen P. and Kroemer G. (2002) Apoptosis-inducing factor (AIF): key to the conserved caspase-independent pathways of cell death? *J.Cell Sci.* **115,** 4727-4734.

Cardone M.H., Roy N., Stennicke H.R., Salvesen G.S., Franke T.F., Stanbridge E., Frisch S. and Reed J.C. (1998) Regulation of cell death protease caspase-9 by phosphorylation. *Science* **282,** 1318-1321.

Castleberry R.P. (1997) Neuroblastoma. *Eur.J.Cancer* **33,** 1430-1437.

Castresana J.S., Bello M.J., Rey J.A., Nebreda P., Queizan A., Garcia-Miguel P. and Pestana A. (1994) No TP53 mutations in neuroblastomas detected by PCR-SSCP analysis. *Genes Chromosomes.Cancer* **10,** 136-138.

Cece R., Barajon I. and Tredici G. (1995) Cisplatin induces apoptosis in SH-SY5Y human neuroblastoma cell line. *Anticancer Res.* **15,** 777-782.

Chan H.S., Thorner P.S., Haddad G. and Ling V. (1990) Immunohistochemical detection of P-glycoprotein: prognostic correlation in soft tissue sarcoma of childhood. *J.Clin.Oncol.* **8,** 689-704.

Chan H.S., Haddad G., Thorner P.S., DeBoer G., Lin Y.P., Ondrusek N., Yeger H. and Ling V. (1991) P-glycoprotein expression as a predictor of the outcome of therapy for neuroblastoma. *N.Engl.J.Med.* **325,** 1608-1614.

Cheung W.L., Ajiro K., Samejima K., Kloc M., Cheung P., Mizzen C.A., Beeser A., Etkin L.D., Chernoff J., Earnshaw W.C. and Allis C.D. (2003) Apoptotic phosphorylation of histone H2B is mediated by mammalian sterile twenty kinase. *Cell* **113,** 507-517.

Clohessy J.G., Zhuang J. and Brady H.J. (2004) Characterisation of Mcl-1 cleavage during apoptosis of haematopoietic cells. *Br.J.Haematol.* **125,** 655-665.

Conradt B. and Horvitz H.R. (1998) The C. elegans protein EGL-1 is required for programmed cell death and interacts with the Bcl-2-like protein CED-9. *Cell* **93,** 519-529.

Cory S. and Adams J.M. (2002) The Bcl2 family: regulators of the cellular life-or-death switch. *Nat.Rev.Cancer* **2,** 647-656.

Cregan S.P., Fortin A., MacLaurin J.G., Callaghan S.M., Cecconi F., Yu S.W., Dawson T.M., Dawson V.L., Park D.S., Kroemer G. and Slack R.S. (2002) Apoptosis-inducing factor is involved in the regulation of caspase-independent neuronal cell death. *J.Cell Biol.* **158,** 507-517.

Cui Y., Konig J., Buchholz J.K., Spring H., Leier I. and Keppler D. (1999) Drug resistance and ATP-dependent conjugate transport mediated by the apical multidrug resistance protein, MRP2, permanently expressed in human and canine cells. *Mol.Pharmacol.* **55,** 929-937.

Damia G., Sanchez Y., Erba E. and Broggini M. (2001) DNA Damage Induces p53-dependent Down-regulation of hCHK1. *J.Biol.Chem.* **276,** 10641-10645.

Danial N.N. and Korsmeyer S.J. (2004) Cell death: critical control points. *Cell* **116,** 205-219.

Datta S.R., Dudek H., Tao X., Masters S., Fu H., Gotoh Y. and Greenberg M.E. (1997) Akt phosphorylation of BAD couples survival signals to the cell-intrinsic death machinery. *Cell* **91,** 231-241.

Datta S.R., Katsov A., Hu L., Petros A., Fesik S.W., Yaffe M.B. and Greenberg M.E. (2000) 14-3-3 proteins and survival kinases cooperate to inactivate BAD by BH3 domain phosphorylation. *Mol.Cell* **6,** 41-51.

Datta S.R., Ranger A.M., Lin M.Z., Sturgill J.F., Ma Y.C., Cowan C.W., Dikkes P., Korsmeyer S.J. and Greenberg M.E. (2002) Survival factor-mediated BAD phosphorylation raises the mitochondrial threshold for apoptosis. *Dev.Cell* **3,** 631-643.

Davidoff A.M., Iglehart J.D. and Marks J.R. (1992) Immune response to p53 is dependent upon p53/HSP70 complexes in breast cancers. *Proc.Natl.Acad.Sci.U.S.A* **89,** 3439-3442.

Davidoff A.M., Pence J.C., Shorter N.A., Iglehart J.D. and Marks J.R. (1992) Expression of p53 in human neuroblastoma- and neuroepithelioma-derived cell lines. *Oncogene* **7,** 127-133.

Deckwerth T.L., Elliott J.L., Knudson C.M., Johnson E.M., Jr., Snider W.D. and Korsmeyer S.J. (1996) BAX is required for neuronal death after trophic factor deprivation and during development. *Neuron* **17,** 401-411.

del Peso L., Gonzalez-Garcia M., Page C., Herrera R. and Nunez G. (1997) Interleukin-3-induced phosphorylation of BAD through the protein kinase Akt. *Science* **278,** 687-689.

Deng H.B., Parekh H.K., Chow K.C. and Simpkins H. (2002) Increased expression of dihydrodiol dehydrogenase induces resistance to cisplatin in human ovarian carcinoma cells. *J.Biol.Chem.* **277,** 15035-15043.

Desagher S., Osen-Sand A., Nichols A., Eskes R., Montessuit S., Lauper S., Maundrell K., Antonsson B. and Martinou J.C. (1999) Bid-induced conformational change of Bax is responsible for mitochondrial cytochrome c release during apoptosis. *J.Cell Biol.* **144,** 891-901.

Deveraux Q.L., Roy N., Stennicke H.R., Van Arsdale T., Zhou Q., Srinivasula S.M., Alnemri E.S., Salvesen G.S. and Reed J.C. (1998) IAPs block apoptotic events induced by caspase-8 and cytochrome c by direct inhibition of distinct caspases. *EMBO J.* **17,** 2215-2223.

Diccianni M.B., Omura-Minamisawa M., Batova A., Le T., Bridgeman L. and Yu A.L. (1999) Frequent deregulation of p16 and the p16/G1 cell cycle-regulatory pathway in neuroblastoma. *Int.J.Cancer* **80,** 145-154.

Dijkers P.F., Medema R.H., Lammers J.W., Koenderman L. and Coffer P.J. (2000) Expression of the pro-apoptotic Bcl-2 family member Bim is regulated by the forkhead transcription factor FKHR-L1. *Curr.Biol.* **10,** 1201-1204.

Ding H.F., Lin Y.L., McGill G., Juo P., Zhu H., Blenis J., Yuan J. and Fisher D.E. (2000) Essential role for caspase-8 in transcription-independent apoptosis triggered by p53. *J.Biol.Chem.* **275,** 38905-38911.

Dole M., Nunez G., Merchant A.K., Maybaum J., Rode C.K., Bloch C.A. and Castle V.P. (1994) Bcl-2 inhibits chemotherapy-induced apoptosis in neuroblastoma. *Cancer Res.* **54,** 3253-3259.

Dole M.G., Jasty R., Cooper M.J., Thompson C.B., Nunez G. and Castle V.P. (1995) Bcl-xL is expressed in neuroblastoma cells and modulates chemotherapy-induced apoptosis. *Cancer Res.* **55,** 2576-2582.

Don R.H., Cox P.T., Wainwright B.J., Baker K. and Mattick J.S. (1991) 'Touchdown' PCR to circumvent spurious priming during gene amplification. *Nucleic Acids Res.* **19,** 4008.

Donnellan R. and Chetty R. (1998) Cyclin D1 and human neoplasia. *Mol.Pathol.* **51,** 1-7.

Doyle L.A., Yang W., Abruzzo L.V., Krogmann T., Gao Y., Rishi A.K. and Ross D.D. (1998) A multidrug resistance transporter from human MCF-7 breast cancer cells. *Proc.Natl.Acad.Sci.U.S.A* **95,** 15665-15670.

Du C., Fang M., Li Y., Li L. and Wang X. (2000) Smac, a mitochondrial protein that promotes cytochrome c-dependent caspase activation by eliminating IAP inhibition. *Cell* **102,** 33-42.

El Deiry W.S. (1998) Regulation of p53 downstream genes. *Semin.Cancer Biol.* **8,** 345-357.

Encinas M., Iglesias M., Liu Y., Wang H., Muhaisen A., Cena V., Gallego C. and Comella J.X. (2000) Sequential treatment of SH-SY5Y cells with retinoic acid and brain-derived neurotrophic factor gives rise to fully differentiated, neurotrophic factor-dependent, human neuron-like cells. *J.Neurochem.* **75,** 991-1003.

Erhardt P., Schremser E.J. and Cooper G.M. (1999) B-Raf inhibits programmed cell death downstream of cytochrome c release from mitochondria by activating the MEK/Erk pathway. *Mol.Cell Biol.* **19,** 5308-5315.

Freedman D.A., Wu L. and Levine A.J. (1999) Functions of the MDM2 oncoprotein. *Cell Mol.Life Sci.* **55,** 96-107.

Fulda S., Lutz W., Schwab M. and Debatin K.M. (1999) MycN sensitizes neuroblastoma cells for drug-induced apoptosis. *Oncogene* **18,** 1479-1486.

Gabarra-Niecko V., Schaller M.D. and Dunty J.M. (2003) FAK regulates biological processes important for the pathogenesis of cancer. *Cancer Metastasis Rev.* **22,** 359-374.

Gavrieli Y., Sherman Y. and Ben Sasson S.A. (1992) Identification of programmed cell death in situ via specific labeling of nuclear DNA fragmentation. *J.Cell Biol.* **119,** 493-501.

Giannakakou P., Sackett D.L., Ward Y., Webster K.R., Blagosklonny M.V. and Fojo T. (2000) p53 is associated with cellular microtubules and is transported to the nucleus by dynein. *Nat.Cell Biol.* **2,** 709-717.

Gilley J., Coffer P.J. and Ham J. (2003) FOXO transcription factors directly activate bim gene expression and promote apoptosis in sympathetic neurons. *J.Cell Biol.* **162,** 613-622.

Godwin A.K., Meister A., O'Dwyer P.J., Huang C.S., Hamilton T.C. and Anderson M.E. (1992) High resistance to cisplatin in human ovarian cancer cell lines is associated with marked increase of glutathione synthesis. *Proc.Natl.Acad.Sci.U.S.A* **89,** 3070-3074.

Gonzalez V.M., Fuertes M.A., Alonso C. and Perez J.M. (2001) Is cisplatin-induced cell death always produced by apoptosis? *Mol.Pharmacol.* **59,** 657-663.

Gottlieb T.M. and Oren M. (1998) p53 and apoptosis. *Semin.Cancer Biol.* **8,** 359-368.

Grasl-Kraupp B., Ruttkay-Nedecky B., Koudelka H., Bukowska K., Bursch W. and Schulte-Hermann R. (1995) In situ detection of fragmented DNA (TUNEL assay) fails to discriminate among apoptosis, necrosis, and autolytic cell death: a cautionary note. *Hepatology* **21,** 1465-1468.

Gross A., McDonnell J.M. and Korsmeyer S.J. (1999) BCL-2 family members and the mitochondria in apoptosis. *Genes Dev.* **13,** 1899-1911.

Hamasaki A., Sendo F., Nakayama K., Ishida N., Negishi I., Nakayama K. and Hatakeyama S. (1998) Accelerated neutrophil apoptosis in mice lacking A1-a, a subtype of the bcl-2-related A1 gene. *J.Exp.Med.* **188,** 1985-1992.

Han J., Flemington C., Houghton A.B., Gu Z., Zambetti G.P., Lutz R.J., Zhu L. and Chittenden T. (2001) Expression of bbc3, a pro-apoptotic BH3-only gene, is regulated by diverse cell death and survival signals. *Proc.Natl.Acad.Sci.U.S.A* **98,** 11318-11323.

Hegde R., Srinivasula S.M., Zhang Z., Wassell R., Mukattash R., Cilenti L., DuBois G., Lazebnik Y., Zervos A.S., Fernandes-Alnemri T. and Alnemri E.S. (2002) Identification of Omi/HtrA2 as a mitochondrial apoptotic serine protease that disrupts inhibitor of apoptosis protein-caspase interaction. *J.Biol.Chem.* **277,** 432-438.

Hengartner M.O. and Horvitz H.R. (1994) C. elegans cell survival gene ced-9 encodes a functional homolog of the mammalian proto-oncogene bcl-2. *Cell* **76,** 665-676.

Hengartner M.O. (2000) The biochemistry of apoptosis. *Nature* **407,** 770-776.

Herr I. and Debatin K.M. (2001) Cellular stress response and apoptosis in cancer therapy. *Blood* **98,** 2603-2614.

Hickman E.S., Moroni M.C. and Helin K. (2002) The role of p53 and pRB in apoptosis and cancer. *Curr.Opin.Genet.Dev.* **12,** 60-66.

Hockenbery D., Nunez G., Milliman C., Schreiber R.D. and Korsmeyer S.J. (1990) Bcl-2 is an inner mitochondrial membrane protein that blocks programmed cell death. *Nature* **348,** 334-336.

Hollstein M., Sidransky D., Vogelstein B. and Harris C.C. (1991) p53 mutations in human cancers. *Science* **253,** 49-53.

Hosoi G., Hara J., Okamura T., Osugi Y., Ishihara S., Fukuzawa M., Okada A., Okada S. and Tawa A. (1994) Low frequency of the p53 gene mutations in neuroblastoma. *Cancer* **73,** 3087-3093.

Hromas R.A., North J.A. and Burns C.P. (1987) Decreased cisplatin uptake by resistant L1210 leukemia cells. *Cancer Lett.* **36,** 197-201.

Hsu Y.T., Wolter K.G. and Youle R.J. (1997) Cytosol-to-membrane redistribution of Bax and Bcl-X(L) during apoptosis. *Proc.Natl.Acad.Sci.U.S.A* **94,** 3668-3672.

Huang D.C. and Strasser A. (2000) BH3-Only proteins-essential initiators of apoptotic cell death. *Cell* **103,** 839-842.

Hunter T. (2000) Signaling--2000 and beyond. *Cell* **100,** 113-127.

Ishida S., Lee J., Thiele D.J. and Herskowitz I. (2002) Uptake of the anticancer drug cisplatin mediated by the copper transporter Ctr1 in yeast and mammals. *Proc.Natl.Acad.Sci.U.S.A* **99,** 14298-14302.

Ishikawa T., Casini A.F. and Nishikimi M. (1998) Molecular cloning and functional expression of rat liver glutathione-dependent dehydroascorbate reductase. *J.Biol.Chem.* **273,** 28708-28712.

Jacobson M.D., Weil M. and Raff M.C. (1997) Programmed cell death in animal development. *Cell* **88,** 347-354.

Jamieson E.R. and Lippard S.J. (1999) Structure, Recognition, and Processing of Cisplatin-DNA Adducts. *Chem.Rev.* **99,** 2467-2498.

Janiak F., Leber B. and Andrews D.W. (1994) Assembly of Bcl-2 into microsomal and outer mitochondrial membranes. *J.Biol.Chem.* **269,** 9842-9849.

Janicke R.U., Ng P., Sprengart M.L. and Porter A.G. (1998) Caspase-3 is required for alpha-fodrin cleavage but dispensable for cleavage of other death substrates in apoptosis. *J.Biol.Chem.* **273,** 15540-15545.

Jeffers J.R., Parganas E., Lee Y., Yang C., Wang J., Brennan J., MacLean K.H., Han J., Chittenden T., Ihle J.N., McKinnon P.J., Cleveland J.L. and Zambetti G.P. (2003) Puma is an essential mediator of p53-dependent and -independent apoptotic pathways. *Cancer Cell* **4,** 321-328.

Kaipia A. and Hsueh A.J. (1997) Regulation of ovarian follicle atresia. *Annu.Rev.Physiol* **59,** 349-363.

Kanamoto T., Mota M., Takeda K., Rubin L.L., Miyazono K., Ichijo H. and Bazenet C.E. (2000) Role of apoptosis signal-regulating kinase in regulation of the c-Jun N-terminal kinase pathway and apoptosis in sympathetic neurons. *Mol.Cell Biol.* **20,** 196-204.

Kaplan D.R., Matsumoto K., Lucarelli E. and Thiele C.J. (1993) Induction of TrkB by retinoic acid mediates biologic responsiveness to BDNF and differentiation of human neuroblastoma cells. Eukaryotic Signal Transduction Group. *Neuron* **11,** 321-331.

Kartalou M. and Essigmann J.M. (2001) Mechanisms of resistance to cisplatin. *Mutat.Res.* **478,** 23-43.

Kaufmann T., Schlipf S., Sanz J., Neubert K., Stein R. and Borner C. (2003) Characterization of the signal that directs Bcl-x(L), but not Bcl-2, to the mitochondrial outer membrane. *J.Cell Biol.* **160,** 53-64.

Kawamata N., Seriu T., Koeffler H.P. and Bartram C.R. (1996) Molecular analysis of the cyclin-dependent kinase inhibitor family: p16(CDKN2/MTS1/INK4A), p18(INK4C) and p27(Kip1) genes in neuroblastomas. *Cancer* **77,** 570-575.

Kerr J.F., Wyllie A.H. and Currie A.R. (1972) Apoptosis: a basic biological phenomenon with wide-ranging implications in tissue kinetics. *Br.J.Cancer* **26,** 239-257.

Kerr J.F., Winterford C.M. and Harmon B.V. (1994) Apoptosis. Its significance in cancer and cancer therapy. *Cancer* **73,** 2013-2026.

Keshelava N., Zuo J.J., Chen P., Waidyaratne S.N., Luna M.C., Gomer C.J., Triche T.J. and Reynolds C.P. (2001) Loss of p53 function confers high-level multidrug resistance in neuroblastoma cell lines. *Cancer Res.* **61,** 6185-6193.

Koberle B., Masters J.R., Hartley J.A. and Wood R.D. (1999) Defective repair of cisplatin-induced DNA damage caused by reduced XPA protein in testicular germ cell tumours. *Curr.Biol.* **9,** 273-276.

Komatsu M., Sumizawa T., Mutoh M., Chen Z.S., Terada K., Furukawa T., Yang X.L., Gao H., Miura N., Sugiyama T. and Akiyama S. (2000) Copper-transporting P-type adenosine triphosphatase (ATP7B) is associated with cisplatin resistance. *Cancer Res.* **60,** 1312-1316.

Kool M., de Haas M., Scheffer G.L., Scheper R.J., van Eijk M.J., Juijn J.A., Baas F. and Borst P. (1997) Analysis of expression of cMOAT (MRP2), MRP3, MRP4, and MRP5, homologues of the multidrug resistance-associated protein gene (MRP1), in human cancer cell lines. *Cancer Res.* **57,** 3537-3547.

Kops G.J., de Ruiter N.D., Vries-Smits A.M., Powell D.R., Bos J.L. and Burgering B.M. (1999) Direct control of the Forkhead transcription factor AFX by protein kinase B. *Nature* **398,** 630-634.

Kubbutat M.H., Jones S.N. and Vousden K.H. (1997) Regulation of p53 stability by Mdm2. *Nature* **387,** 299-303.

Kuida K., Zheng T.S., Na S., Kuan C., Yang D., Karasuyama H., Rakic P. and Flavell R.A. (1996) Decreased apoptosis in the brain and premature lethality in CPP32-deficient mice. *Nature* **384,** 368-372.

Kuida K., Haydar T.F., Kuan C.Y., Gu Y., Taya C., Karasuyama H., Su M.S., Rakic P. and Flavell R.A. (1998) Reduced apoptosis and cytochrome c-mediated caspase activation in mice lacking caspase 9. *Cell* **94,** 325-337.

Kurowski C. and Berthold F. (1998) Presence of classical multidrug resistance and P-glycoprotein expression in human neuroblastoma cells. *Ann.Oncol.* **9,** 1009-1014.

Le Gall M., Chambard J.C., Breittmayer J.P., Grall D., Pouyssegur J. and Obberghen-Schilling E. (2000) The p42/p44 MAP kinase pathway prevents apoptosis induced by anchorage and serum removal. *Mol.Biol.Cell* **11,** 1103-1112.

Ley R., Balmanno K., Hadfield K., Weston C. and Cook S.J. (2003) Activation of the ERK1/2 signaling pathway promotes phosphorylation and proteasome-dependent degradation of the BH3-only protein, Bim. *J.Biol.Chem.* **278,** 18811-18816.

Lindsten T., Ross A.J., King A., Zong W.X., Rathmell J.C., Shiels H.A., Ulrich E., Waymire K.G., Mahar P., Frauwirth K., Chen Y., Wei M., Eng V.M., Adelman D.M., Simon M.C., Ma A., Golden J.A., Evan G., Korsmeyer S.J., MacGregor G.R. and Thompson C.B. (2000) The combined functions of proapoptotic Bcl-2 family members bak and bax are essential for normal development of multiple tissues. *Mol.Cell* **6,** 1389-1399.

Liston P., Young S.S., Mackenzie A.E. and Korneluk R.G. (1997) Life and death decisions: the role of the IAPs in modulating programmed cell death. *Apoptosis.* **2,** 423-441.

Lu W., Pochampally R., Chen L., Traidej M., Wang Y. and Chen J. (2000) Nuclear exclusion of p53 in a subset of tumors requires MDM2 function. *Oncogene* **19,** 232-240.

Makin G.W., Corfe B.M., Griffiths G.J., Thistlethwaite A., Hickman J.A. and Dive C. (2001) Damage-induced Bax N-terminal change, translocation to mitochondria and formation of Bax dimers/complexes occur regardless of cell fate. *EMBO J.* **20,** 6306-6315.

Maliepaard M., van Gastelen M.A., de Jong L.A., Pluim D., van Waardenburg R.C., Ruevekamp-Helmers M.C., Floot B.G. and Schellens J.H. (1999) Overexpression of the BCRP/MXR/ABCP gene in a topotecan-selected ovarian tumor cell line. *Cancer Res.* **59,** 4559-4563.

Mannick J.B., Schonhoff C., Papeta N., Ghafourifar P., Szibor M., Fang K. and Gaston B. (2001) S-Nitrosylation of mitochondrial caspases. *J.Cell Biol.* **154,** 1111-1116.

Marchenko N.D., Zaika A. and Moll U.M. (2000) Death signal-induced localization of p53 protein to mitochondria. A potential role in apoptotic signaling. *J.Biol.Chem.* **275,** 16202-16212.

Maris J.M. and Matthay K.K. (1999) Molecular biology of neuroblastoma. *J.Clin.Oncol.* **17,** 2264-2279.

Martin D.P., Schmidt R.E., DiStefano P.S., Lowry O.H., Carter J.G. and Johnson E.M., Jr. (1988) Inhibitors of protein synthesis and RNA synthesis prevent neuronal death caused by nerve growth factor deprivation. *J.Cell Biol.* **106,** 829-844.

Materna V., Liedert B., Thomale J. and Lage H. (2005) Protection of platinum-DNA adduct formation and reversal of cisplatin resistance by anti-MRP2 hammerhead ribozymes in human cancer cells. *Int.J.Cancer* **115,** 393-402.

Mathai J.P., Germain M. and Shore G.C. (2005) BH3-only BIK Regulates BAX,BAK-dependent Release of Ca2+ from Endoplasmic Reticulum Stores and Mitochondrial Apoptosis during Stress-induced Cell Death. *J.Biol.Chem.* **280,** 23829-23836.

Matsumoto K., Wada R.K., Yamashiro J.M., Kaplan D.R. and Thiele C.J. (1995) Expression of brain-derived neurotrophic factor and p145TrkB affects survival, differentiation, and invasiveness of human neuroblastoma cells. *Cancer Res.* **55,** 1798-1806.

Mayo L.D. and Donner D.B. (2001) A phosphatidylinositol 3-kinase/Akt pathway promotes translocation of Mdm2 from the cytoplasm to the nucleus. *Proc.Natl.Acad.Sci.U.S.A* **98,** 11598-11603.

McDonnell T.J. and Korsmeyer S.J. (1991) Progression from lymphoid hyperplasia to high-grade malignant lymphoma in mice transgenic for the t(14; 18). *Nature* **349,** 254-256.

Melino G., Bernassola F., Ranalli M., Yee K., Zong W.X., Corazzari M., Knight R.A., Green D.R., Thompson C. and Vousden K.H. (2004) p73 Induces apoptosis via PUMA transactivation and Bax mitochondrial translocation. *J.Biol.Chem.* **279,** 8076-8083.

Metzstein M.M., Stanfield G.M. and Horvitz H.R. (1998) Genetics of programmed cell death in C. elegans: past, present and future. *Trends Genet.* **14,** 410-416.

Middlemas D.S., Kihl B.K., Zhou J. and Zhu X. (1999) Brain-derived neurotrophic factor promotes survival and chemoprotection of human neuroblastoma cells. *J.Biol.Chem.* **274,** 16451-16460.

Mihara M., Erster S., Zaika A., Petrenko O., Chittenden T., Pancoska P. and Moll U.M. (2003) p53 has a direct apoptogenic role at the mitochondria. *Mol.Cell* **11,** 577-590.

Molenaar J.J., van Sluis P., Boon K., Versteeg R. and Caron H.N. (2003) Rearrangements and increased expression of cyclin D1 (CCND1) in neuroblastoma. *Genes Chromosomes.Cancer* **36,** 242-249.

Moll U.M., LaQuaglia M., Benard J. and Riou G. (1995) Wild-type p53 protein undergoes cytoplasmic sequestration in undifferentiated neuroblastomas but not in differentiated tumors. *Proc.Natl.Acad.Sci.U.S.A* **92,** 4407-4411.

Montes de Oca L.R., Wagner D.S. and Lozano G. (1995) Rescue of early embryonic lethality in mdm2-deficient mice by deletion of p53. *Nature* **378,** 203-206.

Mora J., Gerald W.L., Qin J. and Cheung N.K. (2001) Molecular genetics of neuroblastoma and the implications for clinical management: a review of the MSKCC experience. *Oncologist.* **6,** 263-268.

Motoyama N., Wang F., Roth K.A., Sawa H., Nakayama K., Nakayama K., Negishi I., Senju S., Zhang Q., Fujii S. and . (1995) Massive cell death of immature hematopoietic cells and neurons in Bcl-x-deficient mice. *Science* **267,** 1506-1510.

Nakagawara A., Arima M., Azar C.G., Scavarda N.J. and Brodeur G.M. (1992) Inverse relationship between trk expression and N-myc amplification in human neuroblastomas. *Cancer Res.* **52,** 1364-1368.

Nakagawara A. (2001) Trk receptor tyrosine kinases: a bridge between cancer and neural development. *Cancer Lett.* **169,** 107-114.

Nakano K. and Vousden K.H. (2001) PUMA, a novel proapoptotic gene, is induced by p53. *Mol.Cell* **7,** 683-694.

Nakayama K., Kanzaki A., Ogawa K., Miyazaki K., Neamati N. and Takebayashi Y. (2002) Copper-transporting P-type adenosine triphosphatase (ATP7B) as a cisplatin based chemoresistance marker in ovarian carcinoma: comparative analysis with expression of MDR1, MRP1, MRP2, LRP and BCRP. *Int.J.Cancer* **101,** 488-495.

Neame S.J., Rubin L.L. and Philpott K.L. (1998) Blocking cytochrome c activity within intact neurons inhibits apoptosis. *J.Cell Biol.* **142,** 1583-1593.

Niedner H., Christen R., Lin X., Kondo A. and Howell S.B. (2001) Identification of genes that mediate sensitivity to cisplatin. *Mol.Pharmacol.* **60,** 1153-1160.

Niimi S., Nakagawa K., Yokota J., Tsunokawa Y., Nishio K., Terashima Y., Shibuya M., Terada M. and Saijo N. (1991) Resistance to anticancer drugs in NIH3T3 cells transfected with c-myc and/or c-H-ras genes. *Br.J.Cancer* **63,** 237-241.

Nijhawan D., Fang M., Traer E., Zhong Q., Gao W., Du F. and Wang X. (2003) Elimination of Mcl-1 is required for the initiation of apoptosis following ultraviolet irradiation. *Genes Dev.* **17,** 1475-1486.

Norris M.D., Smith J., Tanabe K., Tobin P., Flemming C., Scheffer G.L., Wielinga P., Cohn S.L., London W.B., Marshall G.M., Allen J.D. and Haber M. (2005) Expression of multidrug transporter MRP4/ABCC4 is a marker of poor prognosis in neuroblastoma and confers resistance to irinotecan in vitro. *Mol.Cancer Ther.* **4,** 547-553.

O'Reilly L.A., Print C., Hausmann G., Moriishi K., Cory S., Huang D.C. and Strasser A. (2001) Tissue expression and subcellular localization of the pro-survival molecule Bcl-w. *Cell Death.Differ.* **8,** 486-494.

Oltvai Z.N., Milliman C.L. and Korsmeyer S.J. (1993) Bcl-2 heterodimerizes in vivo with a conserved homolog, Bax, that accelerates programmed cell death. *Cell* **74,** 609-619.

Packham G., Porter C.W. and Cleveland J.L. (1996) c-Myc induces apoptosis and cell cycle progression by separable, yet overlapping, pathways. *Oncogene* **13,** 461-469.

Park S.A., Park H.J., Lee B.I., Ahn Y.H., Kim S.U. and Choi K.S. (2001) Bcl-2 blocks cisplatin-induced apoptosis by suppression of ERK-mediated p53 accumulation in B104 cells. *Brain Res.Mol.Brain Res.* **93,** 18-26.

Parker R.J., Eastman A., Bostick-Bruton F. and Reed E. (1991) Acquired cisplatin resistance in human ovarian cancer cells is associated with enhanced repair of cisplatin-DNA lesions and reduced drug accumulation. *J.Clin.Invest* **87,** 772-777.

Perez R.P. (1998) Cellular and molecular determinants of cisplatin resistance. *Eur.J.Cancer* **34,** 1535-1542.

Pettmann B. and Henderson C.E. (1998) Neuronal cell death. *Neuron* **20,** 633-647.

Porter A.G. (1999) Protein translocation in apoptosis. *Trends Cell Biol.* **9,** 394-401.

Print C.G., Loveland K.L., Gibson L., Meehan T., Stylianou A., Wreford N., de Kretser D., Metcalf D., Kontgen F., Adams J.M. and Cory S. (1998) Apoptosis regulator bcl-w is essential for spermatogenesis but appears otherwise redundant. *Proc.Natl.Acad.Sci.U.S.A* **95,** 12424-12431.

Putcha G.V., Moulder K.L., Golden J.P., Bouillet P., Adams J.A., Strasser A. and Johnson E.M. (2001) Induction of BIM, a proapoptotic BH3-only BCL-2 family member, is critical for neuronal apoptosis. *Neuron* **29,** 615-628.

Puthalakath H., Huang D.C., O'Reilly L.A., King S.M. and Strasser A. (1999) The proapoptotic activity of the Bcl-2 family member Bim is regulated by interaction with the dynein motor complex. *Mol.Cell* **3,** 287-296.

Puthalakath H., Villunger A., O'Reilly L.A., Beaumont J.G., Coultas L., Cheney R.E., Huang D.C. and Strasser A. (2001) Bmf: a proapoptotic BH3-only protein regulated by interaction with the myosin V actin motor complex, activated by anoikis. *Science* **293,** 1829-1832.

Raff M.C. (1992) Social controls on cell survival and cell death. *Nature* **356,** 397-400.

Rinkenberger J.L., Horning S., Klocke B., Roth K. and Korsmeyer S.J. (2000) Mcl-1 deficiency results in peri-implantation embryonic lethality. *Genes Dev.* **14,** 23-27.

Roberts D., Schick J., Conway S., Biade S., Laub P.B., Stevenson J.P., Hamilton T.C., O'Dwyer P.J. and Johnson S.W. (2005) Identification of genes associated with platinum drug sensitivity and resistance in human ovarian cancer cells. *Br.J.Cancer* **92,** 1149-1158.

Rodriguez-Lopez A.M., Xenaki D., Eden T.O., Hickman J.A. and Chresta C.M. (2001) MDM2 mediated nuclear exclusion of p53 attenuates etoposide-induced apoptosis in neuroblastoma cells. *Mol.Pharmacol.* **59,** 135-143.

Rodriguez A., Chen P., Oliver H. and Abrams J.M. (2002) Unrestrained caspase-dependent cell death caused by loss of Diap1 function requires the Drosophila Apaf-1 homolog, Dark. *EMBO J.* **21,** 2189-2197.

Ross A.J., Waymire K.G., Moss J.E., Parlow A.F., Skinner M.K., Russell L.D. and MacGregor G.R. (1998) Testicular degeneration in Bclw-deficient mice. *Nat.Genet.* **18,** 251-256.

Roy N., Mahadevan M.S., McLean M., Shutler G., Yaraghi Z., Farahani R., Baird S., Besner-Johnston A., Lefebvre C., Kang X. and . (1995) The gene for neuronal apoptosis inhibitory protein is partially deleted in individuals with spinal muscular atrophy. *Cell* **80,** 167-178.

Rudel T. and Bokoch G.M. (1997) Membrane and morphological changes in apoptotic cells regulated by caspase-mediated activation of PAK2. *Science* **276,** 1571-1574.

Sanchez-Perez I., Murguia J.R. and Perona R. (1998) Cisplatin induces a persistent activation of JNK that is related to cell death. *Oncogene* **16,** 533-540.

Satoh T.H., Surmacz T.A., Nyormoi O. and Whitacre C.M. (2003) Inhibition of focal adhesion kinase by antisense oligonucleotides enhances the sensitivity of breast cancer cells to camptothecins. *Biocell* **27,** 47-55.

Scaffidi P., Misteli T. and Bianchi M.E. (2002) Release of chromatin protein HMGB1 by necrotic cells triggers inflammation. *Nature* **418,** 191-195.

Schreiber M., Kolbus A., Piu F., Szabowski A., Mohle-Steinlein U., Tian J., Karin M., Angel P. and Wagner E.F. (1999) Control of cell cycle progression by c-Jun is p53 dependent. *Genes Dev.* **13,** 607-619.

Schuler M. and Green D.R. (2001) Mechanisms of p53-dependent apoptosis. *Biochem.Soc.Trans.* **29,** 684-688.

Schwab M., Alitalo K., Klempnauer K.H., Varmus H.E., Bishop J.M., Gilbert F., Brodeur G., Goldstein M. and Trent J. (1983) Amplified DNA with limited homology to myc cellular oncogene is shared by human neuroblastoma cell lines and a neuroblastoma tumour. *Nature* **305,** 245-248.

Schwab M. (1999) Human neuroblastoma: from basic science to clinical debut of cellular oncogenes. *Naturwissenschaften* **86,** 71-78.

Seeger R.C., Brodeur G.M., Sather H., Dalton A., Siegel S.E., Wong K.Y. and Hammond D. (1985) Association of multiple copies of the N-myc oncogene with rapid progression of neuroblastomas. *N.Engl.J.Med.* **313,** 1111-1116.

Sheikh M.S. and Fornace A.J., Jr. (2000) Role of p53 family members in apoptosis. *J.Cell Physiol* **182,** 171-181.

Smart P., Lane E.B., Lane D.P., Midgley C., Vojtesek B. and Lain S. (1999) Effects on normal fibroblasts and neuroblastoma cells of the activation of the p53 response by the nuclear export inhibitor leptomycin B. *Oncogene* **18,** 7378-7386.

Srinivasula S.M., Hegde R., Saleh A., Datta P., Shiozaki E., Chai J., Lee R.A., Robbins P.D., Fernandes-Alnemri T., Shi Y. and Alnemri E.S. (2001) A conserved XIAP-interaction motif in caspase-9 and Smac/DIABLO regulates caspase activity and apoptosis. *Nature* **410,** 112-116.

Stambolic V., MacPherson D., Sas D., Lin Y., Snow B., Jang Y., Benchimol S. and Mak T.W. (2001) Regulation of PTEN transcription by p53. *Mol.Cell* **8,** 317-325.

Stommel J.M., Marchenko N.D., Jimenez G.S., Moll U.M., Hope T.J. and Wahl G.M. (1999) A leucine-rich nuclear export signal in the p53 tetramerization domain: regulation of subcellular localization and p53 activity by NES masking. *EMBO J.* **18,** 1660-1672.

Strasser A., Harris A.W., Bath M.L. and Cory S. (1990) Novel primitive lymphoid tumours induced in transgenic mice by cooperation between myc and bcl-2. *Nature* **348,** 331-333.

Strasser A., Harris A.W. and Cory S. (1993) E mu-bcl-2 transgene facilitates spontaneous transformation of early pre-B and immunoglobulin-secreting cells but not T cells. *Oncogene* **8,** 1-9.

Sulston J.E. and Brenner S. (1974) The DNA of Caenorhabditis elegans. *Genetics* **77,** 95-104.

Susin S.A., Lorenzo H.K., Zamzami N., Marzo I., Snow B.E., Brothers G.M., Mangion J., Jacotot E., Costantini P., Loeffler M., Larochette N., Goodlett D.R., Aebersold R., Siderovski D.P., Penninger J.M. and Kroemer G. (1999) Molecular characterization of mitochondrial apoptosis-inducing factor. *Nature* **397,** 441-446.

Suzuki M., Youle R.J. and Tjandra N. (2000) Structure of Bax: coregulation of dimer formation and intracellular localization. *Cell* **103,** 645-654.

Tacconelli A., Farina A.R., Cappabianca L., Desantis G., Tessitore A., Vetuschi A., Sferra R., Rucci N., Argenti B., Screpanti I., Gulino A. and Mackay A.R. (2004) TrkA alternative splicing: a regulated tumor-promoting switch in human neuroblastoma. *Cancer Cell* **6,** 347-360.

Tan T. and Chu G. (2002) p53 Binds and activates the xeroderma pigmentosum DDB2 gene in humans but not mice. *Mol.Cell Biol.* **22,** 3247-3254.

Tang J.Y., Hwang B.J., Ford J.M., Hanawalt P.C. and Chu G. (2000) Xeroderma pigmentosum p48 gene enhances global genomic repair and suppresses UV-induced mutagenesis. *Mol.Cell* **5,** 737-744.

Tashker J.S., Olson M. and Kornbluth S. (2002) Post-cytochrome C protection from apoptosis conferred by a MAPK pathway in Xenopus egg extracts. *Mol.Biol.Cell* **13,** 393-401.

Teitz T., Wei T., Valentine M.B., Vanin E.F., Grenet J., Valentine V.A., Behm F.G., Look A.T., Lahti J.M. and Kidd V.J. (2000) Caspase 8 is deleted or silenced preferentially in childhood neuroblastomas with amplification of MYCN. *Nat.Med.* **6,** 529-535.

Tewari M., Quan L.T., O'Rourke K., Desnoyers S., Zeng Z., Beidler D.R., Poirier G.G., Salvesen G.S. and Dixit V.M. (1995) Yama/CPP32 beta, a mammalian homolog of CED-3, is a CrmA-inhibitable protease that cleaves the death substrate poly(ADP-ribose) polymerase. *Cell* **81,** 801-809.

Thomas L.B., Gates D.J., Richfield E.K., O'Brien T.F., Schweitzer J.B. and Steindler D.A. (1995) DNA end labeling (TUNEL) in Huntington's disease and other neuropathological conditions. *Exp.Neurol.* **133,** 265-272.

Thornberry N.A., Rano T.A., Peterson E.P., Rasper D.M., Timkey T., Garcia-Calvo M., Houtzager V.M., Nordstrom P.A., Roy S., Vaillancourt J.P., Chapman K.T. and Nicholson D.W. (1997) A combinatorial approach defines specificities of members of the caspase family and granzyme B. Functional relationships established for key mediators of apoptosis. *J.Biol.Chem.* **272,** 17907-17911.

Tieu K., Zuo D.M. and Yu P.H. (1999) Differential effects of staurosporine and retinoic acid on the vulnerability of the SH-SY5Y neuroblastoma cells: involvement of bcl-2 and p53 proteins. *J.Neurosci.Res.* **58,** 426-435.

Vassilev L.T., Vu B.T., Graves B., Carvajal D., Podlaski F., Filipovic Z., Kong N., Kammlott U., Lukacs C., Klein C., Fotouhi N. and Liu E.A. (2004) In vivo activation of the p53 pathway by small-molecule antagonists of MDM2. *Science* **303,** 844-848.

Vaux D.L., Cory S. and Adams J.M. (1988) Bcl-2 gene promotes haemopoietic cell survival and cooperates with c-myc to immortalize pre-B cells. *Nature* **335,** 440-442.

Vaux D.L., Weissman I.L. and Kim S.K. (1992) Prevention of programmed cell death in Caenorhabditis elegans by human bcl-2. *Science* **258,** 1955-1957.

Vaux D.L. (1993) Toward an understanding of the molecular mechanisms of physiological cell death. *Proc.Natl.Acad.Sci.U.S.A* **90,** 786-789.

Veis D.J., Sorenson C.M., Shutter J.R. and Korsmeyer S.J. (1993) Bcl-2-deficient mice demonstrate fulminant lymphoid apoptosis, polycystic kidneys, and hypopigmented hair. *Cell* **75,** 229-240.

Verhagen A.M., Ekert P.G., Pakusch M., Silke J., Connolly L.M., Reid G.E., Moritz R.L., Simpson R.J. and Vaux D.L. (2000) Identification of DIABLO, a mammalian protein that promotes apoptosis by binding to and antagonizing IAP proteins. *Cell* **102,** 43-53.

Verma S., Zhao L.J. and Chinnadurai G. (2001) Phosphorylation of the pro-apoptotic protein BIK: mapping of phosphorylation sites and effect on apoptosis. *J.Biol.Chem.* **276,** 4671-4676.

Villunger A., Michalak E.M., Coultas L., Mullauer F., Bock G., Ausserlechner M.J., Adams J.M. and Strasser A. (2003) p53- and drug-induced apoptotic responses mediated by BH3-only proteins puma and noxa. *Science* **302,** 1036-1038.

Vitte-Mony I., Korneluk R.G. and Diaz-Mitoma F. (1997) Role of XIAP protein, a human member of the inhibitor of apoptosis (IAP) protein family, in phytohemagglutinin-induced apoptosis of human T cell lines. *Apoptosis.* **2,** 501-509.

Vogan K., Bernstein M., Leclerc J.M., Brisson L., Brossard J., Brodeur G.M., Pelletier J. and Gros P. (1993) Absence of p53 gene mutations in primary neuroblastomas. *Cancer Res.* **53,** 5269-5273.

Vogelstein B., Lane D. and Levine A.J. (2000) Surfing the p53 network. *Nature* **408,** 307-310.

von Gise A., Lorenz P., Wellbrock C., Hemmings B., Berberich-Siebelt F., Rapp U.R. and Troppmair J. (2001) Apoptosis suppression by Raf-1 and MEK1 requires MEK- and phosphatidylinositol 3-kinase-dependent signals. *Mol.Cell Biol.* **21,** 2324-2336.

Vucic D., Stennicke H.R., Pisabarro M.T., Salvesen G.S. and Dixit V.M. (2000) ML-IAP, a novel inhibitor of apoptosis that is preferentially expressed in human melanomas. *Curr.Biol.* **10,** 1359-1366.

Wang J. and Lenardo M.J. (2000) Roles of caspases in apoptosis, development, and cytokine maturation revealed by homozygous gene deficiencies. *J.Cell Sci.* **113 (Pt 5),** 753-757.

Wang X., Yang C., Chai J., Shi Y. and Xue D. (2002) Mechanisms of AIF-mediated apoptotic DNA degradation in Caenorhabditis elegans. *Science* **298,** 1587-1592.

Wei M.C., Zong W.X., Cheng E.H., Lindsten T., Panoutsakopoulou V., Ross A.J., Roth K.A., MacGregor G.R., Thompson C.B. and Korsmeyer S.J. (2001) Proapoptotic BAX and BAK: a requisite gateway to mitochondrial dysfunction and death. *Science* **292,** 727-730.

Weng C., Li Y., Xu D., Shi Y. and Tang H. (2005) Specific cleavage of Mcl-1 by caspase-3 in tumor necrosis factor-related apoptosis-inducing ligand (TRAIL)-induced apoptosis in Jurkat leukemia T cells. *J.Biol.Chem.* **280,** 10491-10500.

Weston C.R., Balmanno K., Chalmers C., Hadfield K., Molton S.A., Ley R., Wagner E.F. and Cook S.J. (2003) Activation of ERK1/2 by deltaRaf-1:ER* represses Bim expression independently of the JNK or PI3K pathways. *Oncogene* **22,** 1281-1293.

Wetzel C.C. and Berberich S.J. (2001) p53 binds to cisplatin-damaged DNA. *Biochim.Biophys.Acta* **1517,** 392-397.

Whitfield J., Neame S.J., Paquet L., Bernard O. and Ham J. (2001) Dominant-negative c-Jun promotes neuronal survival by reducing BIM expression and inhibiting mitochondrial cytochrome c release. *Neuron* **29,** 629-643.

Wolter K.G., Hsu Y.T., Smith C.L., Nechushtan A., Xi X.G. and Youle R.J. (1997) Movement of Bax from the cytosol to mitochondria during apoptosis. *J.Cell Biol.* **139,** 1281-1292.

Woods D.B. and Vousden K.H. (2001) Regulation of p53 function. *Exp.Cell Res.* **264,** 56-66.

Wyllie A.H., Kerr J.F. and Currie A.R. (1980) Cell death: the significance of apoptosis. *Int.Rev.Cytol.* **68,** 251-306.

Wyllie A.H. (1994) Death from inside out: an overview. *Philos.Trans.R.Soc.Lond B Biol.Sci.* **345,** 237-241.

Yan N., Gu L., Kokel D., Chai J., Li W., Han A., Chen L., Xue D. and Shi Y. (2004) Structural, biochemical, and functional analyses of CED-9 recognition by the proapoptotic proteins EGL-1 and CED-4. *Mol.Cell* **15,** 999-1006.

Yu J., Zhang L., Hwang P.M., Kinzler K.W. and Vogelstein B. (2001) PUMA induces the rapid apoptosis of colorectal cancer cells. *Mol.Cell* **7,** 673-682.

Yu J., Wang Z., Kinzler K.W., Vogelstein B. and Zhang L. (2003) PUMA mediates the apoptotic response to p53 in colorectal cancer cells. *Proc.Natl.Acad.Sci.U.S.A* **100,** 1931-1936.

Yu S.W., Wang H., Poitras M.F., Coombs C., Bowers W.J., Federoff H.J., Poirier G.G., Dawson T.M. and Dawson V.L. (2002) Mediation of poly(ADP-ribose) polymerase-1-dependent cell death by apoptosis-inducing factor. *Science* **297,** 259-263.

Yuan J. and Yankner B.A. (2000) Apoptosis in the nervous system. *Nature* **407,** 802-809.

Zeleznik A.J., Ihrig L.L. and Bassett S.G. (1989) Developmental expression of Ca++/Mg++-dependent endonuclease activity in rat granulosa and luteal cells. *Endocrinology* **125,** 2218-2220.

Zha J., Harada H., Yang E., Jockel J. and Korsmeyer S.J. (1996) Serine phosphorylation of death agonist BAD in response to survival factor results in binding to 14-3-3 not BCL-X(L). *Cell* **87,** 619-628.

Zhao H. and Piwnica-Worms H. (2001) ATR-mediated checkpoint pathways regulate phosphorylation and activation of human Chk1. *Mol.Cell Biol.* **21,** 4129-4139.

Zhou B.P., Liao Y., Xia W., Zou Y., Spohn B. and Hung M.C. (2001) HER-2/neu induces p53 ubiquitination via Akt-mediated MDM2 phosphorylation. *Nat.Cell Biol.* **3,** 973-982.